SIGNALING PATHWAYS REGULATING ENCAPSULATION OF GERMLINE CELLS BY SOMATIC SUPPORT CELLS IN *DROSOPHILA MELANOGASTER*

by

YUE QIAN

(Under the Direction of Cordula Schulz)

ABSTRACT

Most metazoan cells have a short life span and thus are constantly reproduced from stem cells residing in adult tissues. A stem cell normally divides in an asymmetric fashion in that one daughter retains the stem cell properties to replenish the stem cell population while the other produces specialized progeny. The regulation of the stem cell fate decision is determined by intrinsic cues as well as external signals coming from the cellular microenvironment, or niche. Investigating fundamental questions, e.g. how stem cells function to maintain tissue homeostasis, how stem cells communicate with their microenvironment, and how cytophysical influences affect behavior of stem cell daughters, provides essential insights of general mechanisms that regulate metazoan development including growth, aging and regeneration, and also sheds light on clinical potential of stem-cell based tissue engineering and regenerative medicine.

Gonads of *Drosophila melanogaster* have long been studied, which, along with the power of genetic, molecular, biochemical and cytological approaches, make gametogenesis in fruit flies attractive models to study stem cell and developmental biology related questions. In both of male and female fly gonads, germline cells are enclosed in cytoplasmic extensions from supporting somatic cells that serve as the germline cellular microenvironment. This intimate germline-soma interaction is critical for proliferation and differentiation of both lineages. Signaling pathways that regulate germline and soma development can be identified by virtue of viable and infertile mutations and RNA interference (RNAi).

Chapter 1 reviews the role of stem cells in regeneration and homeostasis, the intercellular interaction between stem cells and their microenvironment, and *Drosophila* gonads and gametogenesis. Chapter 2 demonstrates that ecdysone signaling acts antagonistically to Epidermal Growth Factor (EGF) signaling in modulating cyst development in fly testes. Chapter 3 shows that the COP9 signalosome (CSN) is required for the expression of stem cell genes and maintenance of the germline microenvironment through different Cullin RING ubiquitin ligase (CRL) complexes in fly testes. Chapter 4 introduces a novel *Drosophila* specific gene, named *comeback*, that maintains cytoplasmic extensions of somatic support cells to regulate differentiation of germline stem cell (GSC) immediate daughter cells in fly ovaries.

INDEX WORDS: *Drosophila*, Somatic support cell, Germline, Microenvironment, Cytoplasmic extension, Differentiation

SIGNALING PATHWAYS REGULATING ENCAPSULATION OF GERMLINE CELLS BY SOMATIC SUPPORT CELLS IN *DROSOPHILA MELANOGASTER*

by

YUE QIAN

B.S., Shanghai University, People's Republic of China, 2008

A Dissertation Submitted to the Graduate Faculty of The University of Georgia in Partial Fulfillment of the Requirements for the Degree

DOCTOR OF PHILOSOPHY

ATHENS, GEORGIA

2014

SIGNALING PATHWAYS REGULATING ENCAPSULATION OF GERMLINE CELLS BY SOMATIC SUPPORT CELLS IN *DROSOPHILA MELANOGASTER*

by

YUE QIAN

Major Professor: Cordula Schulz

Committee: Edward T. Kipreos
James D. Lauderdale
John P. Shields

Electronic Version Approved:

Julie Coffield
Interim Dean of the Graduate School
The University of Georgia
December 2014

DEDICATION

This dissertation is dedicated to my parents, Lin Qian and Xiaopei Li, who first taught me the value of education and critical thinking. Their support, encouragement, and constant love have sustained me throughout my life. I also dedicate this work to my fiancée, Ming Fang, for his love, patience and companionship in this great venture.

ACKNOWLEDGEMENTS

"It takes a village to raise a child." First Lady Hillary Clinton adopted this proverb for the title of her book published in 1996. While in my case, it took a village to achieve a Doctorate and I would like to express my gratitude to numerous people that assisted me in the completion of this work.

My major advisor and committee chair, Dr. Cordula Schulz, has been an amazing mentor and friend. I greatly appreciate her guidance throughout my time in her lab. Her ongoing supervision and support as well as consistent pushing of my thinking challenged me in all the right ways. I could have never gotten to this point without her. It is such an honor to work with you and it is so much fun to have you teach me many things beyond science!

I would like to thank Dr. Edward Kipreos, Dr. James Lauderdale and Dr. John Shields, for serving on my committee, asking the right questions at the right times, offering constructive comments and directing me in the path to graduation. In particular, I want to appreciate Dr. Edward Kipreos for his detailed and thought-provoking feedback on my projects, which were all exceptionally valuable and helped me to become a more thorough scientist.

I have been fortunate to have two fantastic Graduate Coordinators along the path. I would like to express my deep gratitude to Dr. Marcus Fechheimer for always being fatherly kind and patient, providing so much suggestion, inspiration and support to broaden my horizons in teaching, science and life in general. I am also sincerely grateful to Dr. Scott Dougan for his encouragement in the very beginning, without which I would never grow up to a rounded graduate instructor.

In addition, my special thanks go to Dr. Wolfgang Lukowitz for his every effort in helping writing papers and supporting us during an extraordinarily hard time.

I would also like to appreciate the entirety of the faculty and administrative staff of Cellular Biology Department for being a caring and supportive force. This work could not have been done without your help.

Finally, I want to thank all of those people who, once upon a time, helped me to figure out puzzles in research or life, and inspired me to continue learning and being strong. Their names are too numerous to mention, but I am so grateful to have gone through this experience with all of them – Wish best luck to all of you!

TABLE OF CONTENTS

Page

LIST OF TABLES

Page

LIST OF FIGURES

Page

CHAPTER 1

INTRODUCTION & LITERATURE REVIEW

Multicellular organisms need to constantly make new cells to keep themselves properly functioning. Most specialized cells, such as muscle or blood cells, are unable to replicate themselves simply through cell division. Instead, they are replenished from a unique population of cells – stem cells. Stem cells have two distinctive abilities, self-renewal and differentiation, through which they are able to maintain their own population while producing differentiating cells. These two defining characteristics endow stem cells as the body's natural reservoir of cells – serving in development, tissue regeneration, and homeostatic turnover (Bongso and Richards, 2004). Stem cell research may help us understand many fundamental and long-lasting questions in the field of biology: how does one single fertilized egg turn into a complex organism, how does cancer start, and how does aging occur. In a practical sense, a better understanding of the genetic and molecular controls of stem cell behavior may yield information for expanding fields of regenerative medicine and functional tissue engineering, which could contribute to the treatment of a myriad of diseases, conditions, and disabilities including birth defects, heart disease, diabetes, Alzheimer's disease, and trauma (Daley and Scadden, 2008). In this chapter, I review the role of stem cells in regeneration and homeostasis, the intercellular interaction between stem cells and stem cell microenvironments, and *Drosophila melanogaster* gametogenesis as a valuable tool to study stem cell biology and developmental biology.

Regeneration, homeostasis, and stem cells

Man has long been intrigued by the regenerative abilities of those animals able to rearrange remaining tissues after wounding to generate a missing body part or even create a new organ. Examples are planarians and hydras, which exploit complex processes requiring the collaborative efforts of different cell lineages as well as matrix signals to remodel tissues or organs back to the pre-existing state (Chandebois, 1985; Reiter et al., 2012). Human beings, on the other hand, are incapable of any form of whole-organ regeneration, even though we had all the necessary machinery and instructions to generate tissues and organs during embryogenesis. Nevertheless, some human tissues and organs retain a high capacity of regenerating cells throughout life. For example, epithelial cells found in the epidermis of skin and the intestinal lining are characterized by a process, in which cells constantly proliferate and differentiate with a high turnover rate to make up for the dead cells shed off the body or into the intestine (Martin, 1997; Barker, 2014). Another example is the resected human liver, which can regenerate in a short time through a uniform and homogenous process. During this process, while maintaining all critical differentiated functions, hepatocytes undergo limited dedifferentiation to reenter the cell cycle and proliferate simultaneously, that yield a population of endoderm-like cells (reviewed in Fausto and Campbell, 2003).

But how do the regenerated cells know when to stop proliferation and restrict their original sizes to adapt to the organism? For a long time, scientists from all over the world have been working on the genetic, molecular and cellular mechanisms driving the restoration of structures and functions lost to physiological turnover or damaged by environmental aggressions. They seek a way to understand how metazoan tissues remain

in a state of flux throughout the lifetime of an organism, or more practically, to repair injured tissues or create new organs. In 2003, scientists discovered that hepatocyte growth factor (HGF) and transforming growth factor-beta1 (TGF-β1) function synergistically to regulate the regeneration of liver to a predetermined size after resection, which makes adult-to-adult living donor liver transplantation feasible (Ninomiya et al., 2003). But much earlier than this, researchers noticed that the regeneration dynamics and tissue homeostasis rely on a special cell type, the stem cells, residing in the adult tissues and persisting throughout life as a backup reservoir for replenishing damaged or dead cells. In 1868, the term “stem cell” was coined by German biologist Ernst Haeckel. Later in his books he characterized stem cells in two scenarios: as the unicellular ancestor of all multicellular organisms and as the fertilized egg that gives rise to all cells of the organism (Ramalho-Santos and Willenbring, 2007). In the early 1900s, Russian scientist Alexander Maximow lectured at the Berlin Hematological Society on a theory that all blood cells come from the same ancestor cell, called blood stem cells, that are multipotent and able to differentiate into several types of cells (Maximow, 1909). In 1968, doctors in Minnesota successfully performed the first allogeneic bone marrow transplant to treat two infant siblings with severe combined immunodeficiency (Bortin, 1970). A decade after that, hematopoietic stem cells (HSC) were discovered in human cord blood (Prindull et al., 1978). Scientists started to understand that bone marrow contains somatic stem cells that can produce all of the different cell types that make up the blood. Stem cell-based therapies, using cultured embryonic stem cells (ESCs) or induced pluripotent stem cells (iPSCs), have grown exponentially over the last decade. Recent advances in this field have been reported in animal models for several diseases, including T-cell

immunodeficiency, chronic myeloid leukemia, temporal lobe epilepsy, and spermatogenesis disorder (Awong et al., 2013; Airiau et al., 2013; Miltiadous et al., 2013; Anand et al., 2013).

It has been shown that failure to maintain tissue or stem cell homeostasis disrupts function and structure of tissues and organs of the body, therefore provoking diseases and causing aging (Silva and Conboy, 2008). Cancer biologist Leroy Stevens found large tumors in mouse scrotums in 1958. He reported these tumors, named teratomas, contained mixtures of differentiated and undifferentiated cells, including hair, bone, intestinal and blood tissue (Stevens, 1958). The tumor cells were described as "pluripotent stem cells", meaning they can differentiate into any cell type found in adult animals. Many studies have shown that stem cell behavior is regulated by intrinsic mechanisms (Zon, 2008; de Haan and Van Zant, 1997; Zou et al., 2013; Gogishvili et al., 2013; Nutt et al., 2008). A recent study showed that, Wnt7b, which is an important intrinsic regulator as a direct target of canonical bone morphogenic protein (BMP) signaling in hair follicle stem cells (hfSCs), regulated hair follicle (HF) anagen (growth) length and catagen (cessation) entry. This nonredundant role of Wnt7b in controlling hfSC homeostasis and HF cycling was not compensated by other Wnt ligands (Kandyba and Kobielak, 2014). On the other side, the coordinated extrinsic cues, such as growth factors, signaling molecules, oxygen and mechanical stimuli, have been shown to govern tissue and stem cell homeostasis as well (Przybyla and Voldman, 2012; Yeh et al., 2011; Jiang et al., 2014; Eckes and Krieg, 2004; reviewed in Humphrey, 2008). For example, HSC formation and homeostasis is tightly controlled by chemicals that enhance or block

the synthesis of prostaglandin E2 (PGE2), a hormone-like lipid compound known in medicine as dinoprostone (North et al., 2007).

Stem cell microenvironment, intercellular interactions, and stem cells

The concept of the "stem cell niche" was first postulated almost 40 years ago by mammalian hematologist Ray Schofield, who characterized the "niche" as a specialized microenvironment to house stem cells and regulate their function (Schofield, 1978). In etymology, "niche" is originated from the Latin word "nidus", which literally means "nest". Although a place of habitation would meet the architectural concept of the term "niche", it is insufficient in regard to the multidimensional stem cell surroundings (reviewed in Scadden, 2006). It has been shown that in physiological milieu, stem cells confront complex stimuli including biological, chemical, and physiological cues from neighboring cells and extracellular matrix, which integrate with one another to significantly affect stem cell proliferation and fate determination (Chen et al., 2013; reviewed in Han et al., 2014). Adult stem cells generally have limited function without being situated in the microenvironment. For example, HSCs are known to mostly reside in the bone marrow in a quiescent, immobile state through adhesion interactions with stromal cells (reviewed in Purton and Scadden, 2008). In a study on the impact of the bone marrow microenvironment of hematopoietic stem and progenitor cells, scientists examined the combined effect of hematopoietic niche elements including stromal cells, osteoblasts, and adipocytes. From their findings, they suggested that osteoblasts promoted hematopoietic functions, including repopulating potential by up-regulating Notch-mediated signaling, and adipocytes may down-modulate HSC function (Chitteti et

al., 2010). Another example, a systematic examination of mechanical stimulation on mesenchymal stem cells was performed, using three forces, cyclic stretch, cyclic pressure, and laminar shear stress in parallel to mimic different vascular physiologic conditions, and stem cell behavior changes were seen in morphology, proliferation, and differentiation (Maul et al., 2011).

Studies in regard to identifying and locating stem cell microenvironment in several model organisms have been fruitful in the recent two decades. In *Caenorhabditis elegans*, a somatic distal tip cell (DTC) located at the tip of the germline mitotic region was found to function as an essential microenvironment element in supporting germline stem cells (GSCs) (Crittenden et al., 2002). In female *Drosophila melanogaster*, the germarial anterior tip, composed of terminal filament, cap cells, and escort stem cells, was defined as GSC microenvironment (Xie and Spradling, 2000; Kirilly et al., 2011). Whereas in the males, somatic hub cells and cyst stem cells (CySCs) located at the tip of *Drosophila* testis were confirmed as indispensable to form the GSC microenvironment (Kiger et al., 2001; Tulina and Matunis, 2001; Leatherman and Dinardo, 2010). Although pinpointing stem cells and their correlated microenvironments in mammals is very intricate due to their complicated anatomical structures, scientists have successfully identified locations of epidermal stem cells in the bulge area of hair follicles (Cotsarelis et al., 1990), intestinal stem cells near the crypt base (Potten et al., 2002), neural stem cells regulated by endothelial cells at the base of the subventricular zone (SVZ) and subgranular zone (SGZ) (Shen et al., 2004; Doetsch et al., 1999; Palmer et al., 1997), and HSCs controlled by osteoblastic cells in close proximity to the endosteal surfaces (Zhang et al., 2003; Calvi et al., 2003). All stem cells exemplified hereinabove have been shown

to have intimate associations with their regulatory microenvironmental cells. The stromal cells composing the microenvironment influence cytological and physiological events of stem cells and their daughter cells in direct contact and in proximity, through either the direct intercellular junctions or the secretion of regulatory substances such as signaling ligands or enzymes (Li and Xie, 2005).

In response to signals coming from the microenvironment, intercellular interaction by direct contact between cell surfaces has been established as one of the most crucial mechanisms allowing stem cells including their daughters to decide whether to maintain the "stemness" or to produce a specified lineage on physiological demand (Liu et al., 1997; Parekkadan et al., 2008). In a broader setting, this direct communication is essential for the survival and development of different types of metazoan cells (Verdi et al., 1996; Reinke and Zipursky, 1988). Compared to the complicated compositions within mammalian stem cell microenvironment, male and female *Drosophila* gonads, each consisting of only a few cell types, have been established as valuable models in the studies of intercellular interactions (Palasz and Kaminski, 2009). For example, it was shown that gap junctional contact is required for survival and differentiation of early germ cells during gametogenesis in both sexes of *Drosophila*, possibly by mediating passage of small molecules or signals between germline and somatic cells (Tazuke et al., 2002).

Drosophila testis and spermatogenesis

An adult male *Drosophila* has a pair of testes attached to the anterior ejaculatory duct via seminal vesicles (Fig. 1.1A). Each of the testes is an approximately 2-mm-long

spiral tube, tapered at the apical tip harboring two types of stem cells, germline stem cells (GSCs) and cyst stem cells (CySCs), which give rise to germline cells and cyst cells, respectively (Hardy et al., 1979; Gönczy and DiNardo, 1996). Electron microscopy studies revealed that 5-9 GSCs form a rosette around a single cluster of terminally differentiated somatic support cells, called the hub, at the tip of the testis (Hardy et al., 1979). Each GSC is encapsulated by a pair of CySCs that grow cytoplasmic extensions around the GSC and into the hub. Hub cells express the cytokine-like ligand Unpaired (Upd), which activates the Janus kinase-signal transducer and activator of transcription (JAK-STAT) signaling cascade in adjacent GSCs to control GSC self-renewal and continual maintenance of GSC populations (Kiger et al., 2001; Tulina and Matunis, 2001). Hub cells and somatic cyst cells express two bone morphogenic protein (BMP) molecules, Glass bottom boat (Gbb) and Decapentaplegic (Dpp), which function cooperatively to maintain GSCs (Kawase et al., 2004). Transforming growth factor-beta (TGF-β) signaling represses the expression of the Bag-of-marbles (Bam) protein, which is important to initiate both male and female gametogenesis, to maintain GSCs and spermatogonia (McKearin and Spradling, 1990; Shivdasani and Ingham, 2003; Schulz et al., 2004). Bam and Benign gonial cell neoplasm (Bgcn) restrict the proliferation of amplifying germ cells during spermatogenesis (Gönczy et al., 1997).

Drosophila spermatogenesis starts with the asymmetrical cell divisions of a GSC and two flanking CySCs (Fig. 1.1B). Their daughters that stay in contact with the hub are maintained as stem cells, and the other daughters, correspondingly named as gonialblasts and cyst cells, displace away from the hub and begin to differentiate. The gonialblast undergoes four rounds of transit-amplifying divisions without complete cytokinesis to

produce 16 spermatogonia, which are connected by intercellular bridges called ring canals (Fuller, 1993). After cessation of mitosis, the spermatogonial cells then progress through premeiotic S phase and switch to a spermatocyte stage, when cells grow in size and most of the gene products needed for the development of spermatocytes and spermatids are transcribed (White-Cooper, 2010). After cell growth and gene expression, the spermatocytes undergo meiotic divisions and a series of cellular rearrangements eventually resulting in 64 elongated spermatids. The developmental compartment of germ cells encased by paired somatic cyst cells is called a cyst. During all stages of cyst formation, the two cyst cells continue to grow tremendously in size and continue to project cytoplasmic extensions to fully enclose the germ cells, preventing them from direct contact with any other cell type. This intimate association between the germline and somatic cells is important for both lineages to proliferate and co-differentiate (Schulz et al., 2002; Sarkar, et al., 2007; reviewed in Zoller and Schulz, 2012). As spermatogenesis takes place, the differentiating germline and cyst cells become progressively displaced along the apical to basal axis of the testis, which defines a well-characterized spatio-temporal order allowing researchers to conduct various phenotypic analyses (Fuller, 1993; Hudson et al., 2013).

Drosophila ovary and oogenesis

An adult *Drosophila* female has paired ovaries (Fig. 1.2A) and each consists of an average of 16 ovarioles (Spradling, 1993), depending on genetic or environmental variation (Wayne et al., 1997). An ovariole normally contains 14 stages of developing oocytes, starting from the most anterior structure called the germarium to the most

posterior egg chamber (Fig. 1.2B). At the end of stage 14, the developed egg passes through the lateral oviduct to enter the common oviduct before exiting via the uterus. The most apical cells in the germarium consist of a distinguishable stack of somatic cells known as the terminal filament (TF) cells. The most posterior TF cell is followed by 5-7 cap cells (CpCs). 2-3 GSCs and 4-6 escort stem cells (ESCs) are anchored to the CpCs (reviewed in Kirilly and Xie, 2007). fs(1)Yb, Piwi and Hedgehog function coordinately in TFs and CpCs to control GSC maintenance (King and Lin, 1999; King et al., 2001; Cox et al., 1998; Cox et al., 2000). BMP signal produced by CpCs directly controls GSC fate (Xie and Spradling, 1998; Xie and Spradling, 2000; Song et al., 2004). E-cadherin mediated GSC anchorage to CpCs is essential for GSC maintenance (Song et al., 2002). The CpC number was shown to be correlated to the GSC number (Xie and Spradling, 2000). Notch signaling is important for formation and maintenance of the GSC microenvironment; overexpression of Delta in the germline or activated Notch in the somatic cells resulted in extra CpCs (Ward et al., 2006; Song et al., 2007).

Drosophila oogenesis starts with the asymmetrical cell division of a GSC (Fig. 1.2C). One of the two daughter cells stays adjacent to the anterior tip of the germarium to retain stem cell identity. The other daughter moves out of the local microenvironment to become a cystoblast (CB), which is encased by the cytoplasmic extensions of ESC daughter cells called the inner germarium sheath cells (IGSCs) or escort cells (ECs) (Decotto and Spradling, 2005). The CB undergoes exactly four rounds of synchronous, incomplete mitotic divisions in an assembly-line fashion, and eventually generates 16 interconnected cystocytes. Bam was shown to be required in the germ cell lineage to promote differentiation (McKearin and Ohlstein, 1995). The groups of developing

cystocytes are called germline cysts. ECs extend thin cytoplasmic extensions that surround cysts, prohibiting any direct germ cell-germ cell contact except between sister cyst cells (King, 1970). It was proposed that ovarian germline cysts interact with ECs in a way that, stationary ECs stretch and periodically break their cytoplasmic extensions to allow cysts to move through and get enclosed by more posterior ECs (Decotto and Spradling, 2005). This idea is different from somatic cyst cells moving along basally associating with the developing germline cells as in the testis. This model has been confirmed by live imaging of the microtubules in cytoplasmic extensions that ECs undergo dramatic shape changes allowing cysts to be passed from one EC to another (Morris and Spradling, 2011). The interaction between soma and germline in *Drosophila* ovary was inferred to share similar mechanisms governing coordinated growth, regeneration and homeostasis (Gilboa and Lehmann, 2006). Conventionally, the germarium is divided into four regions that correspond to the various stages of cyst development (Mahowald and Kambysellis, 1980) (Fig. 1.2D). Region 1, adjacent to the TF, houses the GSCs and 2-4 early stage cysts. Once the 16-cell cyst has formed, it enters region 2A. This region contains 4-7 cysts, within which the cells look the same. By the time that a cyst reaches region 2B, one of the two cells that connects four mitotic sister cells will be specified as an oocyte while the remaining 15 become nurse cells. Meanwhile, the cyst will be enclosed by somatic follicle cells to form an egg chamber that buds off from region 3 (King, 1970).

Figure 1.1: The *Drosophila* testis and spermatogenesis.

(A) A drawing of adult male fly reproductive system (modified from Miller, 1950). Testes are color coded in yellow. AG, accessory gland; SV, seminal vesicle.

(B) A cartoon illustration depicting the arrangement and development of germline and its microenvironmental cells at the apical region of the testis. Note that the dotted line simplified the space occupied by developing cysts containing the growing spermatocytes, which continue approximately halfway through the testis and are followed by bundles of 64 elongated spermatids further down to the basal end of the testis.

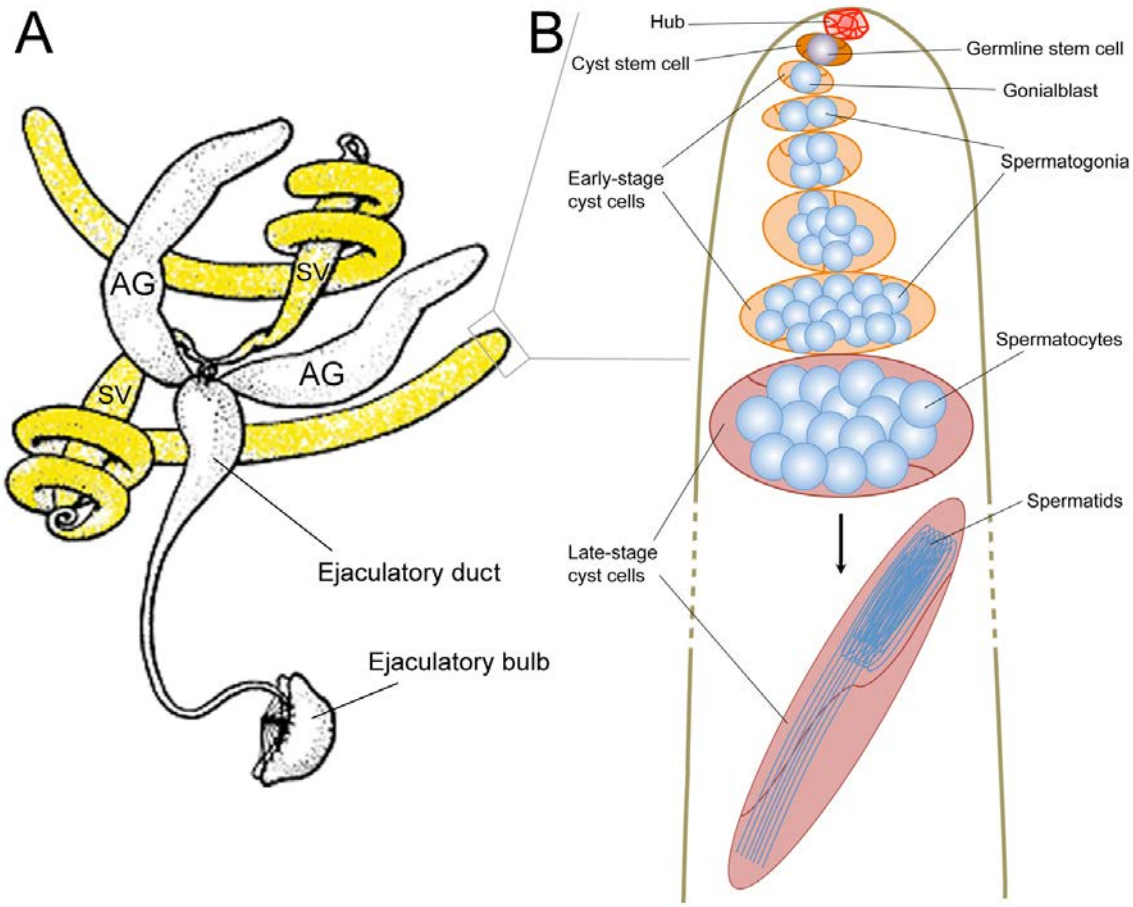
A
AG
SV
AG
SV
Ejaculatory duct
Ejaculatory bulb
B
Hub
Cyst stem cell
Germline stem cell
Gonialblast
Spermatogonia
Early-stage
cyst cells
Spermatocytes
Spermatids
Late-stage
cyst cells

Figure 1.2: The *Drosophila* ovary and oogenesis.

(A) A drawing of a pair of adult fly ovaries (modified from Miller, 1950).

(B) A developing ovariole shows the stages of *Drosophila* oogenesis starting from the germarium followed by the egg chambers (S1-S10), to the oocyte (S14). S7 is the stage at which the spherical egg chamber stretches slightly to be an ovoid, whereas S14 is where the egg is ready to ovulate. G: germarium.

(C) The organization of cells in the germarium. Note that all stages of developing germline cysts are enclosed in somatic cells. CB: cystoblast; CpC: cap cell; DC: developing cystocyte; EC: escort cell; ESC: escort stem cell; FC: follicle cell; GSC: germline stem cell; IGSC: inner germarium sheath cell; O: oocyte; SSC: somatic stem cell; TF: terminal filament.

(D) A drawing demonstrating the female germline cyst formation. The scale at the top indicates the conventional four regions related to the germarium. In the region 2B, a future oocyte highlighted in yellow has been determined.

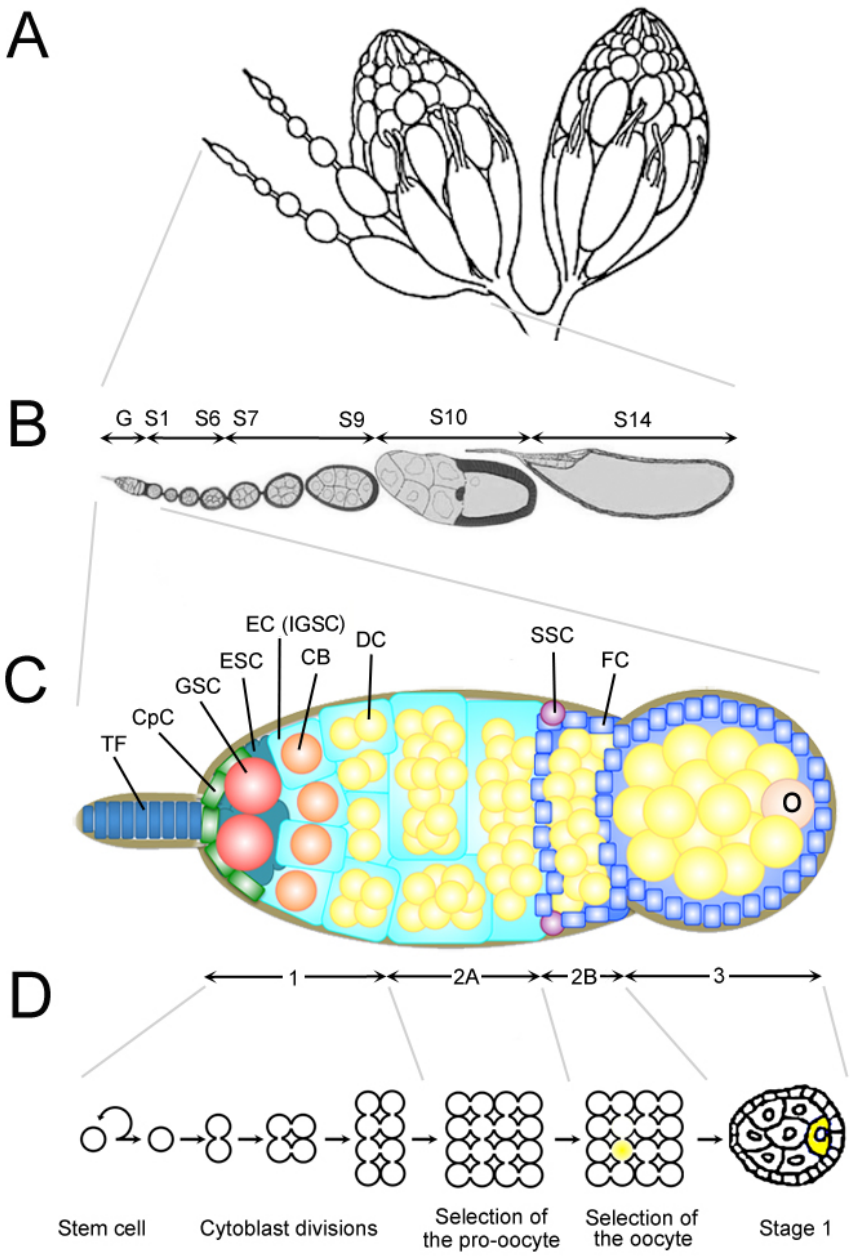
A
B
G S1 S6 S7 S9 S10 S14
C
EC (IGSC)
DC
ESC
CB
SSC
FC
GSC
CpC
TF
O
D
1
2A
2B
3
Stem cell
Cytoblast divisions
Selection of the pro-oocyte
Selection of the oocyte
Stage 1

References

Airiau, K., Mahon, F.X., Josselin, M., Jeanneteau, M., Belloc, F., 2013. PI3K/mTOR pathway inhibitors sensitize chronic myeloid leukemia stem cells to nilotinib and restore the response of progenitors to nilotinib in the presence of stem cell factor. Cell death & disease 4, e827.

Anand, S., Bhartiya, D., Sriraman, K., Patel, H., Manjramkar, D., Bakshi, G., Dhamankar, V., Kurkure, P., 2013. Quiescent Very Small Embryonic-like Stem Cells Resist Oncotherapy and can Restore Spermatogenesis in Germ Cell Depleted Mammalian Testis. Stem cells and development.

Awong, G., Singh, J., Mohtashami, M., Malm, M., La Motte-Mohs, R.N., Benveniste, P.M., Serra, P., Herer, E., van den Brink, M.R., Zuniga-Pflucker, J.C., 2013. Human proT-cells generated in vitro facilitate hematopoietic stem cell-derived T-lymphopoiesis in vivo and restore thymic architecture. Blood 122, 4210-4219.

Barker, N., 2014. Adult intestinal stem cells: critical drivers of epithelial homeostasis and regeneration. Nature reviews. Molecular cell biology 15, 19-33.

Bongso, A., Richards, M., 2004. History and perspective of stem cell research. Best practice & research. Clinical obstetrics & gynaecology 18, 827-842.

Bortin, M.M., 1970. A compendium of reported human bone marrow transplants. Transplantation 9, 571-587.

Calvi, L.M., Adams, G.B., Weibrecht, K.W., Weber, J.M., Olson, D.P., Knight, M.C., Martin, R.P., Schipani, E., Divieti, P., Bringhurst, F.R., Milner, L.A., Kronenberg, H.M., Scadden, D.T., 2003. Osteoblastic cells regulate the haematopoietic stem cell niche. Nature 425, 841-846.

Chandebois, R., 1985. Differentiated epidermal outgrowths in the planarian Dugesia gonocephala: a model for studying cell renewal and patterning in single-layered epithelial tissue. Experimental cell biology 53, 46-58.

Chen, S., Lewallen, M., Xie, T., 2013. Adhesion in the stem cell niche: biological roles and regulation. Development 140, 255-265.

Chitteti, B.R., Cheng, Y.H., Poteat, B., Rodriguez-Rodriguez, S., Goebel, W.S., Carlesso, N., Kacena, M.A., Srour, E.F., 2010. Impact of interactions of cellular components of the bone marrow microenvironment on hematopoietic stem and progenitor cell function. Blood 115, 3239-3248.

Cotsarelis, G., Sun, T.T., Lavker, R.M., 1990. Label-retaining cells reside in the bulge area of pilosebaceous unit: implications for follicular stem cells, hair cycle, and skin carcinogenesis. Cell 61, 1329-1337.

Cox, D.N., Chao, A., Baker, J., Chang, L., Qiao, D., Lin, H., 1998. A novel class of evolutionarily conserved genes defined by piwi are essential for stem cell self-renewal. Genes & development 12, 3715-3727.

Cox, D.N., Chao, A., Lin, H., 2000. piwi encodes a nucleoplasmic factor whose activity modulates the number and division rate of germline stem cells. Development 127, 503-514.

Crittenden, S.L., Bernstein, D.S., Bachorik, J.L., Thompson, B.E., Gallegos, M., Petcherski, A.G., Moulder, G., Barstead, R., Wickens, M., Kimble, J., 2002. A conserved RNA-binding protein controls germline stem cells in Caenorhabditis elegans. Nature 417, 660-663.

Daley, G.Q., Scadden, D.T., 2008. Prospects for stem cell-based therapy. Cell 132, 544-548.

de Haan, G., Van Zant, G., 1997. Intrinsic and extrinsic control of hemopoietic stem cell numbers: mapping of a stem cell gene. The Journal of experimental medicine 186, 529-536.

Decotto, E., Spradling, A.C., 2005. The Drosophila ovarian and testis stem cell niches: similar somatic stem cells and signals. Developmental cell 9, 501-510.

Doetsch, F., Caille, I., Lim, D.A., Garcia-Verdugo, J.M., Alvarez-Buylla, A., 1999. Subventricular zone astrocytes are neural stem cells in the adult mammalian brain. Cell 97, 703-716.

Eckes, B., Krieg, T., 2004. Regulation of connective tissue homeostasis in the skin by mechanical forces. Clinical and experimental rheumatology 22, S73-76.

Fausto, N., Campbell, J.S., 2003. The role of hepatocytes and oval cells in liver regeneration and repopulation. Mechanisms of development 120, 117-130.

Fuller, M. T., 1993. Spermatogenesis in Drosophila., in: Bate, M., Martinez Arias, A. (Ed.), The development of Drosophila melanogaster. Cold Spring Harbor Laboratory Press, Cold Spring Harbor, New York, USA, pp. 71-148.

Gilboa, L., Lehmann, R., 2006. Soma-germline interactions coordinate homeostasis and growth in the Drosophila gonad. Nature 443, 97-100.

Gogishvili, T., Luhder, F., Goebbels, S., Beer-Hammer, S., Pfeffer, K., Hunig, T., 2013. Cell-intrinsic and -extrinsic control of Treg-cell homeostasis and function revealed by induced CD28 deletion. European journal of immunology 43, 188-193.

Gonczy, P., DiNardo, S., 1996. The germ line regulates somatic cyst cell proliferation and fate during Drosophila spermatogenesis. Development 122, 2437-2447.

Gonczy, P., Matunis, E., DiNardo, S., 1997. bag-of-marbles and benign gonial cell neoplasm act in the germline to restrict proliferation during Drosophila spermatogenesis. Development 124, 4361-4371.

Han, Y.L., Wang, S., Zhang, X., Li, Y., Huang, G., Qi, H., Pingguan-Murphy, B., Li, Y., Lu, T.J., Xu, F., 2014. Engineering physical microenvironment for stem cell based regenerative medicine. Drug discovery today 19, 763-773.

Hardy, R.W., Tokuyasu, K.T., Lindsley, D.L., Garavito, M., 1979. The germinal proliferation center in the testis of Drosophila melanogaster. Journal of ultrastructure research 69, 180-190.

Hudson, A.G., Parrott, B.B., Qian, Y., Schulz, C., 2013. A temporal signature of epidermal growth factor signaling regulates the differentiation of germline cells in testes of Drosophila melanogaster. PloS one 8, e70678.

Humphrey, J.D., 2008. Vascular adaptation and mechanical homeostasis at tissue, cellular, and sub-cellular levels. Cell biochemistry and biophysics 50, 53-78.

Jiang, D., Jiang, Z., Zhang, Y., Wang, S., Yang, S., Xu, B., Yang, M., Li, Z., 2014. Effect of Young Extrinsic Environment Stimulated by Hypoxia on the Function of Aged Tendon Stem Cell. Cell biochemistry and biophysics.

Kandyba, E., Kobielak, K., 2014. Wnt7b is an important intrinsic regulator of hair follicle stem cell homeostasis and hair follicle cycling. Stem cells 32, 886-901.

Kawase, E., Wong, M.D., Ding, B.C., Xie, T., 2004. Gbb/Bmp signaling is essential for maintaining germline stem cells and for repressing bam transcription in the Drosophila testis. Development 131, 1365-1375.

Kiger, A.A., Jones, D.L., Schulz, C., Rogers, M.B., Fuller, M.T., 2001. Stem cell self-renewal specified by JAK-STAT activation in response to a support cell cue. Science 294, 2542-2545.

King, F.J., Lin, H., 1999. Somatic signaling mediated by fs(1)Yb is essential for germline stem cell maintenance during Drosophila oogenesis. Development 126, 1833-1844.

King, F.J., Szakmary, A., Cox, D.N., Lin, H., 2001. Yb modulates the divisions of both germline and somatic stem cells through piwi- and hh-mediated mechanisms in the Drosophila ovary. Molecular cell 7, 497-508.

King, R. C., 1970. In Ovarian Development in Drosophila melanogaster. New York: Academic Press.

Kirilly, D., Wang, S., Xie, T., 2011. Self-maintained escort cells form a germline stem cell differentiation niche. Development 138, 5087-5097.

Kirilly, D., Xie, T., 2007. The Drosophila ovary: an active stem cell community. Cell research 17, 15-25.

Leatherman, J.L., Dinardo, S., 2010. Germline self-renewal requires cyst stem cells and stat regulates niche adhesion in Drosophila testes. Nature cell biology 12, 806-811.

Li, L., Xie, T., 2005. Stem cell niche: structure and function. Annual review of cell and developmental biology 21, 605-631.

Liu, A.Y., True, L.D., LaTray, L., Nelson, P.S., Ellis, W.J., Vessella, R.L., Lange, P.H., Hood, L., van den Engh, G., 1997. Cell-cell interaction in prostate gene regulation and cytodifferentiation. Proceedings of the National Academy of Sciences of the United States of America 94, 10705-10710.

Mahowald, A. P. and Kambysellis, M. P., 1980. Oogenesis. In Genetics and Biology of Drosophila 2nd. (eds. M. Ashburner and T. R. F. Wright), pp. 141-223. New York: Academic Press.

Martin, P., 1997. Wound healing--aiming for perfect skin regeneration. Science 276, 75-81.

Maul, T.M., Chew, D.W., Nieponice, A., Vorp, D.A., 2011. Mechanical stimuli differentially control stem cell behavior: morphology, proliferation, and differentiation. Biomechanics and modeling in mechanobiology 10, 939-953.

Maximow A. The Lymphocyte as a stem cell common to different blood elements in embryonic development and during the post-fetal life of mammals (1909). Originally in German: Folia Haematologica 8.1909, 125-134. English translation: Cell Ther Transplant. 2009,1:e.000032.01. doi:10.3205/ctt-2009-en-000032.01

McKearin, D., Ohlstein, B., 1995. A role for the Drosophila bag-of-marbles protein in the differentiation of cystoblasts from germline stem cells. Development 121, 2937-2947.

McKearin, D.M., Spradling, A.C., 1990. bag-of-marbles: a Drosophila gene required to initiate both male and female gametogenesis. Genes & development 4, 2242-2251.

Miller, A, 1950. The internal anatomy and histology of the imago of Drosophila melanogaster. In M. Demerec, editor, Biology of Drosophila. Cold Spring Harbor Laboratory Press, facsimile edition, 1994. Copyright 1994 by Cold Spring Harbor Laboratory Press.

Miltiadous, P., Kouroupi, G., Stamatakis, A., Koutsoudaki, P.N., Matsas, R., Stylianopoulou, F., 2013. Subventricular zone-derived neural stem cell grafts protect against hippocampal degeneration and restore cognitive function in the mouse following intrahippocampal kainic acid administration. Stem cells translational medicine 2, 185-198.

Morris, L.X., Spradling, A.C., 2011. Long-term live imaging provides new insight into stem cell regulation and germline-soma coordination in the Drosophila ovary. Development 138, 2207-2215.

Ninomiya, M., Harada, N., Shiotani, S., Hiroshige, S., Minagawa, R., Soejima, Y., Suehiro, T., Nishizaki, T., Shimada, M., Sugimachi, K., 2003. Hepatocyte growth factor and transforming growth factor beta1 contribute to regeneration of small-for-size liver graft immediately after transplantation. Transplant international : official journal of the European Society for Organ Transplantation 16, 814-819.

North, T.E., Goessling, W., Walkley, C.R., Lengerke, C., Kopani, K.R., Lord, A.M., Weber, G.J., Bowman, T.V., Jang, I.H., Grosser, T., Fitzgerald, G.A., Daley, G.Q., Orkin, S.H., Zon, L.I., 2007. Prostaglandin E2 regulates vertebrate haematopoietic stem cell homeostasis. Nature 447, 1007-1011.

Nutt, S.L., Kallies, A., Belz, G.T., 2008. Blimp-1 connects the intrinsic and extrinsic regulation of T cell homeostasis. Journal of clinical immunology 28, 97-106.

Palasz, A., Kaminski, M., 2009. Stem cell niche in the Drosophila ovary and testis; a valuable model of the intercellular signalling relationships. Advances in medical sciences 54, 143-149.

Palmer, T.D., Takahashi, J., Gage, F.H., 1997. The adult rat hippocampus contains primordial neural stem cells. Molecular and cellular neurosciences 8, 389-404.

Parekkadan, B., Berdichevsky, Y., Irimia, D., Leeder, A., Yarmush, G., Toner, M., Levine, J.B., Yarmush, M.L., 2008. Cell-cell interaction modulates neuroectodermal specification of embryonic stem cells. Neuroscience letters 438, 190-195.

Potten, C.S., Owen, G., Booth, D., 2002. Intestinal stem cells protect their genome by selective segregation of template DNA strands. Journal of cell science 115, 2381-2388.

Prindull, G., Prindull, B., Meulen, N., 1978. Haematopoietic stem cells (CFUc) in human cord blood. Acta paediatrica Scandinavica 67, 413-416.

Przybyla, L.M., Voldman, J., 2012. Attenuation of extrinsic signaling reveals the importance of matrix remodeling on maintenance of embryonic stem cell self-renewal. Proceedings of the National Academy of Sciences of the United States of America 109, 835-840.

Purton, L.E., Scadden, D.T., 2008. The hematopoietic stem cell niche, StemBook, Cambridge (MA).

Ramalho-Santos, M., Willenbring, H., 2007. On the origin of the term "stem cell". Cell stem cell 1, 35-38.

Reinke, R., Zipursky, S.L., 1988. Cell-cell interaction in the Drosophila retina: the bride of sevenless gene is required in photoreceptor cell R8 for R7 cell development. Cell 55, 321-330.

Reiter, S., Crescenzi, M., Galliot, B., Buzgariu, W., 2012. Hydra, a versatile model to study the homeostatic and developmental functions of cell death. The International journal of developmental biology 56, 593-604.

Sarkar, A., Parikh, N., Hearn, S.A., Fuller, M.T., Tazuke, S.I., Schulz, C., 2007. Antagonistic roles of Rac and Rho in organizing the germ cell microenvironment. Current biology : CB 17, 1253-1258.

Scadden, D.T., 2006. The stem-cell niche as an entity of action. Nature 441, 1075-1079.

Schofield, R., 1978. The relationship between the spleen colony-forming cell and the haemopoietic stem cell. Blood cells 4, 7-25.

Schulz, C., Kiger, A.A., Tazuke, S.I., Yamashita, Y.M., Pantalena-Filho, L.C., Jones, D.L., Wood, C.G., Fuller, M.T., 2004. A misexpression screen reveals effects of bag-of-marbles and TGF beta class signaling on the Drosophila male germ-line stem cell lineage. Genetics 167, 707-723.

Schulz, C., Wood, C.G., Jones, D.L., Tazuke, S.I., Fuller, M.T., 2002. Signaling from germ cells mediated by the rhomboid homolog stet organizes encapsulation by somatic support cells. Development 129, 4523-4534.

Shen, Q., Goderie, S.K., Jin, L., Karanth, N., Sun, Y., Abramova, N., Vincent, P., Pumiglia, K., Temple, S., 2004. Endothelial cells stimulate self-renewal and expand neurogenesis of neural stem cells. Science 304, 1338-1340.

Shivdasani, A.A., Ingham, P.W., 2003. Regulation of stem cell maintenance and transit amplifying cell proliferation by tgf-beta signaling in Drosophila spermatogenesis. Current biology : CB 13, 2065-2072.

Silva, H., Conboy, I.M., 2008. Aging and stem cell renewal, StemBook, Cambridge (MA).

Song, X., Call, G.B., Kirilly, D., Xie, T., 2007. Notch signaling controls germline stem cell niche formation in the Drosophila ovary. Development 134, 1071-1080.

Song, X., Wong, M.D., Kawase, E., Xi, R., Ding, B.C., McCarthy, J.J., Xie, T., 2004. Bmp signals from niche cells directly repress transcription of a differentiation-promoting gene, bag of marbles, in germline stem cells in the Drosophila ovary. Development 131, 1353-1364.

Song, X., Zhu, C.H., Doan, C., Xie, T., 2002. Germline stem cells anchored by adherens junctions in the Drosophila ovary niches. Science 296, 1855-1857.

Spradling, A.C., 1993. Developmental genetics of oogenesis. In The development of Drosophila melanogaster 1st. (eds. M. Bate and A. M. Arias). Cold Spring Harbor, NY: Cold Spring Harbor Laboratory Press, pp. 3-4.

Stevens, L.C., 1958. Studies on transplantable testicular teratomas of strain 129 mice. Journal of the National Cancer Institute 20, 1257-1275.

Tazuke, S.I., Schulz, C., Gilboa, L., Fogarty, M., Mahowald, A.P., Guichet, A., Ephrussi, A., Wood, C.G., Lehmann, R., Fuller, M.T., 2002. A germline-specific gap junction protein required for survival of differentiating early germ cells. Development 129, 2529-2539.

Tulina, N., Matunis, E., 2001. Control of stem cell self-renewal in Drosophila spermatogenesis by JAK-STAT signaling. Science 294, 2546-2549.

Verdi, J.M., Groves, A.K., Farinas, I., Jones, K., Marchionni, M.A., Reichardt, L.F., Anderson, D.J., 1996. A reciprocal cell-cell interaction mediated by NT-3 and neuregulins controls the early survival and development of sympathetic neuroblasts. Neuron 16, 515-527.

Ward, E.J., Shcherbata, H.R., Reynolds, S.H., Fischer, K.A., Hatfield, S.D., Ruohola-Baker, H., 2006. Stem cells signal to the niche through the Notch pathway in the Drosophila ovary. Current biology : CB 16, 2352-2358.

Wayne, M. L., Hackett, J. B. and Mackay, T. F. C., 1997. Quantitative Genetics of Ovariole Number in Drosophila melanogaster: I. Segregating Variation and Fitness. Evolution 51, 1156-1163.

White-Cooper, H., 2010. Molecular mechanisms of gene regulation during Drosophila spermatogenesis. Reproduction 139, 11-21.

Xie, T., Spradling, A.C., 1998. decapentaplegic is essential for the maintenance and division of germline stem cells in the Drosophila ovary. Cell 94, 251-260.

Xie, T., Spradling, A.C., 2000. A niche maintaining germ line stem cells in the Drosophila ovary. Science 290, 328-330.

Yeh, J.R., Zhang, X., Nagano, M.C., 2011. Wnt5a is a cell-extrinsic factor that supports self-renewal of mouse spermatogonial stem cells. Journal of cell science 124, 2357-2366.

Zhang, J., Niu, C., Ye, L., Huang, H., He, X., Tong, W.G., Ross, J., Haug, J., Johnson, T., Feng, J.Q., Harris, S., Wiedemann, L.M., Mishina, Y., Li, L., 2003. Identification

of the haematopoietic stem cell niche and control of the niche size. Nature 425, 836-841.

Zoller, R., Schulz, C., 2012. The Drosophila cyst stem cell lineage: Partners behind the scenes? Spermatogenesis 2, 145-157.

Zon, L.I., 2008. Intrinsic and extrinsic control of haematopoietic stem-cell self-renewal. Nature 453, 306-313.

Zou, W.W., Xiao, H.P., Gu, M.N., Liu, K.X., Liu, Z.Q., 2013. Propofol induces rat embryonic neural stem cell apoptosis by activating both extrinsic and intrinsic pathways. Molecular medicine reports 7, 1123-1128.

CHAPTER 2

ECDYSONE SIGNALING OPPOSES EPIDERMAL GROWH FACTOR SIGNALING IN REGULATING CYST DIFFERENTIATION IN THE MALE GONAD OF *DROSOPHILA MELANOGASTER*[1]

[1] Qian Y, Dominado N, Zoller R, Ng C, Kudyba K, Siddall NA, Hime GR, Schulz C. 2014. *Developmental Biology* 394(2), 217-227. Reprinted here with permission of publisher.

Abstract

The development of stem cell daughters into the differentiated state normally requires a cascade of proliferation and differentiation steps that are typically regulated by external signals. The germline cells of most animals, in specific, are associated with somatic support cells and depend on them for normal development. In the male gonad of *Drosophila melanogaster*, germline cells are completely enclosed by cytoplasmic extensions of somatic cyst cells, and these cysts form a functional unit. Signaling from the germline to the cyst cells via the Epidermal Growth Factor Receptor (EGFR) is required for germline enclosure and has been proposed to provide a temporal signature promoting early steps of differentiation. A temperature-sensitive allele of the EGFR ligand Spitz (Spi) provides a powerful tool for probing the function of the EGRF pathway in this context and for identifying other pathways regulating cyst differentiation via genetic interaction studies. Using this tool, we show that signaling via the Ecdysone Receptor (EcR), a known regulator of developmental timing during larval and pupal development, opposes EGF signaling in testes. In *spi* mutant animals, reducing either Ecdysone synthesis or the expression of Ecdysone signal transducers or targets in the cyst cells resulted in a rescue of cyst formation and cyst differentiation. Despite of this striking effect in the *spi* mutant background and the expression of EcR signaling components within the cyst cells, activity of the EcR pathway appears to be dispensable in a wildtype background. We propose that EcR signaling modulates the effects of EGFR signaling by promoting an undifferentiated state in early stage cyst cells.

Introduction

In many metazoan tissues, highly specialized cells need to be constantly reproduced. These cells are derived from the activity of adult stem cells. Over the past decade, considerable progress has been made in our understanding of how these stem cells are organized. It has become clear that the specification and maintenance of most stem cell populations depend on signals from their natural cellular microenvironment (Conover and Notti, 2008; de Rooij, 2009; Ju et al., 2007; Takakura, 2012). For example, blood stem cells in the bone marrow depend on signals from the mesenchymal osteoblasts, including angiopoietin, thrombopoietin, and the chemokine Cxcl12 (Luis et al., 2012; Park et al., 2012). Similarly, gut and skin stem cells depend on signaling via the highly conserved Wnt pathway (Choi et al., 2013; Krausova and Korinek, 2014; Lim and Nusse, 2013). Less is known about the mechanisms that regulate differentiation of stem cell daughters. When cultured, embryonic stem cells can be induced to differentiate into plethora of cell types (Keller, 2005). Comparably few signals that act *in situ* have been identified. In mouse skin, conserved molecules such as p63, Mitogen Activated Protein Kinase (MAPK), Notch, and β-Catenin are essential for skin cell development (Blanpain and Fuchs, 2006; Sotiropoulou and Blanpain, 2012).

The male gonad of *Drosophila melanogaster* provides an excellent model for studying the signaling events regulating differentiation processes. The testis houses two distinct stem cell lineages, a germline stem cell (GSC) lineage and a somatic stem cell lineage, called the cyst stem cell (CySC) lineage. Both stem cell populations are attached to a group of somatic cells at the apical tip, the hub cells, which serve as an organizing center. Each GSC is enclosed by cytoplasmic extensions from two CySCs that extend

around the GSC and into the hub. The divisions of GSCs and CySCs are formative, producing one daughter that remains a stem cell and one daughter that becomes a gonialblast or a cyst cell, respectively. Gonialblasts subsequently become fully enclosed by the cytoplasmic extensions of two cyst cells. Analogous to mammalian stem cell populations, *Drosophila* gonialblasts first undergo mitotic transit amplifying divisions before they differentiate into sperm. Throughout this process, the cyst cells continue to enclose the germline cells and co-differentiate with them (Fuller, 1993; Hardy et al., 1979; Zoller and Schulz, 2012). This developmental sequence is tightly regulated by signaling between the two lineages. For example, the exit of the germline cells from amplifying mitotic divisions depends on Transforming Growth Factor-β signaling in the surrounding cyst cells (Bunt and Hime, 2004; Matunis et al., 1997).

The EGF signaling pathway is involved in embryonic development, cancer, stem cell proliferation, and gametogenesis in numerous species (Moghal and Sternberg, 2003; Normanno et al., 2006; Parrott et al., 2012; Shilo, 2003; Strand and Micchelli, 2013; Wiley et al., 1995). The enclosure of the germline cells by the cyst cells is regulated via EGF signaling (Sarkar et al., 2007; Schulz et al., 2002). Germline cells signal to the cyst cells via Spi, a transmembrane protein that is activated by the germline-specific protease Stet. Once cleaved, Spi stimulates the EGFR on the cyst cells. Mutations in either *spi*, *stet*, or *Egfr* disrupt germline enclosure and result in a failure of the germline cells to differentiate. Testes from *spi* or *stet* mutant animals are tiny compared to wildtype testes and contain tumor-like accumulations of proliferating early-stage germline cells (Kiger et al., 2000; Schulz et al., 2002; Urban et al., 2002). Recent findings further show that the progression of the cysts (germline and surrounding cyst cells) through the early stages of

spermatogenesis is also promoted by EGF signaling. By studying genetic backgrounds in which EGF signaling was reduced but not completely abolished, we were able to show that enclosed germline cells depend on continued EGF signaling for progressing through all four rounds of transit amplifying divisions. Conversely, an increase in EGF signaling caused the cysts to initiate terminal differentiation prior to completing all four rounds of mitosis. These results implied that EGF signaling provides an instructive signal, or a temporal signature that guides the progression of the cysts through the early stages of spermatogenesis (Fuller, 1993; Hudson et al., 2013).

Factors modulating EGF signaling in the gonad have been identified by virtue of their genetic interactions with the temperature-sensitive allele, $spi^{77\text{-}20}$. For example, reducing the expression of the small monomeric GTPase, *rac1*, in cyst cells exacerbated the germline enclosure defects observed in testes of $spi^{77\text{-}20}$ mutant males (*spi/spi*-testes) suggesting that Rac acts downstream of the EGFR. Conversely, reducing the expression of the small monomeric GTPase, *rho1*, in the cyst cells had the opposite effect on *spi/spi*-testes, rescuing the germline enclosure defects. This indicated that Rho1 acts in a pathway opposing EGF for germline enclosure. In conjunction with ultrastructural data and protein binding studies, these findings suggested that EGF signaling from the germline cells organizes a differential of Rac- and Rho-activities in the cyst cells, leading to polarization of the actin cytoskeleton and directional growth around the germline cells (Sarkar et al., 2007).

EcR signaling regulates the timing of key developmental transition, such as molting and metamorphosis. The ligands of the pathway, the Ecdysteroids, are polyhydroxylated compounds that are synthesized from dietary cholesterol in a multi-step

biosynthetic process that produces 20-hydroxyecdysone (20E). During larval development, pulses of ecdysone and other ecdysteroids are released from the prothoracic gland portion of the ring gland and further converted to 20E, the most active form of the ligand, in peripheral tissues (Warren et al., 2006). The prothoracic gland degenerates early in pupal development and the source ecdysteroids in adult flies is not clear (Dai and Gilbert, 1991). However, 20E is still detectable and active in both the adult male and female (Brownes, 1984; Schwedes et al., 2011). In the adult male, 20E signaling has been implicated in long-term memory and male-to-male courtship (Ganter et al., 2011; Simon et al., 2006). In the adult female, 20E signaling is essential for oogenesis and for regulating the wake-sleep cycle (Carney and Bender, 2000; Ishimoto and Kitamoto, 2010; Ishimoto et al., 2009; Schwedes and Carney, 2012).

The EcR is a member of the nuclear steroid receptor superfamily that contains DNA- and hormone-binding domains, indicating that it is a ligand-regulated transcription factor. In order to bind to DNA, EcR forms a heterodimer with Ultraspiracle (Usp), a homologue of the human retinoid X receptor (RXR). This complex binds to 20E and also recruits co-regulators, such as Hsp70/90, Taiman (Tai), and Trithorax-related (Bai et al., 2000; Koelle et al., 1991; Sedkov et al., 2003; Yao et al., 1993). EcR can bind to DNA independent of ligand but displays the highest transcriptional activation when bound to 20E (Braun et al., 2009; Buszczak and Segraves, 1998; Dela Cruz et al., 2000; Hall and Thummel, 1998). Within DNA, EcR binds to specific target sites, known as ecdysone response elements (Perera et al., 2005; Riddihough and Pelham, 1987). During larval development, the EcR complex induces expression of a small group of early regulatory genes. During embryonic and larval development, the complex induces the expression of

Eip74 and Eip75, and at pupariation, also the expression of Broad-Complex (BrC). The protein products of these "early genes" repress their own transcription and also activate or induce the transcription of a larger set of downstream "early-late" and "late-late" genes, producing a genetic hierarchy of transcription (Ashburner and Richards, 1976).

Here, we identify a novel function for EcR signaling in testes, where it acts antagonistically to EGF signaling. We show that reducing the production of 20E restored cyst formation and cyst development in *spi/spi*-testes. Furthermore, EcR signaling components are expressed in cyst cells and reducing EcR signaling specifically in cyst cells of *spi/spi*-testes also resulted in a rescue of the defects caused by the $spi^{77\text{-}20}$ mutation. While EcR signaling is dispensable for normal development of the cysts in a wildtype background, overexpression of EcR in cyst cells induced cell death. On the basis of our observations, we propose that EcR modulates cyst development in the male gonad of *Drosophila* by promoting an undifferentiated state.

Material and methods

Fly Stocks & UAS-Gal4 expression Studies

All fly stocks in this study were raised and maintained on standard cornmeal molasses medium at room temperature. Fly stocks used in this study include $spi^{77\text{-}20}$ (Sarkar et al., 2007), the cyst cell drivers EyaA3-*gal4* (Leatherman and Dinardo, 2008) and C587-*gal4* (Hrdlicka et al., 2002), and UAS-*dnEcR* (Cherbas et al., 2003). The following flies carrying RNAi constructs, alleles of 20E synthesis genes, and overexpression constructs were obtained from the Bloomington Stock Center (The Flybase Consortium, 2003): UAS-$EcRi^{97}$ [BL#9326]; UAS- $EcRi^{104}$ [BL#9327]; UAS-

Uspi$^{TRiP.HMS01620}$ [BL#36729]; UAS-*Eip74EFi*$^{TRiP.JF02515}$ [BL#29353]; UAS-*BrCi*$^{TRiP.JF02585}$ [BL#27272]; UAS-*Taii*$^{TRiP.HMS00673}$ [BL32885]; *spo*^{1} [BL#3276]; *dib*^{2} [BL#2776]; *sad*^{1} [BL#2087]; UAS-*dcr* [BL#24651]; UAS-*EcR-B1* [BL#6469]; UAS-*EcR-B2* [BL#6468]; FRT-*tai*^{61G1} [BL#6379]; *EcR*^{M554fs} [BL#4894]; *EcR*^{V559fs} [BL#4901]; *EcR*^{A483T} [BL#5799]; *EcR*^{Q50ST} [BL#4895]; *EcR*^{W53ST} [BL#5604]. All *spi* mutant flies were raised and maintained at 26.5 °C. Flies for overexpression of *EcR* and expression of RNAi in otherwise wildtype animals were raised at 18 °C and shifted to 29 °C as adult for seven to ten days. *P*-values were calculated using Fisher's and chi-squared exact test.

Molecular Techniques

Total RNA from testes was isolated and purified using TRIzol Reagent with the PureLink RNA Mini Kit as described by the manufacturer. First strand cDNA was generated using Oligo-dT and random hexamer primers provided in Invitrogen SuperScript III First-Strand Synthesis System for RT-PCR kit. Gene-specific PCR primers were designed using GeneRunner oligo analysis. PCR reactions were run on 1% agarose gel to purify products, which were then excised and purified using the QIAquick Gel Extraction Kit and used as a template for secondary PCR to further amplify products and then sequenced by an Applied Biosystem 3730xl 96-capillary DNA Analyzer for Sanger sequencing at the Georgia Genomics Facility. Forward and reverse primers for RT-PCR were designed from neighboring exons, ensuring that products obtained were from RNA and not genomic contamination. Additionally, when products obtained from RT-PCR were sequenced, we noted no intronic sequences present. The following primers were used in this study:

Eip74 F: 5′-CGCACACAGAAACTACACGAC-3′

Eip74 R: 5′-CGGATGAGAGTGCGGATGTGAG-3′

Eip75 F: 5’-GATGGCCAGCAGAACAAGTCGC-3’

Eip75 R: 5′-CTTGTAGGCCTCGTCCATCAGC-3′

BrC F: 5′-GCAGAGGACACACACAGCCATC-3′

BrC R: 5′-GTCGTTGGCATTGGCATTGTTG-3′

EcR-B1 F: 5′-CGCGCAGACAACCATCATTCC-3′

EcR-B1 R: 5′-CTTCGCATCGCAGCTTTCGTTC-3′

Usp F: 5′-CAGCAGTATCCGCCTAACCATC-3′

Usp R: 5′-CGACTGTGGAATAGGGACCAA-3′

Immunofluorescence and microscopy

Testes were dissected and processed for immuno-staining as previously described (Schulz et al., 2002). The following hybridoma/monoclonal antibodies were obtained from the Developmental Studies Hybridoma Bank, developed under the auspices of the NICHD, and maintained by the University of Iowa, Department of Biological Sciences, Iowa City, IA 52242: mouse α-EcR (Aq10.2) [1:10], mouse α-Eya (10H6) [1:10], and mouse α-BrC (25E9.D7) [1:10]. Goat α-Vasa [1:500] and rabbit α-Arm [1:500] was obtained from Santa Cruz Biotechnology. Mouse α-Usp [1:200, a gift from Dr. Rosa Barrio]; guinea pig α-Tj [1:5000, a gift from Dr. Dorothea Godt]; and rabbit α-Tai [1:2000, a gift from Dr. Denise Montell]. Alexa-488-, Cy3-, and Cy5-conjugated secondary antibodies were used at 1:1000 (Invitrogen). Acridine Orange [1.6:100000] was obtained from Sigma. Tissues were embedded in Vectashield (Vector Laboratories)

and observed using a Zeiss Axiophot microscope in fluorescent microscopy. Images were taken with a CCD camera using an Apotome and Axiovision Rel Software.

Results

Reducing 20E production restored germline differentiation in spi/spi-testes

To investigate a genetic interaction between EcR and EGF signaling, we first tested if heterozygous mutations in genes encoding proteins required for 20E synthesis attenuate the germline differentiation defects in a $spi^{77\text{-}20}$ background. In wildtype, developing cysts of germline cells and cyst cells are always arranged in a spatio-temporal order along the apical to basal axis. When testes are stained with the DNA-dye, 4', 6-Diamidino-2-Phenylindole (DAPI), different stages of germline cells can be identified based on their nuclear morphology: early-stage germline cells (GSCs, gonialblasts, and their transit amplifying daughters, the spermatogonia) have small, brightly stained nuclei (Fig. 2.1A-A', arrowhead) and they are found exclusively in the apical region (Fig. 2.1A); post-mitotic germline cells, the spermatocytes, have larger, less brightly stained nuclei (Fig. 2.1A-A', small arrows) and are located in the apical region of the testis basal to the spermatogonia; spermatids are found at the basal end and have sickle-shaped nuclei (Fig. 2.1A, large arrow).

spi/*spi*-testes display phenotypes of differing severity dependent on the temperature at which animals are raised and maintained. When raised at 18 °C, *spi*/*spi*-testes appear normal but, when raised at 26.5 °C, the majority of the *spi*/*spi*-testes are tiny and filled with small, bright DAPI-stained nuclei (Fig. 2.1B, arrowheads) (Sarkar et al., 2007). When we introduced single mutant copies of various 20E biosynthetic genes into

the *spi*$^{77\text{-}20}$ background, the testes of most animals were longer and contained differentiating germline cells (spermatocytes and spermatids). To quantify the effects of reduced 20E production testes were binned into one of three phenotypic groups: Type I testes (Fig. 2.1B) were tiny and contained only small, bright DAPI-stained nuclei, indicative of early-stage germline cells; Type II testes (Fig. 2.1C) were small and contained small, bright DAPI-stained nuclei as well as large, less brightly DAPI-stained nuclei, indicative of early-stage germline cells and spermatocytes; Type III testes (Fig. 2.1D) were long and contained germline cells at all stages of spermatogenesis; small, brightly DAPI-stained nuclei, large, less brightly DAPI-stained nuclei, and sickle-shaped nuclei. However, Type III testes did not appear wildtype, as they still contained clusters of over-proliferating germline cells (Fig. 2.1D), small arrowheads) due to the presence of the *spi*-mutation.

As expected, all wildtype testes were of Type III and 74% of the *spi/spi*-testes were of Type I (Table 1). A detailed comparison made apparent that reduction of either *spook* (*spo*), *disembodied* (*dib*), or *shadow* (*sad*) from the *spi*$^{77\text{-}20}$ background significantly reduced the frequency of Type I testes (Fig. 2.1E, Table 1). These results suggest that 20E signaling opposes EGF signaling in promoting germline differentiation.

Components of EcR signaling were expressed in the cyst cells of adult testes

We next examined whether components of the EcR signaling pathway (Fig. 2.2A) were expressed in testes. To detect components and targets of EcR signaling at the level of RNA transcription, we amplified transcripts from testes dissected from adult wildtype animals by Reverse Transcriptase Polymerase Chain Reaction (RT-PCR). When primers

specific for *Eip74*, *Eip75*, *BrC*, the B1 isoform of *EcR* (*EcR-B1*), and *Usp* were used in PCR reactions with testes cDNA as a template, we obtained products of the expected sizes (Fig. 2.2B). Sequencing of these products confirmed the identity of these amplicons. In order to determine whether protein products of these genes are present in cyst cells, we employed commercially available antibodies specific for EcR, Usp, Tai, and BrC in immunofluorescence detection. As a counterstain, antibodies against Traffic jam (Tj) and Eyes absent (Eya) were used. Tj marks the nuclei of early-stage cyst cell nuclei, while Eya is expressed at increasing levels in early-stage cyst cell nuclei and at high levels in all late-stage cyst cell nuclei (Fabrizio et al., 2003; Li et al., 2003).

We found that EcR signaling components were expressed in cyst cells. Antibodies specific for isoform EcR-A were primarily detected in the spermatocytes (data not shown), while antibodies against the isoform EcR-B1 decorated the nuclei of Tj-positive cyst cells (Fig. 2.2C-C'', arrowhead) as well as Tj-negative cyst cells (Fig. 2.2C-C'', arrows). Usp and Tai were also expressed in early- and late-stage cyst cell nuclei, with a clear co-localization of Usp (Fig. 2.2D-D'', arrows) and Tai (Fig. 2.2E-E'', arrows) with Eya. BrC, in contrast, specifically localized to Tj-positive cyst cell nuclei (Fig. 2.2F-F'', arrowhead) but not to Tj-negative cyst cell nuclei, suggesting that EcR signaling is most active at the apical tip. The BrC expression pattern was not changed in *spi/spi*-testes (Fig. 2.2G-G'').

Reducing EcR signaling in cyst cells rescued spi/spi-testes

Since the EcR pathway appears to be active in cyst cells of wildtype and *spi/spi*-testes, we next assessed whether reducing the activity of EcR signaling components specifically in cyst cells of *spi/spi*-testes restored germline differentiation. Towards this

aim, we expressed RNA-Interference (RNAi) constructs targeting components of the pathway with the UAS-*gal4* system (Brand and Perrimon, 1993; Phelps and Brand, 1998). To confine the expression of the RNA hairpins to cyst cells, the cyst cell-specific Eya-*gal4* Gal4 transactivator line was used. A transgene of the Dicer-2 enzyme (UAS-*dcr*), which is involved in the RNAi silencing mechanism, was co-expressed along with RNA hairpin constructs in order to enhance the production of small interfereing RNAs (Dietzl et al., 2007). Expressing RNAi constructs against *EcR, Usp, BrC*, and *Eip74* in cyst cells of *spi/spi*-testes caused a decrease in the percentage of Type I testes (Fig. 2.3, Table 1) and these changes were highly statistically significant (Fig. 2.3, asterisks). Conversely, expression of the RNAi constructs in germline cells of *spi/spi*-testes had no effect on the phenotype (data not shown). Considering the substantial rescue of *spi/spi*-testes by reducing any of the EcR signaling components or targets in cyst cells, we conclude that EcR signaling antagonizes the differentiation-inducing EGF signal within the cyst cells.

Reducing EcR signaling restored cyst cell differentiation in spi/spi-testes

Since proper germline differentiation depends cyst cells, we next compared how many cyst cells continued to develop in *spi/spi*-testes and *spi/spi*-testes with reduced 20E signaling. In a wildtype testis, only the apical region that houses the early-stage germline cells (Fig. 2.4A, arrowhead) contains Tj-positive early-stage cyst cell nuclei (red in Fig. 2.4A'), while the remainder of the testis contains late-stage Eya-positive cyst cell nuclei (green in Fig. 2.4A'). The cyst cell cytoplasmic extensions around the germline cells can

be visualized using the membrane marker anti-Armadillo (Arm) and they appear as a net-like pattern in wildtype testes (green in Fig. 2.4B).

Type I *spi/spi*-testes, filled with small, brightly DAPI-stained nuclei (Fig. 2.4C), contained both Tj-positive and Eya-positive cyst cell nuclei (Fig. 2.4C'). However, it appeared that more Tj-positive nuclei and fewer Eya-positive nuclei were present than in wildtype testis (compare Fig. 2.4C' to Fig. 2.4A'). This suggests that differentiation of the cyst cells was delayed upon strong reduction of EGF signaling. Furthermore, the cyst cells in *spi/spi*-testes did not form cytoplasmic extensions around the germline cells as evident by a lack of the Arm-positive net-like pattern (Fig. 2.4D, note that Arm was still detected in the apical hub cells). The lack of cytoplasmic extensions in *spi/spi*-testes is consistent with previous observations (Sarkar et al., 2007). Testes from *spi/spi* mutant animals that were also heterozygous for a mutation in either of the 20E biosynthetic genes (*spi/spi* + reduced 20E-testes) appeared to contain fewer Tj-positive and more Eya-positive cyst cell nuclei than *spi/spi*-testes (compare Fig. 2.4E' to Fig. 2.4C'). To quantify this effect, we counted Tj and Eya-positive nuclei in the median focal plane of wildtype, *spi/spi*, and *spi/spi* + reduced 20E-testes (Table 2). The substantial decrease in early-stage, Tj-positive cyst cells in *spi/spi* + reduced 20E-testes compared to *spi/spi*-testes suggests that reducing EcR signaling enables the cyst cells in *spi/spi*-testes to differentiate into a later stage. In addition, Arm-positive cytoplasmic extensions were apparent (Fig. 2.4F, arrows) in all Type II and Type III *spi/spi* + reduced 20E-testes, revealing that germline enclosure was at least partially restored. The same effects on cyst cell differentiation were observed upon expression of RNAi-constructs against EcR signaling components specifically in the cyst cells of *spi/spi*-testes (data not shown). We

conclude that, in *spi/spi*-testes, EcR signaling is limiting the ability of germline and cyst cells to enter the differentiation program.

High levels of EcR signaling caused cyst death

Unexpectedly, none of the RNAi constructs that restored cyst differentiation in *spi/spi*-testes caused defects in germline enclosure, germline proliferation, or cyst differentiation when expressed in cyst cells of otherwise wildtype testes. The testes appeared normal by anatomy and the males were fertile, even though the RNAi hairpin constructs disrupted oogenesis in the female siblings (data not shown). Likewise, cysts of testes from animals carrying temperature sensitive alleles of the EcR and shifted to restrictive temperatures for several days, or cysts from animals expressing dominant negative versions of EcR in the cyst cells, or cysts lacking Tai function upon induction of cyst cell clones using mosaic analysis proceeded through the early stages of differentiation normally (data not shown). These findings agree with previous studies suggesting that EcR signaling is dispensable for spermatogenesis (Morris and Spradling, 2012) but are surprising considering the strong interaction of EGFR and EcR signaling in this process.

Next, we investigated whether it is possible to induce a phenotype in otherwise wildtype testes by overexpressing the *EcR* in cyst cells. Indeed, overexpression of the isoforms *EcR-B1* and *EcR-B2* (cyst cell-*EcR-B*-testes), but not of isoform *EcR-A*, using two different Gal4-transactivators (Eya-*gal4* and C587-*gal4*) had a drastic effect. When wildtype testes were labeled with DAPI and the germline marker anti-Vasa, small early-stage germline cells were seen at the tip (Fig. 2.5A, arrowhead), larger spermatocytes

were found basal to the early-stage germline cells and along the testis coil (Fig. 2.5A and C, small arrows), and spermatids with sickle-shaped nuclei were apparent at the base (Fig. 2.5A, large arrow, n=100). Cyst cell-*EcR-B*-testes were much thinner than control testes and contained few cysts, which were mostly found in the apical region (Fig. 2.5B, arrowhead and small arrows, n>50). The remainder of the cyst cell-*EcR-B*-testes did not contain Vasa-positive germline cells (Fig. 2.5B). Massive cell death was detected in cyst cell-*EcR-B*-testes on the basis of positive staining with the cell death marker Acridine Orange (Arama and Steller, 2006). While only 11% of testes from control animals contained some Acridine Orange-stained cells (Fig. 2.5C, arrows, n=19), 81% of testes overexpressing *EcR-B1* (Fig. 2.5D, arrows, n=16) and 63% of testes overexpressing *EcR-B2* (n=38) under the control of the Eya-*gal4*-transactivator contained many Acridine Orange-stained cells throughout the testes.

A Terminal deoxynucleotidyl transferase dUtp Nick End Labeling (TUNEL) cell death assay revealed that cell death occurred primarily in the germline cells of cyst cell-*EcR-B*-testes. Testes from control animals (n=50) normally did not show TUNEL-positive signals (Fig. 2.5E). Only small spots of TUNEL-positive cells were detected and occurred in less than 33% of the control testes. Cyst cell-*EcR-B*-testes (n=15), in contrast, had several clusters of TUNEL-positive cells in 85% of the testes. A careful analysis of these clusters revealed that they were mostly germline cells, based on the expression of Vasa and the size of the TUNEL-labeled clusters (Fig. 2.5F, arrowheads). 45% of the dying germline clusters were not associated with Eya-positive cyst cells, while 55% of the dying germline clusters were associated with cyst cells that expressed Eya (Fig. 2.5F, arrow). We did not detected clusters of germline cells associated with an Eya-positive,

TUNEL-positive cyst cell. Together these observations suggest that overexpression of *EcR-B* isoforms induced germline death, which in turn might have caused the loss of the associated cyst cells. Massive germline death was not apparent in *spi*/*spi*-testes raised at 26 °C.

To examine if overexpression of *EcR-B* caused cyst cell loss, we labeled control and experimental testes with the cyst cell markers, Tj and Eya, respectively. Immuno-labeling of testes with Vasa, Tj, and Arm revealed that the germline was properly enclosed in cyst cells in wildtype (Fig. 2.6A-A′) and cyst cell-*EcR-B*-testes (Fig. 2.6B-B′). However, not all of the Tj-positive cyst cell nuclei were associated with germline and thus appeared as single cell in cyst cell-*EcR-B*-testes (Fig. 2.6B, arrows). Likewise, we detected single, Eya-positive cyst cell nuclei in cyst cell-*EcR-B*-testes (Fig. 2.6D, arrows), but not in wildtype testes (Fig. 2.6C). Eventually, cyst cells accumulated and were present at excessive numbers in 30% of cyst cell-*EcR-B*-testes (n=47), likely due to the lack of germline. Our observation that cyst cells were present in cyst cell-*EcR-B*-testes shows that overexpression of *EcR-B* in the cyst cells does not directly cause cyst cell death. Similarly, only very few dying cyst cell nuclei were observed in *spi*/*spi*-testes raised at 26 °C, with an average of 2 (±2) cyst cell nuclei per testis (n=20).

Discussion

Previous research has established that signaling from the apical hub cells via the Janus Kinase signal transducer and activator of transcription pathway is required and instructive for CySC fate (Kiger et al., 2001; Tulina and Matunis, 2001). Likewise, signaling from the germline via EGF is required and instructive for cyst cell

differentiation (Hudson et al., 2013). Here we show that a hormonal signal, 20E, also plays a role in cyst differentiation. Reducing EcR signaling by two independent genetic approaches (introduction of a single mutant copy of 20E biosynthetic genes or expressing RNA hairpins against the EcR signaling complex and its target genes in the cyst cells) restored germline enclosure and cyst differentiation in *spi/spi*-testes. These findings reveal that EcR activity severely limits differentiation in this mutant background. The EcR early response target BrC was only expressed in early-stage cyst cells but not in late-stage cyst cells; thus, we propose that EcR signaling normally acts within the early-stage cyst cells. Importantly, BrC expression is essentially unchanged in *spi/spi*-testes, indicating that EcR signaling operates independently of EGF signaling.

The number of early-stage cyst cells were vastly increased in *spi*/*spi*-testes, but returned to close to normal when EcR signaling was also disrupted. This observation implies that EcR acts to prolong the timing of early differentiation steps or to prevent the onset of differentiation in *spi*/*spi*-testes. Despite these striking effects, loss of EcR signaling in otherwise wildtype testes, forced by a number of different experimental methods, remained without apparent consequences for cyst development, confirming that EcR signaling is not required for normal cyst cell and germline differentiation. One possible explanation for this lack of phenotype may be that the EcR pathway acts redundantly with other, yet to be identified signals to prevent cyst differentiation. Alternatively, EGF signaling may be sufficient for regulating early cyst differentiation independently, with the EcR pathway playing an accessory role. According to this view, EcR signaling would bias the early-stage cyst cells to an undifferentiated state, but this effect would normally be over-ridden by the independent, instructive EGF signals

originating from the germline cells (Fig. 2.7). 20E is a systemic signal, and it is tempting to speculate that it may be utilized to modulate the production of sperm in response to physiological parameters by slowing the rate of early-state cyst differentiation. In testes where EGF signaling is lost or reduced, EcR signaling would remain unchecked and thus prevent the normal progression of development.

In contrast to the lack of a testis phenotype upon loss of EcR signaling, overexpression of EcR in the cyst cells of otherwise wildtype testes produced a strong phenotype. This finding confirms that increased activity of EcR has an effect on the cysts. In our overexpression experiments, the level of EcR may have been too high to be attenuated by EGF. This high level of EcR may have blocked or prolonged cyst cell differentiation in this genetic background. This, in turn, may have upset the developmental balance between the cyst cells and the enclosed germline cells, upon which the germline entered the cell death program. The phenotype produced by overexpression of EcR in cyst cells is different from loss of EGF. This is not surprising, as germline cells and cyst cells are normally not associated in *spi*/*spi*-testes. Furthermore, one would expect EGF to have additional roles than just attenuating EcR signaling and therefore to produce a far more drastic phenotype when lost.

Several scenarios can be envisioned for how EcR and EGF signaling act antagonistically in the cyst cells. For example, both pathways can affect cell morphogenesis. In the female gonad, loss of EcR signaling disrupts formation of the cytoplasmic extensions from somatic cells to early-stage germline cells (Morris and Spradling, 2012). In the developing leg, 20E signaling appears to promote the cell shape changes associated with leg morphogenesis (von Kalm et al., 1995). A genetic modifier

screen revealed that mutations in Rho1 increased the severity of these defects in leg morphogenesis, suggesting the possibility that EcR signaling promotes activation of Rho1 (Ward et al., 2003). We have previously shown that the directional outgrowth of cyst cell cytoplasmic extensions is organized by a differential of Rho1 and Rac1 activity in the cyst cells, with Rac acting downstream of the EGFR and Rho1 acting antagonistic to EGF signaling (Sarkar et al., 2007). Potentially, EcR may affect germline enclosure by regulating Rho1.

A second possible convergence point of the two pathways may be provided by MAPK, which has been placed downstream of the EGFR (Lemmon and Schlessinger, 2010). The function of the human Usp homolog, RXR, depends on phosphorylation (Gronemeyer et al., 2004; Macoritto et al., 2008; Solomon et al., 1999). In benign tumors of the uterus, RXR-alpha appears to be phosphorylated by MAPK, based on a reduction of RXR phosphorylation upon administering MAPK-inhibitors (Lattuada et al., 2007). In *Caenorhabditis elegans*, the Usp homolog was identified as a target for MAPK phosphorylation by a computational approach (Arur et al., 2009). However, potential phosphorylation sites in human and *C. elegans* RXR are not present in *Drosophila* Usp, making it difficult to predict whether MAPK is involved in regulating EcR signaling in *Drosophila*.

Perhaps the most likely scenario is that EGF and EcR interact at the level of transcriptional regulation of target genes. For example, the EcR complex or its direct early response genes could bind to regulatory regions of genes that are either required for the differentiated or the undifferentiated state of the cyst cells. The same genes may also be targeted by EGF-controlled transcriptional regulators. Accordingly, the correct

expression of these genes would be predicted to depend on an appropriate balance of EcR- and EGF-controlled transcriptional regulators. As the cysts develop and the EGF signal becomes stronger, EGF-controlled transcriptional regulators may push the transcriptional profile toward differentiation functions. In our experiments, reducing EcR signaling in *spi*/*spi*-testes may have restored the normal balance between EGF and EcR signaling and, thus, enabled a more normal expression profile. Testing this model awaits the characterization of EGF-regulated target genes in testes of *Drosophila*.

Acknowledgments

The authors are indebted to Manashree Malpe and Alicia Hudson for technical assistance and Judith Willis, Scott Dougan, and Mark Brown for helpful discussion. We thank Manashree Malpe, Alicia Hudson, and Wolfgang Lukowitz for critical reading of the manuscript. This work was supported by the NSF Grants #0841419 and #1355009 given to CS and ARC Discovery Project 120100224 given to GH.

Genotype	**Total**	**Type I**	**Type II**	**Type III**	**Ratio (%)**
Wildtype	500	0	0	500	00:00:100
spi/spi	341	253	24	64	74:07:19
spi/spi; spo^{1}/+	93	31	10	52	33:11:56
spi/spi; dib^{2}/+	93	31	16	46	33:17:50
spi/spi; sad^{1}/+	83	5	7	71	06:08:86
spi/spi; Eya-*gal4;* UAS-*dcr*/+	191	111	40	40	58:21:21
spi/spi; UAS-*EcRi*; *U*AS-*EcRi*/+	162	87	15	60	54:09:37
spi/spi; UAS-*Uspi*/+	63	49	2	12	78:03:19
spi/spi; UAS-*BrCi*/+	155	110	18	27	71:12:17
spi/spi; UAS-*Eip74i*/+	126	94	7	25	75:05:20
spi, Eya-*gal4/spi*-UAS-*EcRi*; UAS-*dcr*/UAS-*EcRi*	240	30	20	190	13:08:79
spi/spi; Eya-*gal4*; UAS-*Uspi*/UAS-*dcr*	163	12	9	142	07:06:87
spi/sp; Eya-*gal4*; UAS-*BrCi*/UAS-*dcr*	175	30	15	130	17:09:74
spi/spi; Eya-*gal4;* UAS-*Eip74i*/UAS-*dcr*	161	20	6	135	12:04:84

Table 2.1:

Reducing 20E signaling decreased the percentage of Type I *spi/spi*-testes. For each genotype, the total number of testes examined, the total numbers of Type I, Type II, and Type III testes, and the percentage distribution (Ratio) of Type I, Type II, and Type III testes, respectively, are listed.

Genotype	# Testes	Tj-positive cells	Tj-negative, Eya-positive cells
Wildtype	20	42 (±12)	60 (±20)
spi/spi	25	73 (±16)	7 (±5)
spi/spi + reduced 20E	20	57 (±16)	45 (±8)

Table 2.2:

Reducing EcR signaling in *spi/spi*-testes decreased the average number of Tj-positive cyst cells. Genotypes and marked cells, as indicated.

Figure 2.1: Reduction in 20E production promoted germline differentiation in *spi/spi*-testes.

(A)-(D) DAPI-stained preparations of testes. Arrowheads point to early-stage germline nuclei, small arrows point to spermatocyte nuclei, large arrows point to sperm heads, and asterisks mark the apical tip of the testes. Scale bars: 30 μm.

(A) A whole wildtype testis.

(A') High magnification of the nuclei in the apical region of (A).

(B)-(D) Type I, II, and III *spi*/*spi*-testes, as indicated. Note that the testes are shown in the same magnification.

(E) Bar graph showing percentage of Type I, II, and III *spi*/*spi*-testes (*X*-axis) from animals without and with single copy mutations in genes required for 20E production (*Y*-axis). Asterisks represent statistical significance in the percentage of Type I testes between *spi*/*spi*-testes and suppressed *spi*/*spi*-testes (*P*-value<0.0001).

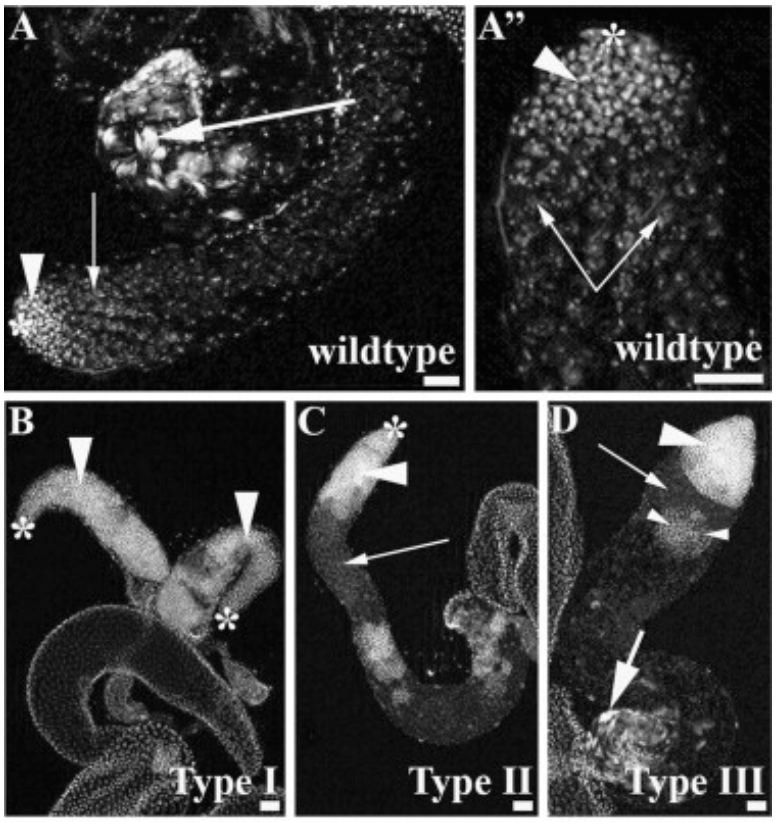
A
wildtype
A''
wildtype
B
Type I
C
Type II
D
Type III

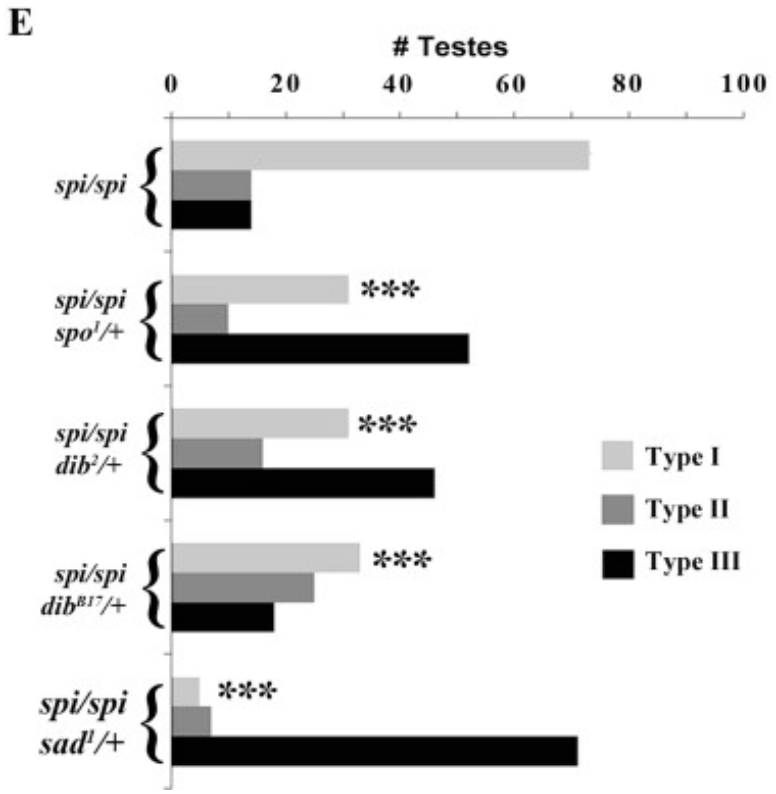
E
Testes
0
20
40
60
80
100
spi/spi
spi/spi
spo1/+
***
spi/spi
dib2/+
***
spi/spi
dibR17/+
***
spi/spi
sad1/+
***
Type I
Type II
Type III

Figure 2.2: EcR signaling components and the target BrC are expressed in cyst cells.

(A) Illustration depicting the EcR transcriptional complex and the early response genes. Co-R: Co-regulators.

(B) A photograph of an agarose gel showing the amplified RT-PCR products, as indicated. The correct band for Usp is marked by an asterisk.

(C)-(F") Apical tips of wildtype testes.

(C) and (C") Co-expression of Tj and EcR, as indicated.

(D) and (D") Co-expression of Eya and Usp, as indicated.

(E) and (E") Co-expression of Eya and Tai, as indicated.

(F) and (F") Co-expression of Tj and BrC, as indicated.

(G) and (G") Co-expression of Tj and BrC in *spi*/*spi*-testes, as indicated.

Arrowheads point to early-stage cyst cell nuclei, arrows point to late-stage cyst cell nuclei, and asterisks mark the apical tip of the testes. Scale bars: 30 μm.

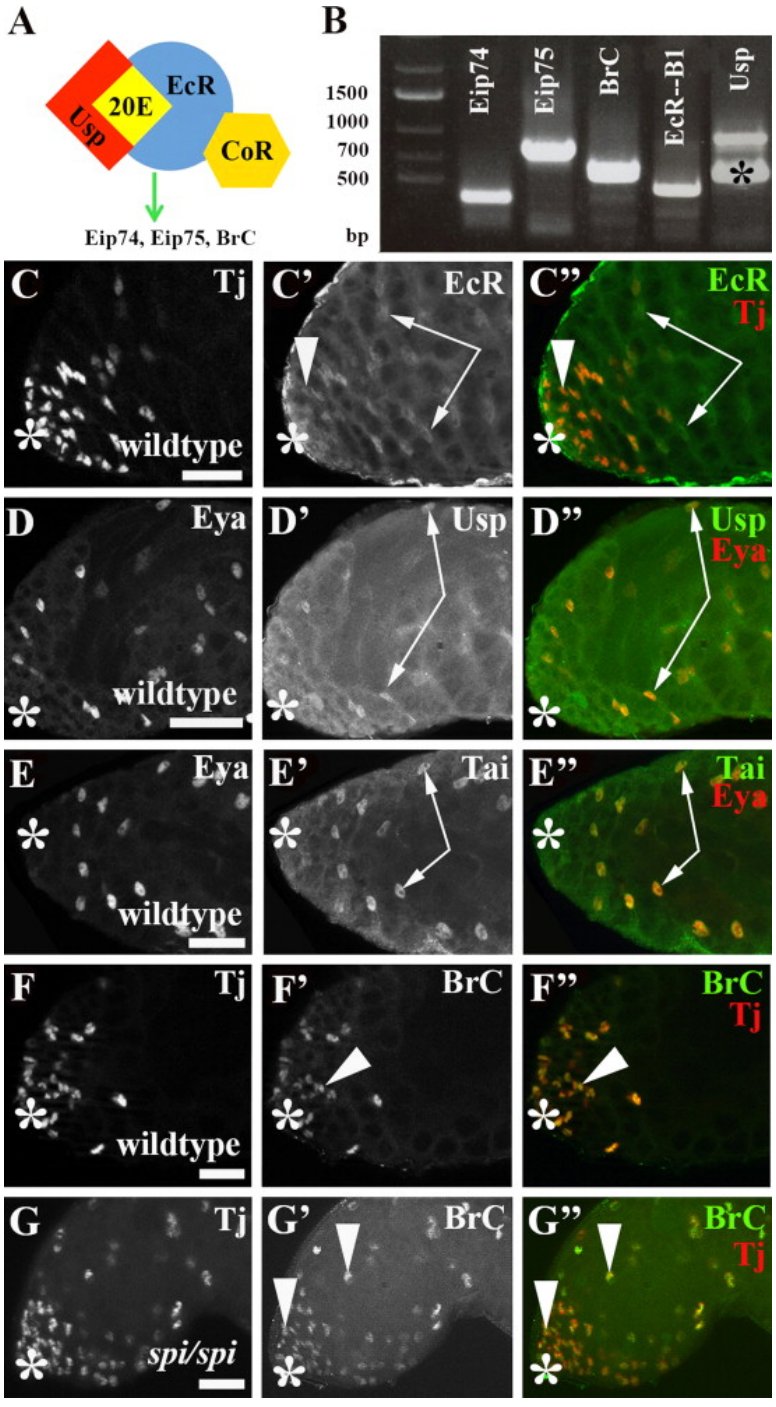
A
EcR
20E
Usp
CoR
Eip74, Eip75, BrC
B
1500
1000
700
500
bp
Eip74
Eip75
BrC
EcR--B1
Usp
C
Tj
wildtype
C'
EcR
C''
EcR
Tj
D
Eya
wildtype
D'
Usp
D''
Usp
Eya
E
Eya
wildtype
E'
Tai
E''
Tai
Eya
F
Tj
wildtype
F'
BrC
F''
BrC
Tj
G
Tj
spi/spi
G'
BrC
G''
BrC
Tj

Figure 2.3: Reduction of Ecdysone signaling components in cyst cells reduced the percentage of Type I *spi*/*spi*-testes.

Bar graph showing the percentage of Type I, II, and III *spi*/*spi*-testes (*X*-axis) of control and experimental animals (*Y*-axis). Asterisks represent statistical relevance in the percentage of Type I testes between *spi*/*spi*-testes and suppressed *spi*/*spi*-testes (*P*-value<0.0001).

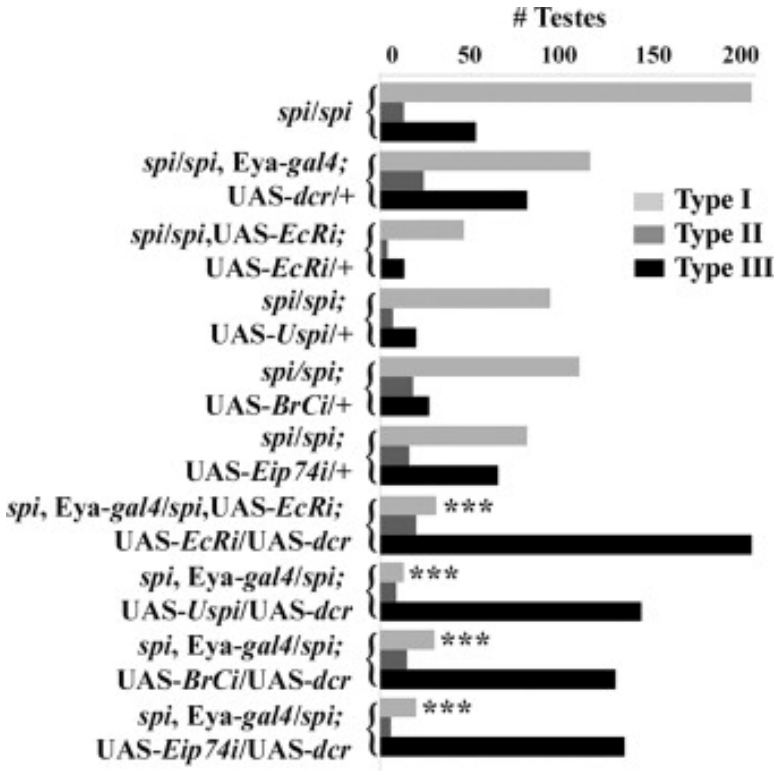
Testes
0
50
100
150
200
spi/spi
spi/spi, Eya-gal4;
UAS-dcr/+
spi/spi,UAS-EcRi;
UAS-EcRi/+
spi/spi;
UAS-Uspi/+
spi/spi;
UAS-BrCi/+
spi/spi;
UAS-Eip74i/+
spi, Eya-gal4/spi,UAS-EcRi;
UAS-EcRi/UAS-dcr
spi, Eya-gal4/spi;
UAS-Uspi/UAS-dcr
spi, Eya-gal4/spi;
UAS-BrCi/UAS-dcr
spi, Eya-gal4/spi;
UAS-Eip74i/UAS-dcr
***
***
***
Type I
Type II
Type III

Figure 2.4: Reduction of EcR signaling in *spi* mutant animals restored cyst cell differentiation.

(A)-(F) Apical regions of testes.

(A) and (B) from wildtype animals, (C) and (D) from *spi*/*spi* mutant animals (*spi*/*spi*), (E) and (F) from *spi*/*spi* mutant animals, heterozygous for *sad1*(*spi*/*spi* + reduced 20E). Testes are stained with DAPI and cell type-specific antibodies, as indicated (for details, please see main body text).

Arrowhead points to early-stage germline cells, arrows point to cyst cell cytoplasmic extensions, and asterisks mark the apical tip of the testes. Scale bars: 30 µm.

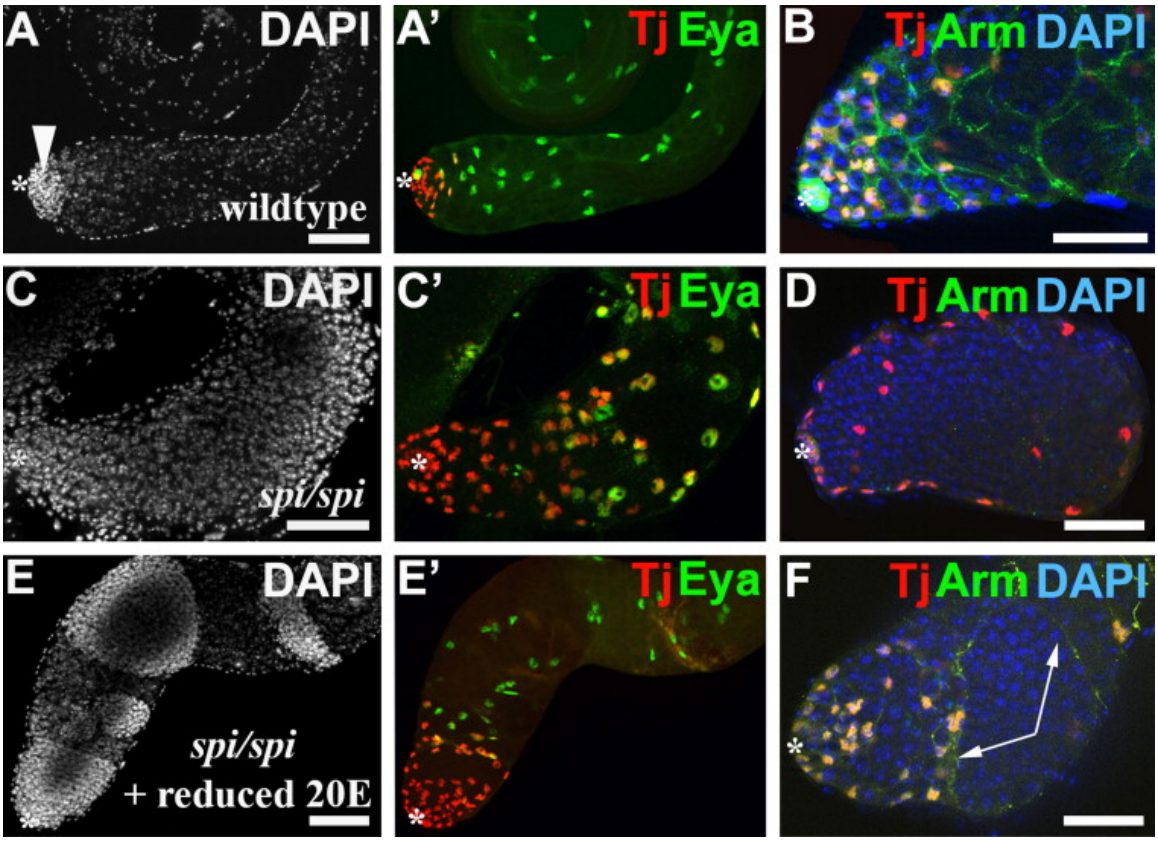
A
DAPI
wildtype
A'
Tj Eya
B
Tj Arm DAPI
C
DAPI
spi/spi
C'
Tj Eya
D
Tj Arm DAPI
E
DAPI
spi/spi
+ reduced 20E
E'
Tj Eya
F
Tj Arm DAPI

Figure 2.5: Overexpression of *EcR* resulted in cell death.

(A) and (B) Whole testes labeled with the germline marker Vasa and the nuclear marker DAPI. Arrowheads point to early-stage germline cells, small arrowheads point to empty regions of the testes, small arrows point to spermatocytes, and large arrow points to spermatid heads.

(A) A wildtype testis is filled with Vasa-positive germline cells in the apical region and along the testis coil, and contains many sperm heads with sickle-shaped, DAPI-positive nuclei at the base.

(B) A cyst cell-*EcR-B1* testis contains only a few germline cells in the apical region.

(C) and (D) Whole testes labeled for cell death using Acridine Orange. Small arrows point to dying cells.

(C) A wild type testis with only a few dying cells.

(D) A cyst cell-*EcR-B1*-testis with massive cell death.

(E) and (F) Apical to mid-testes region showing developing germline clusters in

(E) wildtype, and (F) cyst cell-*EcR-B1*. Note dying clusters of germline (arrowheads). Arrow points to Eya-positive cyst cell associated with a cluster of dying germline cells. Asterisks mark the apical tip of the testes. Scale bars: 30 μm.

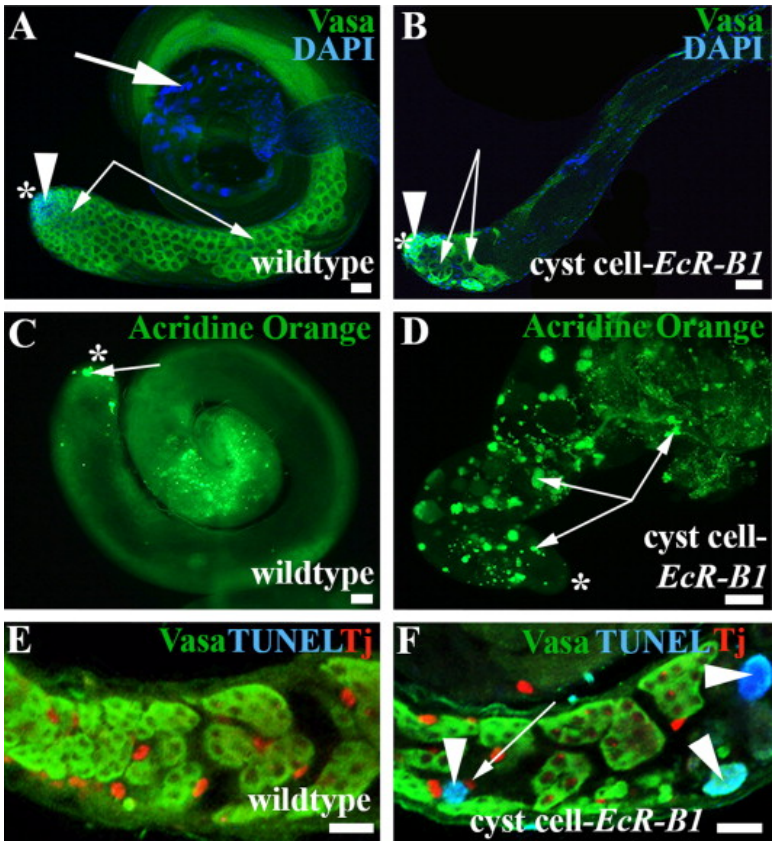
A
Vasa
DAPI
wildtype
B
Vasa
DAPI
cyst cell-EcR-B1
C
Acridine Orange
wildtype
D
Acridine Orange
cyst cell-
EcR-B1
E
VasaTUNELTj
wildtype
F
Vasa TUNEL Tj
cyst cell-EcR-B1

Figure 2.6: In testes with overexpression of *EcR*, single cyst cells accumulate.

(A)-(D') Apical testes regions, immuno-labeled as indicated.

(A)-(B') Single, Tj-positive cyst cell nuclei were not detected in (A) wildtype, but were clearly present in (B) cyst cell-*EcR-B1*-testes. Note, that the germline cells were enclosed by cyst cell bodies (arrowheads).

(C) and (D) Eya-positive cyst cell nuclei were single in (D) cyst cell-*EcR-B1*-testes, but not in (C) wildtype.

Asterisks mark the apical tip of the testes, arrows point to cyst cell nuclei that are not associated with germline, scale bars: 30 µm.

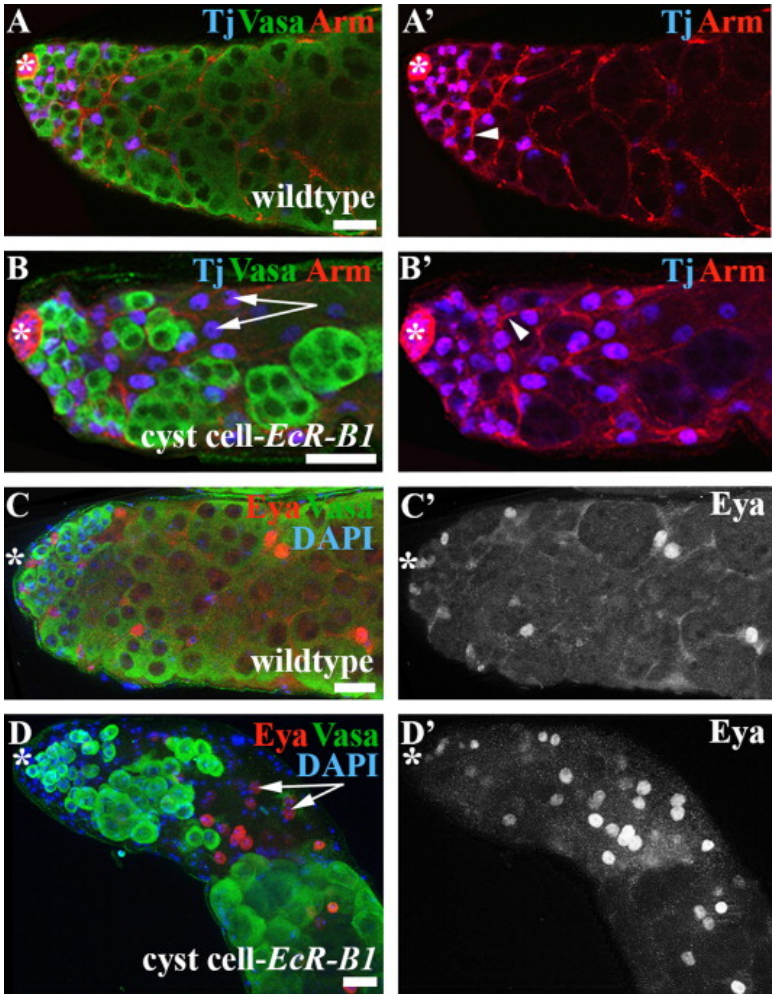
A
Tj Vasa Arm
wildtype
A'
Tj Arm
B
Tj Vasa Arm
cyst cell-EcR-B1
B'
Tj Arm
C
Eya Vasa
DAPI
wildtype
C'
Eya
D
Eya Vasa
DAPI
cyst cell-EcR-B1
D'
Eya

Figure 2.7: Opposing roles of EcR and EGF signaling in regulating cyst differentiation.

Illustration of the early stages of cyst development and the interaction between EGF and EcR in regulating differentiation of the cyst cells into later stages. The bottom of the image shows the stem cell region (CySC fate depends on signals from the hub) and developing cysts. The developmental state of the cyst is indicated by large triangles: the black triangle represents cyst cell differentiation and the grey triangle represents the undifferentiated state of the cyst cells. The activities of the EcR and EGF signaling pathway is outlined on the top. In this model, EGF is the major pathway inducing cyst differentiation (black arrow) and attenuating EcR (black lines). EcR plays a promoting role in maintaining cyst cells undifferentiated (grey arrow).

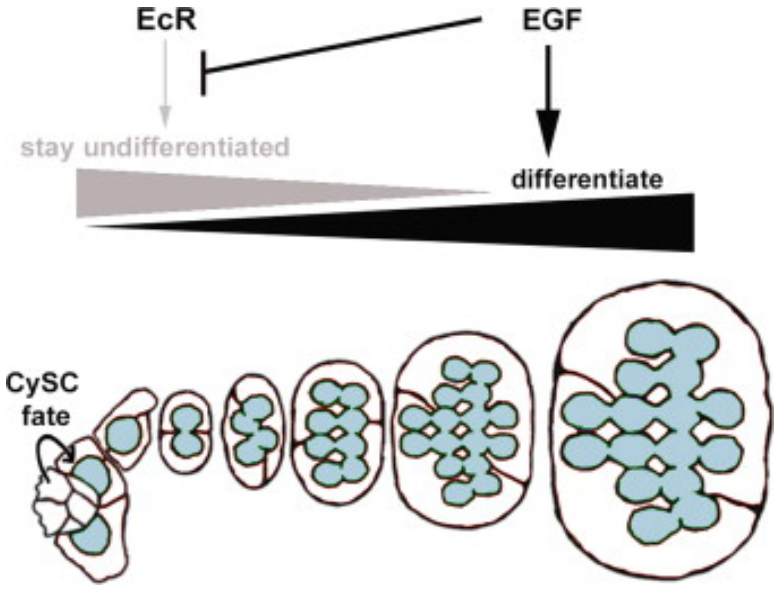
EcR
EGF
stay undifferentiated
differentiate
CySC
fate

References

Arama, E., Steller, H., 2006. Detection of apoptosis by terminal deoxynucleotidyl transferase-mediated dUTP nick-end labeling and acridine orange in Drosophila embryos and adult male gonads. Nature protocols 1, 1725-1731.

Arur, S., Ohmachi, M., Nayak, S., Hayes, M., Miranda, A., Hay, A., Golden, A., Schedl, T., 2009. Multiple ERK substrates execute single biological processes in Caenorhabditis elegans germ-line development. Proc. Natl. Acad. Sci. U. S. A. 106, 4776-4781.

Ashburner, M., Richards, G., 1976. Sequential gene activation by ecdysone in polytene chromosomes of Drosophila melanogaster. III. Consequences of ecdysone withdrawal. Dev. Biol. 54, 241-255.

Bai, J., Uehara, Y., Montell, D.J., 2000. Regulation of invasive cell behavior by taiman, a Drosophila protein related to AIB1, a steroid receptor coactivator amplified in breast cancer. Cell 103, 1047-1058.

Blanpain, C., Fuchs, E., 2006. Epidermal stem cells of the skin. Annu. Rev. Cell Dev. Biol. 22, 339-373.

Brand, A.H., Perrimon, N., 1993. Targeted gene expression as a means of altering cell fates and generating dominant phenotypes. Development 118, 401-415.

Braun, S., Azoitei, A., Spindler-Barth, M., 2009. DNA-binding properties of Drosophila ecdysone receptor isoforms and their modification by the heterodimerization partner ultraspiracle. Arch. Insect Biochem. Physiol. 72, 172-191.

Brownes, M., Dudendorfer, A., Smith, T., 1984. Ecdysteroids in adult males and females in Drosophila. J. Insect Physiol. 30, 823-830.

Bunt, S.M., Hime, G.R., 2004. Ectopic activation of Dpp signalling in the male Drosophila germline inhibits germ cell differentiation. Genesis 39, 84-93.

Buszczak, M., Segraves, W.A., 1998. Drosophila metamorphosis: the only way is USP? Curr. Biol. 8, R879-882.

Carney, G.E., Bender, M., 2000. The Drosophila ecdysone receptor (EcR) gene is required maternally for normal oogenesis. Genetics 154, 1203-1211.

Cherbas, L., Hu, X., Zhimulev, I., Belyaeva, E., Cherbas, P., 2003. EcR isoforms in Drosophila: testing tissue-specific requirements by targeted blockade and rescue. Development 130, 271-284.

Choi, Y.S., Zhang, Y., Xu, M., Yang, Y., Ito, M., Peng, T., Cui, Z., Nagy, A., Hadjantonakis, A.K., Lang, R.A., Cotsarelis, G., Andl, T., Morrisey, E.E., Millar, S.E., 2013. Distinct functions for Wnt/beta-catenin in hair follicle stem cell proliferation and survival and interfollicular epidermal homeostasis. Cell stem cell 13, 720-733.

Conover, J.C., Notti, R.Q., 2008. The neural stem cell niche. Cell Tissue Res. 331, 211-224.

Dai, J.D., Gilbert, L.I., 1991. Metamorphosis of the corpus allatum and degeneration of the prothoracic glands during the larval-pupal-adult transformation of Drosophila melanogaster: a cytophysiological analysis of the ring gland. Dev. Biol. 144, 309-326.

de Rooij, D.G., 2009. The spermatogonial stem cell niche. Microsc. Res. Tech. 72, 580-585.

Dela Cruz, F.E., Kirsch, D.R., Heinrich, J.N., 2000. Transcriptional activity of Drosophila melanogaster ecdysone receptor isoforms and ultraspiracle in Saccharomyces cerevisiae. J. Mol. Endocrinol. 24, 183-191.

Dietzl, G., Chen, D., Schnorrer, F., Su, K.C., Barinova, Y., Fellner, M., Gasser, B., Kinsey, K., Oppel, S., Scheiblauer, S., Couto, A., Marra, V., Keleman, K., Dickson, B.J., 2007. A genome-wide transgenic RNAi library for conditional gene inactivation in Drosophila. Nature 448, 151-156.

Fabrizio, J.J., Boyle, M., DiNardo, S., 2003. A somatic role for eyes absent (eya) and sine oculis (so) in Drosophila spermatocyte development. Dev. Biol. 258, 117-128.

Fuller, M.T., 1993. Spermatogenesis in Drosophila, in: Bate, M., Martinez Arias, A. (Ed.), The development of Drosophila melanogaster. Cold Spring Harbor Laboratory Press, Cold Spring Harbor, New York, USA, pp. 71-148.

Ganter, G.K., Panaitiu, A.E., Desilets, J.B., Davis-Heim, J.A., Fisher, E.A., Tan, L.C., Heinrich, R., Buchanan, E.B., Brooks, K.M., Kenney, M.T., Verde, M.G., Downey, J., Adams, A.M., Grenier, J.S., Maddula, S., Shah, P., Kincaid, K.M., O'Brien, J.R., 2011. Drosophila male courtship behavior is modulated by ecdysteroids. J. Insect Physiol. 57, 1179-1184.

Gronemeyer, H., Gustafsson, J.A., Laudet, V., 2004. Principles for modulation of the nuclear receptor superfamily. Nature reviews. Drug discovery 3, 950-964.

Hall, B.L., Thummel, C.S., 1998. The RXR homolog ultraspiracle is an essential component of the Drosophila ecdysone receptor. Development 125, 4709-4717.

Hardy, R.W., Tokuyasu, K.T., Lindsley, D.L., Garavito, M., 1979. The germinal proliferation center in the testis of Drosophila melanogaster. J. Ultrastruct. Res. 69, 180-190.

Hrdlicka, L., Gibson, M., Kiger, A., Micchelli, C., Schober, M., Schock, F., Perrimon, N., 2002. Analysis of twenty-four Gal4 lines in Drosophila melanogaster. Genesis 34, 51-57.

Hudson, A.G., Parrott, B.B., Qian, Y., Schulz, C., 2013. A temporal signature of epidermal growth factor signaling regulates the differentiation of germline cells in testes of Drosophila melanogaster. PloS one 8, e70678.

Ishimoto, H., Kitamoto, T., 2010. The steroid molting hormone Ecdysone regulates sleep in adult Drosophila melanogaster. Genetics 185, 269-281.

Ishimoto, H., Sakai, T., Kitamoto, T., 2009. Ecdysone signaling regulates the formation of long-term courtship memory in adult Drosophila melanogaster. Proc. Natl. Acad. Sci. U. S. A. 106, 6381-6386.

Ju, X.F., An, T.Z., Teng, C.B., 2007. [Advances in the study of stem cell niche]. Sheng li ke xue jin zhan [Progress in physiology] 38, 213-218.

Keller, G., 2005. Embryonic stem cell differentiation: emergence of a new era in biology and medicine. Genes Dev. 19, 1129-1155.

Kiger, A.A., Jones, D.L., Schulz, C., Rogers, M.B., Fuller, M.T., 2001. Stem cell self-renewal specified by JAK-STAT activation in response to a support cell cue. Science 294, 2542-2545.

Kiger, A.A., White-Cooper, H., Fuller, M.T., 2000. Somatic support cells restrict germline stem cell self-renewal and promote differentiation. Nature 407, 750-754.

Koelle, M.R., Talbot, W.S., Segraves, W.A., Bender, M.T., Cherbas, P., Hogness, D.S., 1991. The Drosophila EcR gene encodes an ecdysone receptor, a new member of the steroid receptor superfamily. Cell 67, 59-77.

Krausova, M., Korinek, V., 2014. Wnt signaling in adult intestinal stem cells and cancer. Cell. Signal. 26, 570-579.

Lattuada, D., Vigano, P., Mangioni, S., Sassone, J., Di Francesco, S., Vignali, M., Di Blasio, A.M., 2007. Accumulation of retinoid X receptor-alpha in uterine leiomyomas is associated with a delayed ligand-dependent proteasome-mediated degradation and an alteration of its transcriptional activity. Mol. Endocrinol. 21, 602-612.

Leatherman, J.L., Dinardo, S., 2008. Zfh-1 controls somatic stem cell self-renewal in the Drosophila testis and nonautonomously influences germline stem cell self-renewal. Cell stem cell 3, 44-54.

Lemmon, M.A., Schlessinger, J., 2010. Cell signaling by receptor tyrosine kinases. Cell 141, 1117-1134.

Li, M.A., Alls, J.D., Avancini, R.M., Koo, K., Godt, D., 2003. The large Maf factor Traffic Jam controls gonad morphogenesis in Drosophila. Nature cell biology 5, 994-1000.

Lim, X., Nusse, R., 2013. Wnt signaling in skin development, homeostasis, and disease. Cold Spring Harbor perspectives in biology 5.

Luis, T.C., Killmann, N.M., Staal, F.J., 2012. Signal transduction pathways regulating hematopoietic stem cell biology: introduction to a series of Spotlight Reviews. Leukemia 26, 86-90.

Macoritto, M., Nguyen-Yamamoto, L., Huang, D.C., Samuel, S., Yang, X.F., Wang, T.T., White, J.H., Kremer, R., 2008. Phosphorylation of the human retinoid X receptor alpha at serine 260 impairs coactivator(s) recruitment and induces hormone resistance to multiple ligands. J. Biol. Chem. 283, 4943-4956.

Matunis, E., Tran, J., Gonczy, P., Caldwell, K., DiNardo, S., 1997. punt and schnurri regulate a somatically derived signal that restricts proliferation of committed progenitors in the germline. Development 124, 4383-4391.

Moghal, N., Sternberg, P.W., 2003. The epidermal growth factor system in Caenorhabditis elegans. Exp. Cell Res. 284, 150-159.

Morris, L.X., Spradling, A.C., 2012. Steroid signaling within Drosophila ovarian epithelial cells sex-specifically modulates early germ cell development and meiotic entry. PloS one 7, e46109.

Normanno, N., De Luca, A., Bianco, C., Strizzi, L., Mancino, M., Maiello, M.R., Carotenuto, A., De Feo, G., Caponigro, F., Salomon, D.S., 2006. Epidermal growth factor receptor (EGFR) signaling in cancer. Gene 366, 2-16.

Park, D., Sykes, D.B., Scadden, D.T., 2012. The hematopoietic stem cell niche. Front. Biosci. 17, 30-39.

Parrott, B.B., Hudson, A., Brady, R., Schulz, C., 2012. Control of germline stem cell division frequency--a novel, developmentally regulated role for epidermal growth factor signaling. PloS one 7, e36460.

Perera, S.C., Zheng, S., Feng, Q.L., Krell, P.J., Retnakaran, A., Palli, S.R., 2005. Heterodimerization of ecdysone receptor and ultraspiracle on symmetric and asymmetric response elements. Arch. Insect Biochem. Physiol. 60, 55-70.

Phelps, C.B., Brand, A.H., 1998. Ectopic gene expression in Drosophila using GAL4 system. Methods 14, 367-379.

Riddihough, G., Pelham, H.R., 1987. An ecdysone response element in the Drosophila hsp27 promoter. EMBO J. 6, 3729-3734.

Sarkar, A., Parikh, N., Hearn, S.A., Fuller, M.T., Tazuke, S.I., Schulz, C., 2007. Antagonistic roles of Rac and Rho in organizing the germ cell microenvironment. Curr. Biol. 17, 1253-1258.

Schulz, C., Wood, C.G., Jones, D.L., Tazuke, S.I., Fuller, M.T., 2002. Signaling from germ cells mediated by the rhomboid homolog stet organizes encapsulation by somatic support cells. Development 129, 4523-4534.

Schwedes, C., Tulsiani, S., Carney, G.E., 2011. Ecdysone receptor expression and activity in adult Drosophila melanogaster. J. Insect Physiol. 57, 899-907.
Schwedes, C.C., Carney, G.E., 2012. Ecdysone signaling in adult Drosophila melanogaster. J. Insect Physiol. 58, 293-302.

Sedkov, Y., Cho, E., Petruk, S., Cherbas, L., Smith, S.T., Jones, R.S., Cherbas, P., Canaani, E., Jaynes, J.B., Mazo, A., 2003. Methylation at lysine 4 of histone H3 in ecdysone-dependent development of Drosophila. Nature 426, 78-83.

Shilo, B.Z., 2003. Signaling by the Drosophila epidermal growth factor receptor pathway during development. Exp. Cell Res. 284, 140-149.

Simon, A.F., Liang, D.T., Krantz, D.E., 2006. Differential decline in behavioral performance of Drosophila melanogaster with age. Mech. Ageing Dev. 127, 647-651.

Solomon, C., White, J.H., Kremer, R., 1999. Mitogen-activated protein kinase inhibits1,25-dihydroxyvitamin D3-dependent signal transduction by phosphorylating human retinoid X receptor alpha. J. Clin. Invest. 103, 1729-1735.

Sotiropoulou, P.A., Blanpain, C., 2012. Development and homeostasis of the skin epidermis. Cold Spring Harbor perspectives in biology 4, a008383.

Strand, M., Micchelli, C.A., 2013. Regional control of Drosophila gut stem cell proliferation: EGF establishes GSSC proliferative set point & controls emergence from quiescence. PloS one 8, e80608.

Takakura, N., 2012. Formation and regulation of the cancer stem cell niche. Cancer science 103, 1177-1181.

The Flybase Consortium, 2003. The FlyBase database of the Drosophila genome projects and community literature. Nucleic Acids Res 31, 172-175.

Tulina, N., Matunis, E., 2001. Control of stem cell self-renewal in Drosophila spermatogenesis by JAK-STAT signaling. Science 294, 2546-2549.

Urban, S., Lee, J.R., Freeman, M., 2002. A family of Rhomboid intramembrane proteases activates all Drosophila membrane-tethered EGF ligands. EMBO J. 21, 4277-4286.

von Kalm, L., Fristrom, D., Fristrom, J., 1995. The making of a fly leg: a model for epithelial morphogenesis. Bioessays 17, 693-702.

Ward, R.E., Evans, J., Thummel, C.S., 2003. Genetic modifier screens in Drosophila demonstrate a role for Rho1 signaling in ecdysone-triggered imaginal disc morphogenesis. Genetics 165, 1397-1415.

Warren, J.T., Yerushalmi, Y., Shimell, M.J., O'Connor, M.B., Restifo, L.L., Gilbert, L.I., 2006. Discrete pulses of molting hormone, 20-hydroxyecdysone, during late larval development of Drosophila melanogaster: correlations with changes in gene activity. Dev. Dyn. 235, 315-326.

Wiley, L.M., Adamson, E.D., Tsark, E.C., 1995. Epidermal growth factor receptor function in early mammalian development. Bioessays 17, 839-846.

Yao, T.P., Forman, B.M., Jiang, Z., Cherbas, L., Chen, J.D., McKeown, M., Cherbas, P., Evans, R.M., 1993. Functional ecdysone receptor is the product of EcR and Ultraspiracle genes. Nature 366, 476-479.

Zoller, R., Schulz, C., 2012. The Drosophila cyst stem cell lineage: Partners behind the scenes? Spermatogenesis 2, 145-157.

CHAPTER 3

CSN CONTROLS LEVELS OF STEM CELL GENES AND MAINTENANCE OF THE GERMLINE CELLULAR MICROENVIRONMENT VIA DISTINCT CRLS IN TESTES OF *DROSOPHILA MELANOGASTER*[1]

[1] Qian Y, Ng C, and Schulz C. 2014. *Developmental Biology* (in press).

Abstract

Stem cells and their daughters are often associated with and depend on cues from their cellular microenvironment. In *Drosophila* testes, each Germline Stem Cell (GSC) contacts apical hub cells and is enclosed by cytoplasmic extensions from two Cyst Stem Cells (CySCs). Each GSC daughter becomes enclosed by cytoplasmic extensions from two CySC daughters, called cyst cells. CySC fate depends on an Unpaired (Upd) signal from the hub cells, which activates the Janus Kinase and Signal Transducer and Activator of Transcription (Jak/STAT) pathway in the stem cells. Germline enclosure depends on Epidermal Growth Factor (EGF) signals from the germline to the somatic support cells. Expression of RNA-hairpins against subunits of the COnstitutively Photomorphogenic-9- (COP9-) signalosome (CSN) in somatic support cells disrupted germline enclosure. Furthermore, CSN-depleted somatic support cells in the CySC position next to the hub had reduced levels of the Jak/STAT effectors Zinc finger homeotic-1 (Zfh-1) and Chronologically inappropriate morphogenesis (Chinmo). Knockdown of CSN in the somatic support cells does not disrupt EGF and Upd signal transduction as downstream signal transducers, phosphorylated STAT (pSTAT) and phosphorylated Mitogen Activated Protein Kinase (pMAPK), were still localized to the somatic support cell nuclei. The CSN modifies fully formed Cullin RING ubiquitin ligase (CRL) complexes to regulate selective proteolysis. Reducing *cullin2* (*cul2*) from the somatic support cells disrupted germline enclosure, while reducing *cullin1* (*cul1*) from the somatic support cells led to a low level of Chinmo. We propose that different CRLs enable the responses of somatic support cells to Upd and EGF.

Introduction

The continuous production of specialized cells in animal tissue relies on the abilities of stem cells to self-renew and to produce differentiating daughter cells. Mechanistically, these traits are mostly regulated by extrinsic signals from the cellular microenvironment, or niche (Fuchs et al., 2004; Walker et al., 2009; Watt and Hogan, 2000). For example, in the bone marrow, quiescent Hematopoietic Stem Cells (HSCs) reside close to the bone within the osteoblastic niche that is composed of mesenchymal osteoblasts, osteoclasts, and CXC-chemokine ligand (CXCL) 12-Abundant Reticular (CAR) cells (Suarez-Alvarez et al., 2012). Signals from the osteoblastic niche regulate stem cell activity. Angiopoietin-1 from the osteoblasts directly binds to the Tie-1 receptor on the HSCs to regulate their quiescence and adhesion to the niche (Arai et al., 2004). The actively dividing HSCs are believed to reside more centrally within the bone marrow, in the vascular niche that lacks osteoblasts and osteoclasts. The vascular niche contains endothelial and CAR cells. The release of CXCL 12 from the CAR cells regulates their self-renewal, mobilization, and homing (Ara et al., 2003; Ceradini et al., 2004).

Similarly, germline cells occupy different microenvironments dependent on their developmental stage. In mammalian testes, all germline cells are enclosed by somatic Sertoli cells. The Spermatogonial Stem Cells (SSCs) and their mitotic daughters are found along the basal membrane of the seminiferous tubules but the distinct morphology of the SSC microenvironment is yet to be distinguished (de Rooij, 2009). According to the current understanding, the SSCs are concentrated in those areas of the seminiferous tubules that are above interstitial cells and bloods vessels (Chiarini-Garcia et al., 2001;

Yoshida et al., 2007). SSC self-renewal is regulated by several extrinsic factors, such as Glial cell line-Derived Neurotrophic Factor (GDNF) and Fibroblast Growth Factor 2 (FGF2) from the Sertoli cells, and Colony Stimulating Factor 1 (CSF1) from the interstitial Leydig cells (Goriely et al., 2005; Kokkinaki et al., 2009; Meng et al., 2000). Differentiating germline cells are displaced away from the basal membrane and receive instructive signals for their differentiation from the Sertoli cells. These signals include Steel factor, Activin A and Bone Morphogenic Protein 4 (Filipponi et al., 2007; Griswold, 1998; Nagano et al., 2003).

Despite the importance of the cellular microenvironment for tissue homeostasis, comparably little is known about how microenvironment cells are regulated. In the gonad of *Drosophila melanogaster*, two different microenvironments were identified, one for GSCs and one for developing GSC daughters. A plethora of genetic manipulations and molecular tools have been established that allow for the study of these microenvironment cells. In testes, GSCs and CySCs contact an apical stem cell organizing center, called the hub. Two CySCs have cytoplasmic extensions around one GSC and into the hub (Fig. 3.1A) (Hardy et al., 1979). The hub cells and the CySCs provide regulatory signals to the GSCs and are considered the GSC cellular microenvironment (de Cuevas and Matunis, 2011). Specifically, hub cells signal via the ligand Upd to activate the Jak/STAT pathway in the contacting germline and somatic support cells (Fig. 3.1B). Upon phosphorylation, pSTAT localizes into the nuclei of cells to regulate the transcription of target genes. In the CySCs, two effectors of Jak/STAT signaling have been identified, Zfh-1 and Chinmo. Loss of any of the components of the pathway leads to loss of CySCs, while hyperstimulation of the pathway, or overexpression of Zfh-1 or Chinmo induces CySC

fate in the somatic support cells in positions away from the hub (Flaherty et al., 2010; Kiger et al., 2001; Leatherman and Dinardo, 2008, 2010; Tulina and Matunis, 2001).

GSCs and CySCs self-renew and produce daughters that differentiate as gonialblasts and cyst cells, respectively. The gonialblast recruits two cyst cells to grow cytoplasmic extensions around it. The growth of cytoplasmic extensions from the somatic support cells (CySCs and cyst cells) and the differentiation of the cyst cells depend on signaling from the germline cells to the somatic support cells via EGF. Stimulation of the EGF-receptor (EGFR) activates downstream signaling cascades that act through the small monomeric GTPases, Rac1, and MAPK, respectively (Fig. 3.1B) (Hudson et al., 2013; Sarkar et al., 2007; Schulz et al., 2002). Once phosphorylated, pMAPK translocates into the nucleus to regulate the expression of target genes (Schlessinger, 2004). However, the transcriptional targets of EGF in testes remain unknown.

Once a gonialblast is enclosed by two cyst cells the three cells develop as a unit, called a cyst. The enclosed gonialblast enters mitotic transit amplifying divisions to generate spermatogonia. Cytokinesis is incomplete in germline cells. Thus, each group of cells derived from a GSC remains interconnected by cytoplasmic bridges that facilitate their synchronous development and gives them the appearance of clusters of cells. After spermatogonia exit transit amplifying divisions the clusters of cells develop into spermatocytes. Spermatocytes grow in size, divide by meiosis, and differentiate into spermatids (Fig. 3.1A) (Fuller, 1993; Hardy et al., 1979). The cyst cells continue to enclose and co-differentiate with the germline, as evident by their increase in size and the expression of stage-specific nuclear markers. CySCs express high levels of Zfh-1, CySCs and early-stage cyst cells (cyst cells associated with spermatogonia) express high levels

of Traffic jam (Tj), and late-stage cyst cells (cyst cells associated with spermatocytes) express high levels of Eyes absent (Eya, Fig. 3.1A-A') (Fabrizio et al., 2003; Leatherman and Dinardo, 2008; Li et al., 2003). Signals from the cyst cells regulate germline differentiation (Zoller and Schulz, 2012). Signaling via Transforming Growth Factor-beta (TGF-β), for example, restricts the number of mitotic amplification divisions in spermatogonia (Bunt and Hime, 2004; Matunis et al., 1997; Schulz et al., 2004).

Here, we address a requirement for the CSN and distinct downstream Cullins in the somatic support cells. The CSN complex is composed of eight subunits of varying sizes, termed CSN1 to CSN8. CSN was originally identified due to its role in light responses in *Arabidopsis thaliana* (Stratmann and Gusmaroli, 2012; Wei et al., 1994). Subsequently, other members of the complex were identified in numerous species (Freilich et al., 1999; Mundt et al., 1999; Seeger et al., 1998; Wei and Deng, 1998; Wei et al., 1998). Subunits of the CSN are nuclear enriched and have been implicated in important processes, such as cell proliferation, lipid metabolism, and cancer (Licursi et al., 2014; Richardson and Zundel, 2005; Yan et al., 2003). In *Drosophila*, the CSN has been associated with many developmental processes, including muscle development, development of the immune system, and the temporal regulation of gene expression during the transitions between larval stages (Bech-Otschir et al., 2002; Goubeaud et al., 1996; Harari-Steinberg et al., 2007; Oron et al., 2007).

The CSN complex modulates the activity of CRL complexes. A CRL complex consists of a catalytic region containing the E3 RING Ubiquitin ligase, a Cullin scaffold, and a substrate-binding region that connects to Cullin, often via an adaptor protein. The combination of different Cullins and substrate receptors provides the complexes with

specificity in targeting different substrates for poly-ubiquitination by the proteasome (Bosu and Kipreos, 2008; Sarikas et al., 2011). The activity of CRLs is regulated by the presence or absence of a covalently linked Ubiquitin-like molecule, termed Nedd8, to the Cullin scaffold (Pan et al., 2004). CSN, specifically, removes Nedd8 from the Cullin scaffold. This modification prevents auto-ubiquitination and promotes disassembly of the CRL (Bosu and Kipreos, 2008; Cope and Deshaies, 2006; Cope et al., 2002; Lyapina et al., 2001).

Here, we show that knockdown of CSN-subunits and distinct *cullins* disrupted the function of the somatic support cells in *Drosophila* testes. Expression of an RNA-hairpin directed against the subunit *CSN2*, also known as *Drosophila alien*, or other subunits of the CSN complex in the somatic support cells resulted in two distinct responses: a failure of the somatic support cells to grow and maintain cytoplasmic extensions around the germline cells, and a reduction in the levels of the CySC-specific transcription factors Zfh-1 and Chinmo in the somatic support cell nuclei. The upstream signaling pathways regulating germline enclosure and CySC fate, EGF and Jak/STAT, respectively, appeared to be stimulated normally, based on the nuclear localization of the signal transducers, pMAPK and pSTAT. This places CSN function downstream of, or parallel to these signaling events. Finally, we show that Cul2 is required for germline enclosure, while Cul1 is required for maintaining a high level of Chinmo in the CySCs. We propose that CSN acts via different CRLs to enable the somatic support cell's response to the external EGF and Upd signals.

Material and methods

Fly husbandry

All fly lines in this study were raised and maintained on standard cornmeal molasses agar diet at room temperature, unless otherwise stated. The following flies carrying RNAi and overexpression constructs were obtained from the Bloomington Stock Center: *UAS-alien-RNAi*$^{TRiP.HM05119}$ [BL#28908]; *UAS-lin19-RNAi*$^{TRiP.HM05197}$ [BL#29520]; *UAS-cul-2-RNAi*$^{TRiP.HM05237}$ [BL#30494]; *UAS-cul-3-RNAi*$^{TRiP.HMS01572}$ [BL#36684]; *UAS-CSN1b-RNAi*$^{TRiP.JF02612}$ [BL#27303]; UAS-*CSN3-RNAi*$^{TRiP.HMS00242}$ [BL#33369]; *UAS-CSN4-RNAi*$^{TRiP.GL01169}$ [BL#42798]; *UAS-CSN5-RNAi*$^{TRiP.JF03159}$ [BL#28732]; *UAS-CSN6-RNAi*$^{TRiP\ HMS02392}$ [BL# 41991]; *UAS-CSN7-RNAi*$^{TRiP.HMS00073}$ [BL#33663]; *C784-Gal4* [BL#6985]; *tubulin-Gal80*^{ts} [BL#7018]. *UAS-cul-4-RNAi*$^{P\{GD14006\}}$ [v44829] was obtained from the Vienna *Drosophila* Research Center and the *tj-Gal4* stock from the Kyoto stock center [#104-055]. The *eya-Gal4* stock was a gift from Steve DiNardo.

UAS/Gal4 expression studies

Animals carrying the *Gal4*-transactivators and the temperature sensitive *tubulin-Gal80* were crossed to animals carrying the *UAS-RNAi*-constructs. Flies were placed on apple juice plates in an 18°C incubator with humidity control and day/night cycle. Apple juice plates were transferred into food bottles and the progeny were raised at 18°C. After eclosure, adult animals carrying all three constructs were either kept at 18°C as non-shifted controls or shifted to 29°C to induce high activity of the *UAS/Gal4*-system (Duffy, 2002). Animals carrying only the *Gal4*- and *Gal80*-constructs (*Gal4/Gal80*), and

wild-type animals were raised and kept under the same conditions and served as controls. Unless otherwise stated, testes from experimental animals were dissected seven days after the temperature shift.

Immunofluorescence experiments and microscopy

Immunofluorescence experiments were performed as previously described (Flaherty et al., 2010; Schulz et al., 2002). The following hybridoma/monoclonal antibodies were obtained from the Developmental Studies Hybridoma Bank, developed under the auspices of the NICHD, and maintained by The University of Iowa, Department of Biological Sciences, Iowa City, IA 52242: mouse anti-α-Spectrin (3A9) (1:10), mouse anti-Eya (1:10), mouse anti-Fasciclin III (Fas III, 1:10), rat anti-ECad (1:5), and rat anti-NCad (1:5). Goat anti-Vasa (1:150) and rabbit anti-Arm (1:500) were obtained from Santa Cruz Biotechnology. Rabbit anti-pMAPK (P-p44/42 MAPK, T202/Y204, 1:200) was obtained from Cell Signaling and rabbit anti-pHH3 (1:800) was obtained from Millipore. Guinea-pig anti-Tj (1:5000) was a gift from Dorothea Godt. Rabbit anti-pSTAT (1:1000) and rabbit anti-Chinmo (1:1000) were gifts from Erika Bach. Rabbit anti-Zfh-1 (1:100) was a gift from Ruth Lehman. Alexa-488-, Cy3, and Cy5-conjugated secondary antibodies (Invitrogen) were used at 1:1000. Testes were embedded in SlowFade Gold Antifade Reagent with 4’,6-diamidino-2-phenylindole (DAPI, Life Technologies) and were observed using a Zeiss Axiophot microscope. Images were taken with a CCD camera using an Apotome and Axiovision Rel Software, using the same exposure time within each set of control and experimental genotypes.

Pixel counts were performed using the Axiovision Rel Software. The TUNEL assay was performed following the manufacturer's (Roche) instructions.

Results

Expression of an RNA-hairpin against alien in the somatic support cells resulted in an accumulation of early-stage germline cells

To investigate a role for CSN in the adult male gonad an RNA-hairpin construct directed against *alien* (*UAS-alienRNAi*) was expressed in the testes using the tissue-specific *UAS/Gal4* expression system (Brand and Perrimon, 1993; Phelps and Brand, 1998). Staining with the molecular marker, anti-Vasa, distinguishes the early-stage germline cells (GSCs, gonialblasts, and spermatogonia) from the spermatocytes. While the early-stage germline cells are small (Fig. 3.1C, arrowhead) and found in the most apical region of a control testis, the spermatocytes are large (Fig. 3.1C, small arrow) and found more basally. The long spermatids can be seen in the lumen and at the base of the testis (Fig. 3.1C, large arrow, n>100). Expression of *UAS-alienRNAi* in the somatic support cells of otherwise wild-type testes (cyst cell-*alienRNAi*-testes) using three different somatic *Gal4*-transactivators (*tj-Gal4*, *eya-Gal4*, or *C784-Gal4*) produced a drastic phenotype in 100% of the testes. When shifted to 29°C for one week, the apical region of a testis contained large areas of small, Vasa-positive cells (Fig. 3.1D, small arrowheads), indicative of early-stage germline cells (n>100). The remainder of the testis was filled with cell debris indicating that expression of *UAS-alienRNAi* induced cell death in the developing germline-soma cysts (Fig. 3.1D, large arrowhead). We never observed such a phenotype in non-shifted animals kept at 18°C for up to two weeks

(n>50), or in testes from shifted control *UAS-alienRNAi* or control *Gal4/Gal80* flies (n>50, data not shown). We conclude that the observed germline phenotype was due to the expression of UAS-*alienRNAi* in the somatic support cells. We did not observe a mutant phenotype upon expression of *UAS-alienRNAi* in the germline cells (n>30, data not shown), suggesting that *alien* may be required specifically in somatic support cells.

The germline cells at various stages of differentiation contain subcellular structures of different shape and size, the fusomes (Lin et al., 1994). These can be visualized with antibodies against α-spectrin. GSCs and gonialblasts are single cells that each contain a single round fusome (Fig. 3.2A-A', arrowheads). Developing germline cells within one cyst are interconnected by cytoplasmic bridges. In these cells, the fusome grows and reaches through the intercellular bridges, making it appear progressively more branched as the number of interconnected germline cells increases (Fig. 3.2A-A', small arrows). The fusomes in the spermatocytes are wider (Fig. 3.2A-A', large arrows) than the fusomes in spermatogonia due to the differences in cell sizes. The germline cells in all of the cyst cell-*alienRNAi*-testes contained round fusomes (Fig. 3.2B-B', arrowheads) and thin, slightly branched fusomes (Fig. 3.2B-B', small arrows) normally seen in early-stage germline cells but lacked fusomes characteristic of spermatocytes (n>50).

Another excellent criterion for determining the developmental stage of the germline cells is their cell division pattern revealed by the expression of cell cycle-specific proteins (Gonczy and DiNardo, 1996). The single GSCs and gonialblasts divide independently of the divisions of other cells and when labeled with Vasa and a mitosis marker, anti-phosphorylated Histone-H3 (pHH3), are detectable as single Vasa-positive, pHH3-positive cells located close to the hub (Fig. 3.2C, arrowhead). The clusters of

spermatogonia within one cyst, on the other hand, divide in synchrony and are detectable in groups of two, four (Fig. 3.2C, arrow), or eight Vasa-positive, pHH3-positive cells located away from the hub. In cyst cell-*alienRNAi*-testes, single dividing, Vasa-positive germline cells (Fig 2D, arrowheads, inset) and groups of two or four dividing cells (data not shown) were scattered throughout the apical region (100%, n>50). This finding confirms that the accumulating germline cells in cyst cell-*alienRNAi*-testes were groups of interconnected spermatogonia and single cells that could have been GSCs, gonialblasts, or both.

To examine if the single germline cells away from the hub were GSCs or gonialblasts, we used antibodies targeted against pSTAT. In control (Fig. 3.2E, arrow, n>30) and cyst cell-*alienRNAi*-testes (Fig. 3.2F, arrow, n>30), we always detected germline cells with nuclear pSTAT located in the stem cell position next to the hub, but germline cells with nuclear pSTAT away from the hub were never observed. Together, our data show that the accumulating germline cells in cyst cell-*alienRNAi*-testes were gonialblasts and spermatogonia.

Somatic support cells in cyst cell-alienRNAi-testes lacked cytoplasmic extensions

Differentiation of the germline cells is dependent on their enclosure by cytoplasmic extensions from the somatic support cells (Schulz et al., 2002). The cytoplasmic extensions can be visualized using antibodies against cell surface markers. For example, the Vasa-positive germline cells are enclosed in cytoplasmic extensions that are positive for the adherens junction protein Armadillo (Arm). The cytoplasmic extensions are seen as a net-like pattern that surrounds the clusters of germline cells (Fig.

3.3A-A', small arrows). We never detected this net-like pattern of cytoplasmic extensions around the germline upon expression of *UAS-alienRNAi* in the somatic support cells. In cyst cell-*alienRNAi*-testes, Vasa-positive germline cells were not enclosed by Arm-positive cytoplasmic extensions (Fig. 3.3B-B'), even though Arm was expressed in the apical hub and some cytoplasmic extensions were seen near the testis sheath (Fig. 3.3B', large arrow, n>50). Despite the lack of cytoplasmic extensions around the germline, the early-stage somatic support cells were readily detectable in cyst cell-*alienRNAi*-testes based on nuclear Tj-staining (compare Fig. 3.3D to Fig. 3.3C, arrowheads, n>100). Other cell surface markers, such as the cell adhesion molecules E-Cadherin (ECad) and N-Cadherin (NCad) also detected cytoplasmic extensions in a net-like pattern in control testes (Fig. 3.3C-C' and 3E-E', respectively, small arrows, n>50). Only very few and short cytoplasmic extensions (Fig. 3.3D-D' and 3. 3F-F', respectively, large arrows, n>50) but no net-like pattern of cytoplasmic extensions were seen in cyst cell-*alienRNAi*-testes. We conclude that the knockdown of *alien* disrupted the cellular microenvironment of the germline cells.

A timeline experiment revealed that the cytoplasmic extensions were quickly lost in response to the knockdown of *alien*. Testes from cyst cell-*alienRNAi* and control flies were dissected prior to (day 0) and 1, 2, or 3 days after the shift from 18°C to 29°C. All testes from non-shifted cyst cell-*alienRNAi*-animals (Fig. 3.4A-A') and from all other control animals appeared normal when co-labeled for Tj and Arm. However, by day 1 after the shift to the restrictive temperature, holes in the net-like pattern of cytoplasmic extensions were observed in 50% of the cyst cell-*alienRNAi*-testes (Fig. 3.4B-B', small arrowheads, n>50). By day 2, large areas that did not contain Arm-positive cytoplasmic

extensions were observed in 70% of the cyst cell-*alienRNAi*-testes (Fig. 3.4C-C', large arrowhead, n>50), and by day 3, the cytoplasmic extensions had almost vanished from the majority (95%) of the cyst cell-*alienRNAi*-testes (Fig. 3.4D-D', n>50). The cytoplasmic extensions from the somatic support cells are rapidly growing to accommodate the dividing, enclosed germline cells. A simple explanation for the quick response to reduction in *alien* is a requirement for *alien* either in the growth or in the stability of the cytoplasmic extensions. None of the testes from control animals displayed disruptions in the cytoplasmic extensions (data not shown, n>50). No signs of cell death were observed in the Tj-positive somatic support cells in the apical region of cyst cell-*alienRNAi*-testes based on the Terminal deoxynucleotidyl transferase dUtp Nick End Labeling (TUNEL) cell death assay (data not shown, n>50). This suggests that knockdown of *alien* did not impair viability of these somatic support cells.

A possible explanation for the failure of the somatic support cells in cyst cell-*alienRNAi*-testes to maintain cytoplasmic extensions could be a lack of EGF signaling. In control testes, pMAPK was detected in the nuclei of all Tj-positive somatic support cells (Fig. 3.4E-E', large arrows). We also detected pMAPK in the cytoplasm of all somatic support cells (Fig. 3.4E-E', small arrows), resembling the net-like pattern of the cytoplasmic extensions seen with the surface markers shown above (n>50). In 100% of cyst cell-*alienRNAi*-testes, pMAPK always co-localized with Tj in the somatic cell nuclei (Fig. 3.4F-F', large arrows, n>50). This finding shows that somatic support cells in cyst cell-*alienRNAi*-testes did receive and transduce the EGF signal, and excludes the possibility that Alien regulates MAPK phosphorylation or nuclear translocation. Due to

the lack of cytoplasmic extensions, we did not detect a net-like pattern of pMAPK-staining in cyst cell-*alienRNAi*-testes (Fig. 3.4F-F').

The levels of transcription factors that act downstream of Jak/STAT signaling were reduced in cyst cell-alienRNAi-testes

Expression of *UAS-alienRNAi* in the somatic support cells led to a severe reduction in the levels of CySC stage-specific transcription factors. STAT activation in CySCs appeared normal in control and cyst cell-*alienRNAi*-testes, as all Tj-positive cell nuclei next to the hub were positive for the pSTAT antibody (compare Fig. 3.5B-B' to Fig. 3.5A-A', arrows). In response to JAK/STAT signaling, CySCs express high levels of the transcription factors Zfh1 and Chinmo. In control testes, we always detected Zfh1 at a high level in CySC nuclei (Fig. 3.5C-C', arrow) and at lower levels in the cyst cell nuclei (n>50). Surprisingly, Tj-positive nuclei in the CySC position next to the hub did not express a high level of Zfh1 in any of the cyst cell-*alienRNAi*-testes (Fig. 3.5D-D', arrow, n>50). For unknown reasons, a high level of Zfh-1 was detected in random Tj-positive nuclei positioned away the hub (Fig. 3.5D-D', large arrowhead) and in nuclei of the testis sheath (Fig. 3.5D-D', small arrowhead).

In control testes, Chinmo was expressed at high levels in CySC nuclei (Fig. 3.5E-E', arrows) and to some degree in the cyst cell nuclei. In cyst cell-*alienRNAi*-testes, Chinmo was hardly detectable in Tj-positive nuclei next to the hub (Fig. 3.5F-F', arrows). Pixel counts that quantify the level of Chinmo confirmed that Chinmo was significantly reduced in the Tj-positive cells next to the hub in cyst cell-*alienRNAi*-testes compared to controls (Fig. 3.6A, Table 1). Together, this suggests that knockdown of *alien* either

reduces the expression or leads to degradation of the transcription factors Zfh-1 and Chinmo in the CySCs. Notably, the expression levels of Tj did not appear to be affected in cyst cell-*alienRNAi*-testes (Fig. 3.5B, 3.5D, and 3.5F), suggesting that the observed reduction in Chimno and Zfh-1 was due to a selective process.

Despite the reduction in the levels of Zfh-1 and Chinmo, knockdown of *alien* did not disrupt the ability of the somatic support cells to divide by mitosis. In control testes, Tj-positive, pHH3-positive cells were mostly found close to the hub (Fig. 3.6B, arrowheads). In cyst cell-*alienRNAi*-testes as well, we detected Tj-positive, pHH3-positive somatic support cells close to the hub (Fig. 3.6C, arrowheads) indicating that the somatic support cells in the stem cell position responded to proliferative signals.

Finally, we investigated if the somatic support cells in cyst cell-*alienRNAi*-testes had the ability to differentiate into late stage. The transcription factor Eya is normally only expressed at low levels in early-stage cyst cells but at high levels in late-stage cyst cells (Fig. 3.6D-D', arrows). In cyst cell-*alienRNAi*-testes, Eya was barely detectable (Fig. 3.6E-E', arrows), strongly implicating that the somatic support cells remained at early stage. As the upstream signaling pathway activating high levels of Eya is not known, we were not able to examine whether or not the pathway was activated upon knockdown of *alien* from somatic support cells.

Alien acts through its role in the CSN and via distinct Cullins to regulate germline enclosure and the level of Chinmo

Cyst cell-RNA*i* against several other members of CSN (CSN1b, CSN3, and CSN6) caused identical phenotypes to cyst cell-*alienRNAi*. For example, expression of an

RNA-hairpin directed against CSN1b (cyst cell-*CSN1bRNAi*-testes) always resulted in cells that expressed Tj but lacked Arm-positive cytoplasmic extensions (compare Fig. 3.7B to Fig. 3.7A, n>50). Furthermore, somatic support cells in cyst cell-*CSN1bRNAi*-testes and cyst cell-*CSN3RNAi*-testes had a low level of Chinmo in the Tj-positive nuclei next to the hub (Fig. 3.6A, Table 1). Cyst cell-RNAi against other subunits of the CSN complex (CSN4, CSN5, CSN7) produced similar but weaker defects in germline enclosure and differentiation (data not shown). We conclude that Alien acts though its role in the CSN in the somatic support cells of the testes.

Finally, we asked if a loss or reduction of any of the *cullins* produced a similar phenotype to knockdown of *alien*. For this, we expressed available hairpins against *Drosophila cul1*, *cul2*, *cullin3* (*cul3*), or *cullin4* (*cul4*) in the somatic support cells. We discovered that the expression of an RNA-hairpin against *cul2* led to strong defects in germline enclosure in 100% of the testes (Fig. 3.7C-C'). These defects were identical to the defects seen upon expression of the RNA-hairpin against *alien* (compare to Fig. 3.3B). Expression of RNA-hairpins against *cul1*, *cul3*, or *cul4* did not disrupt germline enclosure, as cytoplasmic extensions were clearly detected in a net-like pattern around the germline in 100% of the cyst cell-*cul1RNAi*-testes (Fig. 3.7D-D', small arrows, n>30), cyst cell-*cul3RNAi*-testes (data not shown, n>30), and cyst cell-*cul4RNAi*-testes (data not shown, n>30). We cannot exclude the possibility that the RNA-hairpins did not fully knockdown *cul1*, *cul3*, and/or *cul4* in our experiments. However, the RNA-hairpin against *cul2* produced a different phenotype than the RNA-hairpins against *cul1*, *cul3*, or *cul4*, strongly suggesting that they play distinct roles.

While a reduction in *cul2* disrupted germline enclosure it did not affect the level of Chinmo. In cyst cell-*cul2RNAi*-testes, normal levels of Chinmo were easily detectable in the somatic support cells next to the hub (Fig. 3.7E-E', arrows, Fig. 3.6A, Table 1). In contrast, Chinmo was hardly detectable in the somatic support cells next to the hub in cyst cell-*cul1RNAi*-testes (Fig. 3.7F-F', arrows, Fig. 3.6A, Table 1). We conclude that CSN and Cul2 maintain the germline cellular microenvironments while CSN and Cul1 maintain a high level of Chinmo in the CySCs.

Discussion

Here we show that knockdown of *alien* from somatic support cells disrupted the cellular microenvironment of the germline cells. Interestingly, Alien activity was associated with the regulation of nuclear hormone signaling. When transformed into Hela cells, Alien interacts with the thyroid hormone receptor in a ligand-dependent manner. A similar role for Alien as a co-regulator for the Ecdysone receptor (EcR) has been suggested (Dressel et al., 1999). However, Alien does not appear to act as a co-regulator of the EcR in somatic support cells as depletion of EcR signaling molecules from these cells did not produce a mutant phenotype (Qian et al., 2014). Instead, Alien acts though its role in the CSN. As with the expression of the RNA-hairpin directed against *alien* in the somatic support cells, the expression of RNA-hairpins against other subunits of the CSN complex in these cells disrupted germline enclosure. The CSN has not been associated with the maintenance or function of cellular microenvironments in any species. Given the importance of cellular microenvironments for tissues homeostasis and the conservation of the CSN complex among plant and animal species, it seems highly

likely that a similar role for CSN may be discovered in other tissue maintained by stem cells.

The knockdown of *alien* from the somatic support cells also caused an accumulation of early-stage germline cells within the mutant testes. A similar germline phenotype was observed in other mutants that affect the structure of the microenvironment cells, such as those in Tj, Dynein Light Chain, or those in components of EGF signaling (Joti et al., 2011; Li et al., 2003; Schulz et al., 2002). We therefore propose that the observed failure of germline cells to differentiate in cyst cell-*alienRNAi*-testes was an indirect effect due to the loss of the cellular microenvironment.

In addition to the defects in germline enclosure, cyst cell-*alienRNAi*-testes had reduced levels of Zfh-1 and Chinmo in the somatic support cells next to the hub, suggesting that these cells were not CySCs. Yet, these cells occupied the CySC position, had pSTAT and nuclear pMAPK in their nuclei, and divided by mitosis, indicating that they had CySC characteristics. These latter observations suggest that high levels of Zfh-1 and Chinmo may be dismissible for CySC fate or function. A low level of Zfh-1 and Chinmo could be sufficient for CySC fate as long as the cells remain in contact with the hub. Possibly, pSTAT or other signal transducers activate additional downstream effectors for CySC fate or function.

The CSN complex has been associated with stem cell maintenance in human embryonic stem cells and GSCs in the *Drosophila* ovary (Chia et al., 2010; Pan et al., 2014; Yan et al., 2003). In the *Drosophila* ovary, germline cells were depleted of CSN function using mosaic analysis. In this technique, the homozygous mutant GSCs were quickly lost from the stem cell position while the heterozygous GSCs were maintained

(Pan et al., 2014). Recently, competition for the position next to the hub has been shown to be one of the mechanisms to assure that a healthy population of stem cells is maintained in the gonad (Issigonis et al., 2009; Sheng et al., 2009). In the context of mosaic analysis, a CSN-depleted CySC may be disadvantaged and lose the competition for the position next to the hub. In our experiments, we depleted the CSN from all CySCs. CySCs, in turn, are instructive for GSC fate (Leatherman and Dinardo, 2010). Thus, we can assume that we created a non-competitive environment that allowed CSN-depleted CySCs to be maintained next to the hub.

In the ovary, CSN4 was reported to specifically interact with the cytoplasmic differentiation factor Bag of marbles (Bam) and this interaction was proposed to regulate the balance between GSC self-renewal and differentiation (Pan et al., 2014). fmc is not expressed in somatic support cells of the testes and thus is not likely to regulate CSN function in the CySC lineage. We did not observe a loss of germline cells in the position next to the hub upon expressing the RNA-hairpins against subunits of CSN in all germline cells (data not shown). This could be due to a lack of competition between the CSN-depleted GSCs, or because we did not sufficiently reduce the CSN subunits from the germline.

We showed that different Cullins, which are known to function downstream of the CSN complex, mediate different cellular responses of the somatic support cells. Cyst cell-*cul1RNAi*-testes had reduced levels of Chinmo. We propose that Cul1 promotes CySC fate via controlling the levels of Zfh-1 and Chinmo downstream of Jak/STAT activation. Cyst cell-*cul2RNAi*-testes showed defects in germline enclosure. We propose that Cul2 regulates germline enclosure in the CySCs and the cyst cells downstream of MAPK

activation, possibly by regulating EGF-targets. Different roles for the Cullin scaffolds downstream of the CSN have been described in dendrite morphogenesis. In this aspect of development, the CSN acts through Cul1 to stimulate dendritic branching and through Cul3 to inhibit it (Djagaeva and Doronkin, 2009a, b). It would be interesting to address if and how selected protein degradation acts in mammalian tissues maintained by stem cells. Specifically, studying the role of different Cullins may provide useful information for furthering our understanding of tissue homeostasis.

Acknowledgments

The authors are indebted to Richard Zoller, Alicia Hudson, Manashree Malpe, and Karl Kudyba for technical assistance. We thank Dorothea Godt, Erika Bach, Ruth Lehmann, and Steve DiNardo for reagents, and Allan Spradling and Edward Kipreos for critical discussions. Furthermore, we are grateful to Edward Kipreos and members of the Schulz laboratory for comments on the manuscript. This work was supported by NSF grants #0841419 and #1355099 given to CS.

Genotype	**#testes**	**#cells**	**Chinmo**	**s.d.**
UAS-alienRNAi/+	20	51	222.12	58.76
Cyst cell-*alienRNAi*	21	40	96.05	36.87
UAS-CSN1bRNAi/+	27	65	125.12	45.42
Cyst cell-*CSN1bRNAi*	18	53	52.65	15.18
UAS-CSN3RNAi/+	25	61	193.72	56.89
Cyst cell-*CSN3RNAi*	23	56	114.46	41.20
UAS-cul2RNAi/+	24	59	230.77	94.50
Cyst cell-*cul1RNAi*	30	69	122.60	50.47
Cyst cell-*cul2RNAi*	18	33	208.26	64.12
Cyst cell-*cul3RNAi*	25	67	200.99	87.52

Table 3.1:

The levels of Chinmo in the Tj-positive cells next to the hub. Genotypes, number of testes, and number of somatic support cell next to the hub analyzed (cells) are as indicated. A reduction of Chinmo (measured as pixels per inch) was observed upon knockdown of subunits of the CSN and upon knockdown of Cul2, s.d.= standard deviation.

Figure 3.1: Expression of the RNA-hairpin against *alien* in somatic support cells produced a strong phenotype.

(A) Illustration of the arrangement and development of germline and somatic support cells. The apical hub is shown in yellow, germline cells in light blue, and cyst cells are color-coded according to their developmental stage; CySCs in pink, early-stage cyst cells in purple, and late-stage cyst cells in green.

(A') The apical region of a wild-type testis labeled for stage-specific, nuclear markers for somatic support cells, as indicated.

(B) Illustration of the key players in Jak/STAT and EGF signaling that regulate CySC fate, germline enclosure, and cyst differentiation. Cell types in light grey, receptors in blue, signal transducers that translocalize into nuclei in red, other signal transducers in black, transcription factors in green.

(C) A whole testis from a control animal showing small, Vasa-positive, early-stage germline cells (arrowhead), and large, Vasa-positive spermatocytes (small arrow). Sperm bundles are seen at the base (large arrow).

(D) A whole testis from a cyst cell-*alienRNAi*-animal with excess small, Vasa-positive, early-stage germline cells (small arrowheads) in the apical region but lacking spermatocytes and sperm bundles. Note that cell debris (large arrowhead) is filling the basal region of the testis, indicative of massive cell death.

Asterisks mark the hubs, scale bars: 30 μm.

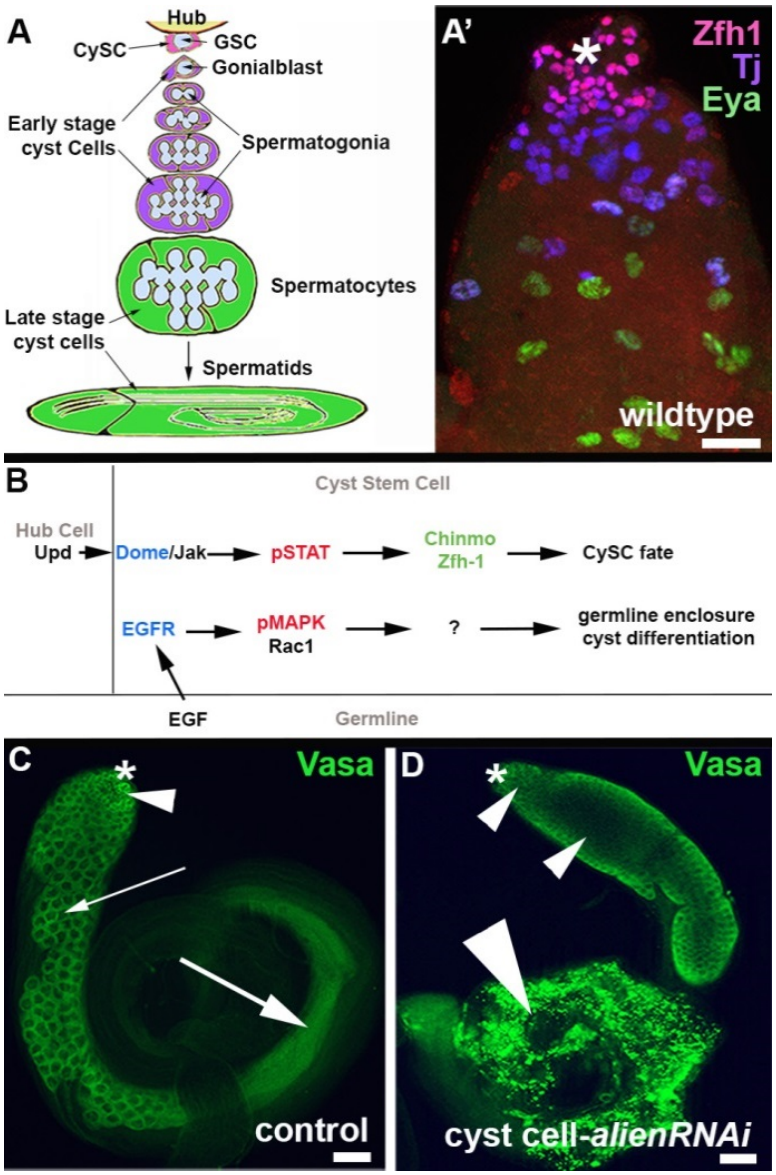
A
Hub
CySC
GSC
Gonialblast
Early stage
cyst Cells
Spermatogonia
Spermatocytes
Late stage
cyst cells
Spermatids
A'
Zfh1
Tj
Eya
wildtype
B
Cyst Stem Cell
Hub Cell
Upd
Dome/Jak
pSTAT
Chinmo
Zfh-1
CySC fate
EGFR
pMAPK
Rac1
?
germline enclosure
cyst differentiation
EGF
Germline
C
Vasa
control
D
Vasa
cyst cell-alienRNAi

Figure 3.2: Germline differentiation was blocked in cyst cell-*alienRNAi*-testis.

(A)-(F) Immuno-labeling with molecular markers, as indicated.

(A) and (A') A control testis tip with a round fusome (arrowheads) in GSCs and gonialblasts, thin fusomes (small arrows) interconnecting spermatogonia, and thick fusomes (large arrows) interconnecting spermatocytes.

(B) and (B') Apical region of a cyst cell-*alienRNAi*-testis showing round fusomes (arrowheads) and short, thin fusomes (arrows).

(C) A control testis tip with a single dividing GSC (arrowhead) next to the hub and a group of four dividing spermatogonia (arrow) displaced away from the hub.

(D) Apical region of a cyst cell-*alienRNAi*-testis showing single dividing germline cells (arrowheads) in positions away from the hub. Inset shows two dividing Vasa-positive germline cells at a high magnification.

(E) and (F) Nuclear pSTAT (green) was only detected in the cells around the apical hub in (E) a control testis and (F) a cyst cell-*alienRNAi*-testis.

Asterisks mark the hubs, scale bars: 30 μm.

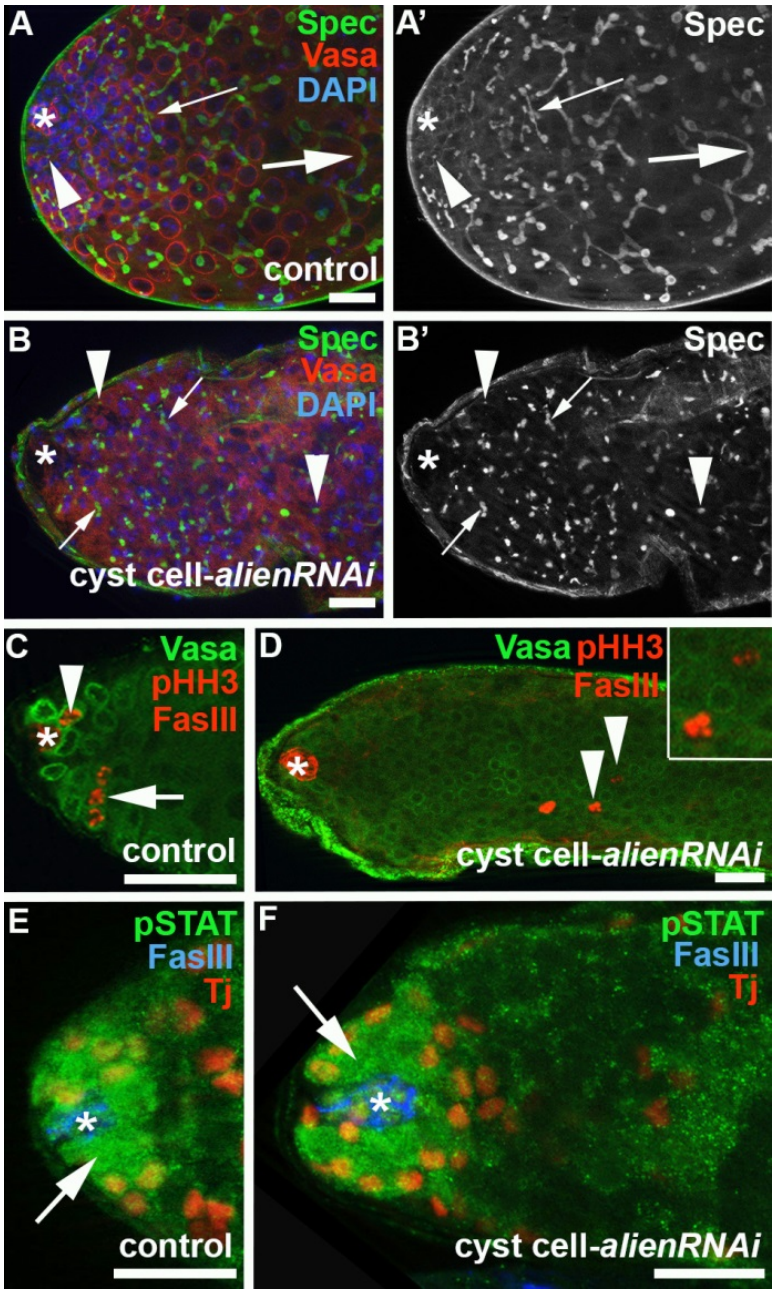
A
Spec
Vasa
DAPI
control
A'
Spec
B
Spec
Vasa
DAPI
cyst cell-alienRNAi
B'
Spec
C
Vasa
pHH3
FasIII
control
D
Vasa pHH3
FasIII
cyst cell-alienRNAi
E
pSTAT
FasIII
Tj
control
F
pSTAT
FasIII
Tj
cyst cell-alienRNAi

Figure 3.3: In cyst cell-*alienRNAi*-testis, the germline cells lacked their cellular microenvironment.

(A)-(F') Apical regions of testes immuno-labeled with molecular markers, as indicated. Small arrows point to cytoplasmic extensions surrounding the germline cells, large arrows point to cytoplasmic extensions in the mutant testes, and arrowheads point to somatic support cell nuclei.

(A) and (A') A control testis showing an Arm-positive, net-like pattern of cytoplasmic extensions around the germline.

(B) and (B') A cyst cell-*alienRNAi*-testis without an Arm-positive, net-like pattern of cytoplasmic extensions around the germline. Note that the hub is positive for Arm.

(C) and (C') A control testis showing Tj-positive cyst cell nuclei and an ECad-positive, net-like pattern of cytoplasmic extensions.

(D) and (D') A cyst cell-*alienRNAi*-testis contains Tj-positive cyst cell nuclei but lacks the ECad-positive, net-like pattern of cytoplasmic extensions.

(E) and (E') A control testis with Tj-positive cyst cell nuclei and an NCad-positive, net-like pattern of cytoplasmic extensions.

(F) and (F') A cyst cell-*alienRNAi*-testis contains Tj-positive cyst cell nuclei but lacks the NCad-positive, net-like pattern of cytoplasmic extensions.

Asterisks mark the hubs, scale bars: 30 μm.

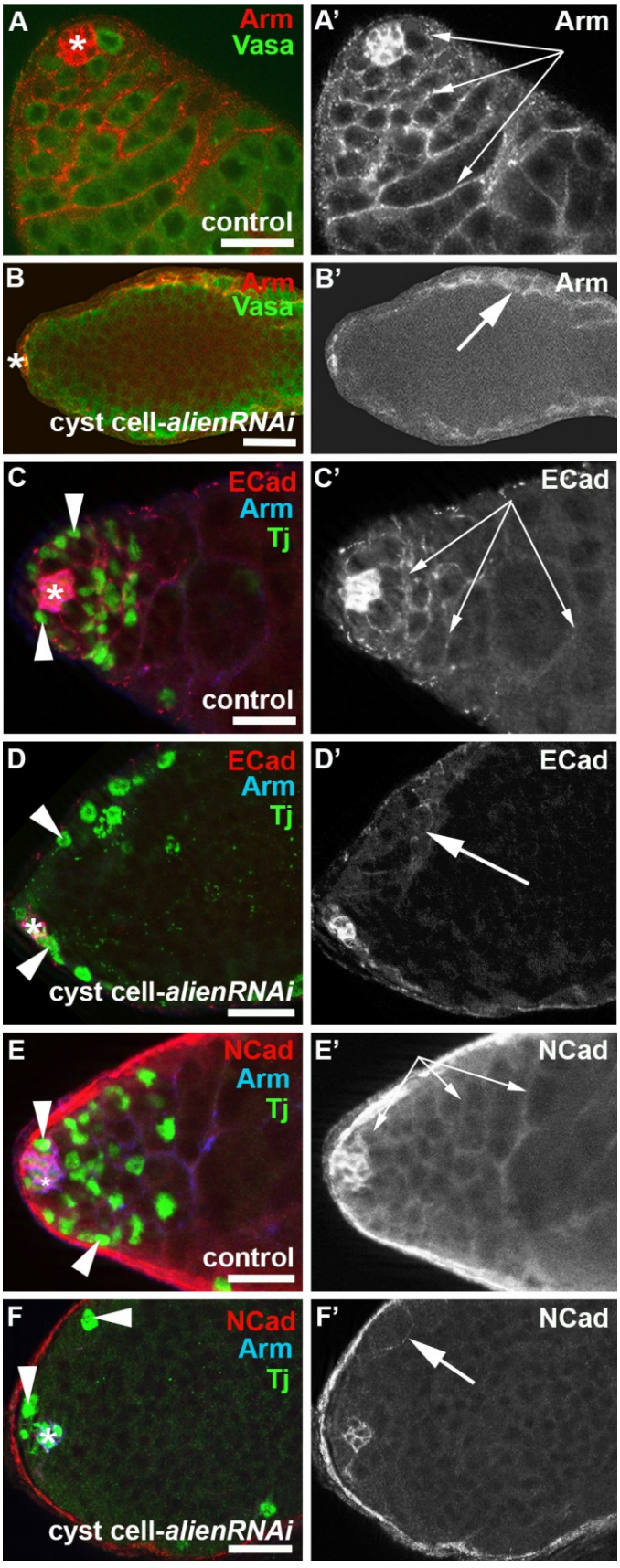
A
Arm
Vasa
control
A'
Arm
B
Arm
Vasa
cyst cell-alienRNAi
B'
Arm
C
ECad
Arm
Tj
control
C'
ECad
D
ECad
Arm
Tj
cyst cell-alienRNAi
D'
ECad
E
NCad
Arm
Tj
control
E'
NCad
F
NCad
Arm
Tj
cyst cell-alienRNAi
F'
NCad

Figure 3.4: Reduction of *alien* in somatic support cells led to a quick loss of cytoplasmic extensions.

(A)-(F') Apical tips of testes, immuno-labeling as indicated.

(A)-(D') Arm-positive cytoplasmic extensions in cyst cell-*alienRNAi*-testis

(A) and (A') appear normal prior to the shift to 29°C (day 0),

(B) and (B') show holes (small arrowheads) by day 1 after the shift to 29°C,

(C) and (C') have large disruption (large arrowhead) by day 2 after the shift to 29°C,

(D) and (D') are almost gone by day 3 after the shift to 29°C.

(E) In a control testis, Tj-positive somatic support cells had pMAPK in their nuclei (large arrows) and in their cytoplasm (small arrows).

(F) and (F') In a cyst cell-*alienRNAi*-testis, pMAPK co-localized with Tj in somatic support cell nuclei.

Asterisks mark the hubs, scale bars: 30 μm.

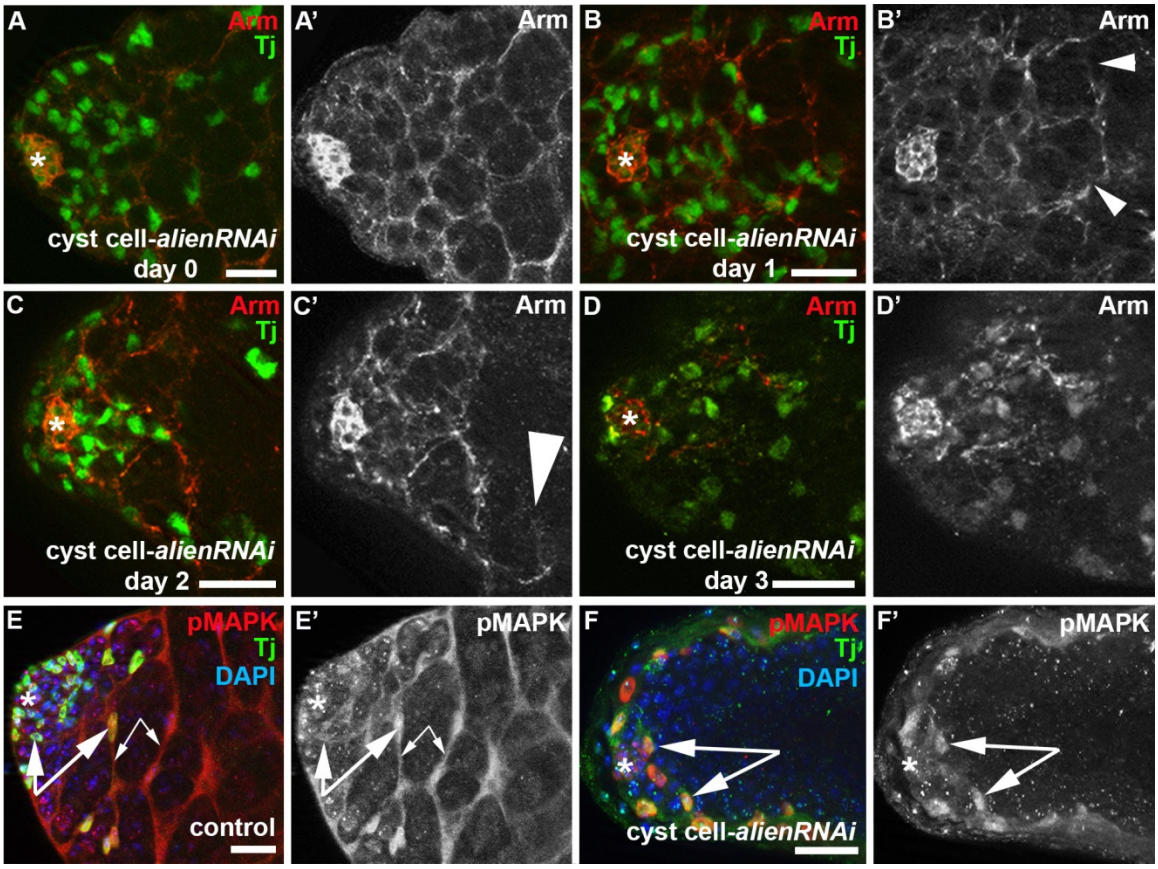
A
Arm
Tj
cyst cell-alienRNAi
day 0
A'
Arm
B
Arm
Tj
cyst cell-alienRNAi
day 1
B'
Arm
C
Arm
Tj
cyst cell-alienRNAi
day 2
C'
Arm
D
Arm
Tj
cyst cell-alienRNAi
day 3
D'
Arm
E
pMAPK
Tj
DAPI
control
E'
pMAPK
F
pMAPK
Tj
DAPI
cyst cell-alienRNAi
F'
pMAPK

Figure 3.5: *alien*-depleted somatic support cells have lower levels of the transcription factors Zfh-1 and Chinmo.

(A)-(F') Apical testes tips immuno-stained with molecular markers, as indicated.

(A)-(B') pSTAT in Tj-positive nuclei next to the hub in (A) and (A') a control testis and (B) and (B') a cyst cell-*alienRNAi*-testis.

(C) and (C') In control, Tj-positive nuclei next to the hub had a high levels of Zfh-1 (arrows) while the Tj-positive nuclei away from the hub had decreasing levels of Zfh-1.

(D) and (D') In a cyst cell-*alienRNAi*-testis, Zfh-1 was hardly detectable in Tj-positive nuclei next to the hub (arrows). Note that a high level of Zfh-1 was detected in nuclei of the testis sheath (small arrowhead) and random Tj-positive cells located away from the tip (large arrowhead).

(E) and (E') In a control testis, Tj-positive cell nuclei (large arrows) next to the hub showed a high level of Chinmo.

(F) and (F') In a cyst cell-*alienRNAi*-testis, a low level of Chinmo was detected in Tj-positive nuclei next to the hub (large arrows).

Asterisks mark the hubs, scale bars: 30 μm.

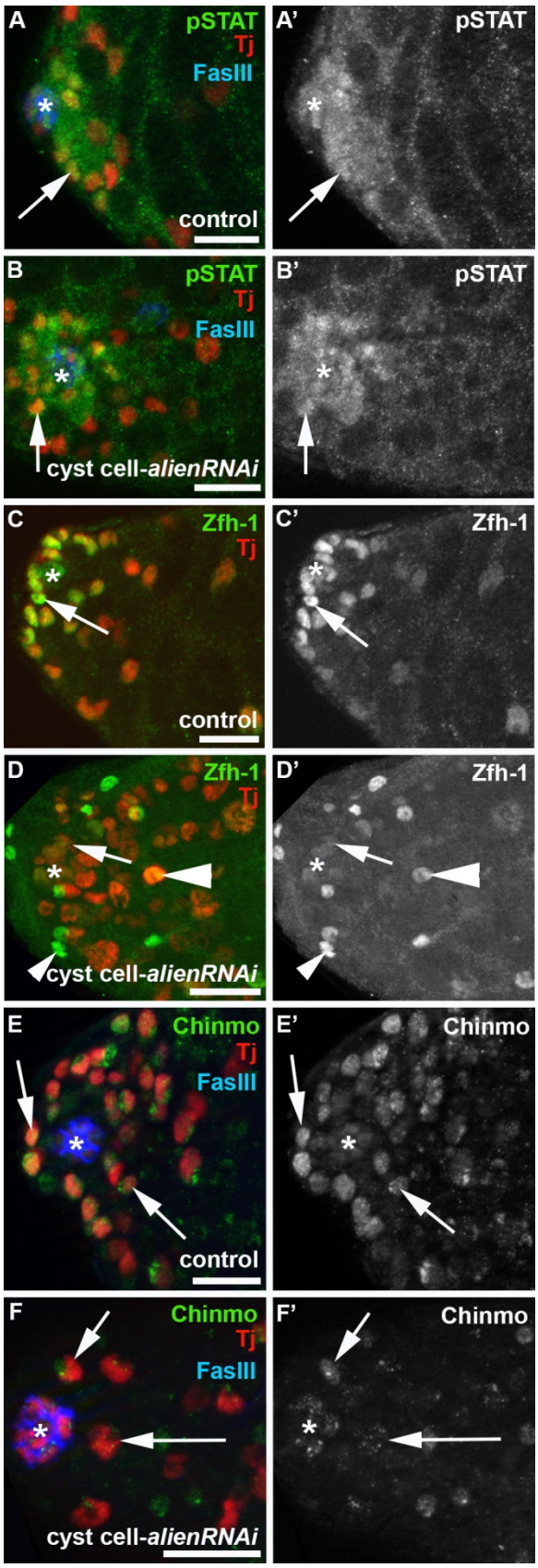
A
pSTAT
Tj
FasIII
control
A'
pSTAT
B
pSTAT
Tj
FasIII
cyst cell-alienRNAi
B'
pSTAT
C
Zfh-1
Tj
control
C'
Zfh-1
D
Zfh-1
Tj
cyst cell-alienRNAi
D'
Zfh-1
E
Chinmo
Tj
FasIII
control
E'
Chinmo
F
Chinmo
Tj
FasIII
cyst cell-alienRNAi
F'
Chinmo

Figure 3.6: *alien* is required for the levels of transcription factors but not for mitosis.

(A) Bar graph showing pixel counts for Chinmo in a variety of genotypes, as indicated. Pixel counts of control genotypes shown as light grey bars, and those of experimental genotypes as black bars. Control and experimental genotypes are grouped as they have been stained and analyzed the same day. P= statistical relevance of the difference in pixel count between experimental genotypes and the corresponding control genotype.

(B)-(E) Apical testes regions immuno-labeled with molecular markers, as indicated.

(B) and (C) Tj-positive cells next to the hub undergoing mitotic divisions (arrowheads) in (B) a control, and (C) a cyst cell-*alienRNAi*-testis.

(D) and (D') A control testis with Tj- and Eya-positive (arrows) cyst cell nuclei.

(E) and (E') In a cyst cell-*alienRNAi*-testis, many nuclei were positive for Tj, but Eya was hardly detectable (arrows).

Asterisks mark the hubs, scale bars: 30 μm.

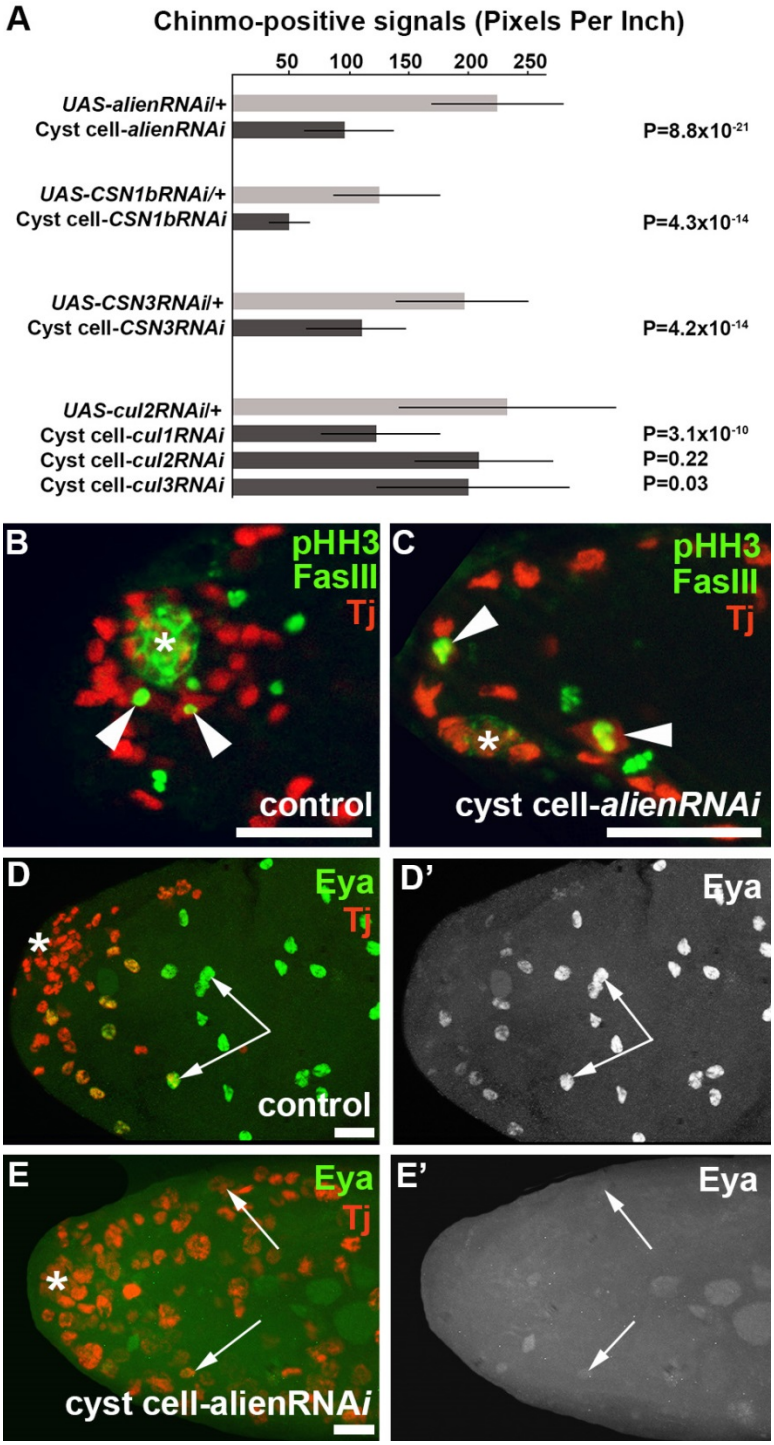
A
Chinmo-positive signals (Pixels Per Inch)
50
100
150
200
250
UAS-alienRNAi/+
Cyst cell-alienRNAi
P=8.8x10-21
UAS-CSN1bRNAi/+
Cyst cell-CSN1bRNAi
P=4.3x10-14
UAS-CSN3RNAi/+
Cyst cell-CSN3RNAi
P=4.2x10-14
UAS-cul2RNAi/+
Cyst cell-cul1RNAi
P=3.1x10-10
Cyst cell-cul2RNAi
P=0.22
Cyst cell-cul3RNAi
P=0.03
B
pHH3
FasIII
Tj
control
C
pHH3
FasIII
Tj
cyst cell-alienRNAi
D
Eya
Tj
control
D'
Eya
E
Eya
Tj
cyst cell-alienRNAi
E'
Eya

Figure 3.7: Alien acts through the CSN and Cullins.

(A)-(G') Apical testes tips immuno-labeled with molecular markers, as indicated.

(A) A control testis with Tj-positive nuclei (arrowhead) and an Arm-positive, net-like pattern of cyst cell cytoplasmic extensions (red).

(B) A cyst cell-*CSN1bRNAi*-testis with Tj-positive nuclei (arrowhead) but lacking cytoplasmic extensions.

(C) and (C') A cyst cell-*cul2RNAi*-testis with Tj-positive nuclei (arrowhead) but lacking cytoplasmic extensions.

(D) and (D') A cyst cell-*cul1RNAi*-testis with cytoplasmic extensions around the germline (small arrows).

(E) and (F') Tj-positive nuclei (arrows) next to the hub had (E) and (E') a high level of Chinmo in a cyst cell-*cul2RNAi*-testis, but (F) and (F') a low level of Chinmo in a cyst cell-*cul1RNAi*-testis.

Asterisks mark the hubs, scale bars: 30 μm.

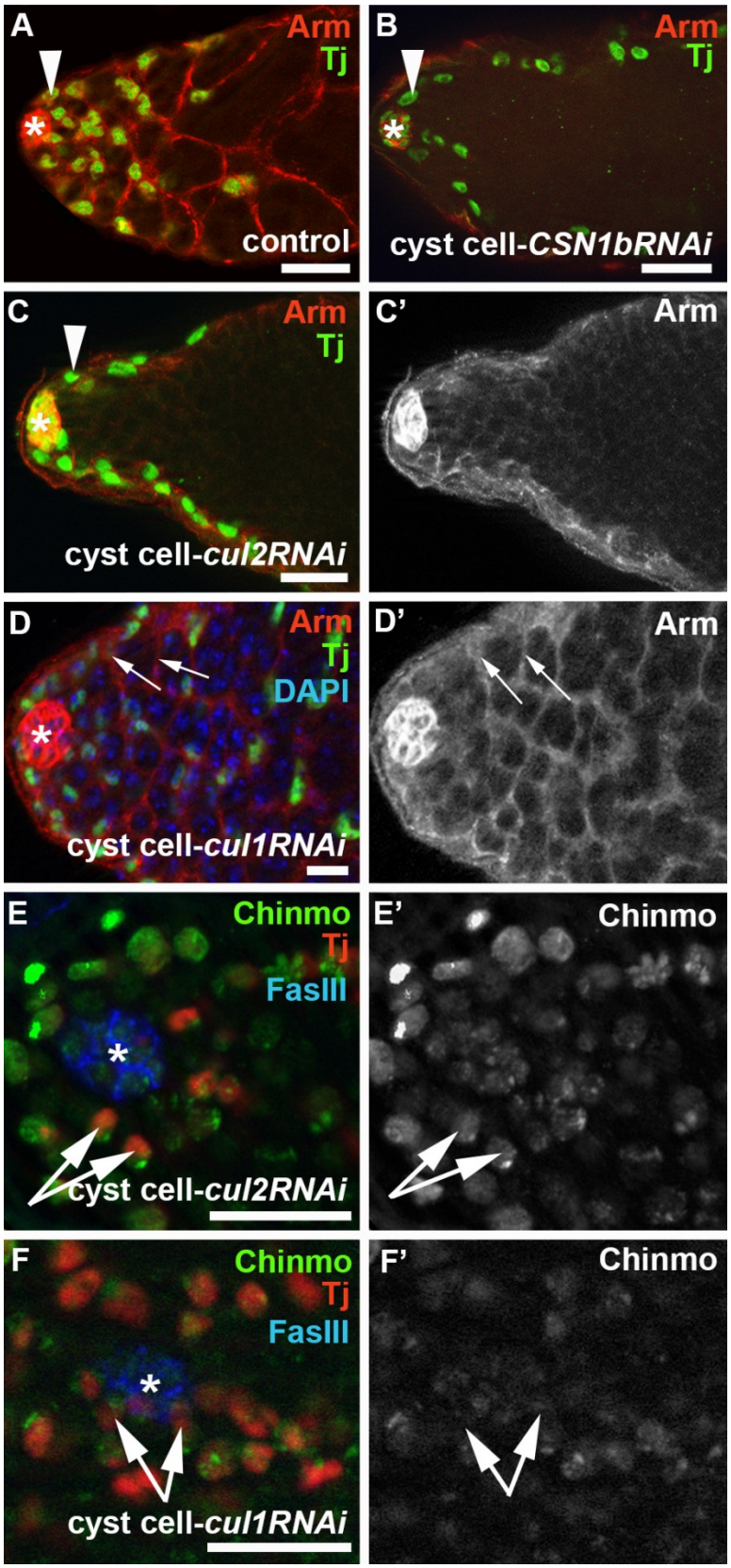
A
Arm
Tj
control
B
Arm
Tj
cyst cell-CSN1bRNAi
C
Arm
Tj
cyst cell-cul2RNAi
C'
Arm
D
Arm
Tj
DAPI
cyst cell-cul1RNAi
D'
Arm
E
Chinmo
Tj
FasIII
cyst cell-cul2RNAi
E'
Chinmo
F
Chinmo
Tj
FasIII
cyst cell-cul1RNAi
F'
Chinmo

References

Ara, T., Tokoyoda, K., Sugiyama, T., Egawa, T., Kawabata, K., Nagasawa, T., 2003. Long-term hematopoietic stem cells require stromal cell-derived factor-1 for colonizing bone marrow during ontogeny. Immunity 19, 257-267.

Arai, F., Hirao, A., Ohmura, M., Sato, H., Matsuoka, S., Takubo, K., Ito, K., Koh, G.Y., Suda, T., 2004. Tie2/angiopoietin-1 signaling regulates hematopoietic stem cell quiescence in the bone marrow niche. Cell 118, 149-161.

Bech-Otschir, D., Seeger, M., Dubiel, W., 2002. The COP9 signalosome: at the interface between signal transduction and ubiquitin-dependent proteolysis. J. Cell Sci. 115, 467-473.

Bosu, D.R., Kipreos, E.T., 2008. Cullin-RING ubiquitin ligases: global regulation and activation cycles. Cell division 3, 7.

Brand, A.H., Perrimon, N., 1993. Targeted gene expression as a means of altering cell fates and generating dominant phenotypes. Development 118, 401-415.

Bunt, S.M., Hime, G.R., 2004. Ectopic activation of Dpp signalling in the male Drosophila germline inhibits germ cell differentiation. Genesis 39, 84-93.

Ceradini, D.J., Kulkarni, A.R., Callaghan, M.J., Tepper, O.M., Bastidas, N., Kleinman, M.E., Capla, J.M., Galiano, R.D., Levine, J.P., Gurtner, G.C., 2004. Progenitor cell trafficking is regulated by hypoxic gradients through HIF-1 induction of SDF-1. Nat. Med. 10, 858-864.

Chia, N.Y., Chan, Y.S., Feng, B., Lu, X., Orlov, Y.L., Moreau, D., Kumar, P., Yang, L., Jiang, J., Lau, M.S., Huss, M., Soh, B.S., Kraus, P., Li, P., Lufkin, T., Lim, B.,

Clarke, N.D., Bard, F., Ng, H.H., 2010. A genome-wide RNAi screen reveals determinants of human embryonic stem cell identity. Nature 468, 316-320.

Chiarini-Garcia, H., Hornick, J.R., Griswold, M.D., Russell, L.D., 2001. Distribution of type A spermatogonia in the mouse is not random. Biol. Reprod. 65, 1179-1185.

Cope, G.A., Deshaies, R.J., 2006. Targeted silencing of Jab1/Csn5 in human cells downregulates SCF activity through reduction of F-box protein levels. BMC biochemistry 7, 1.

Cope, G.A., Suh, G.S., Aravind, L., Schwarz, S.E., Zipursky, S.L., Koonin, E.V., Deshaies, R.J., 2002. Role of predicted metalloprotease motif of Jab1/Csn5 in cleavage of Nedd8 from Cul1. Science 298, 608-611.

de Cuevas, M., Matunis, E.L., 2011. The stem cell niche: lessons from the Drosophila testis. Development 138, 2861-2869.

de Rooij, D.G., 2009. The spermatogonial stem cell niche. Microsc. Res. Tech. 72, 580-585.

Djagaeva, I., Doronkin, S., 2009a. COP9 limits dendritic branching via Cullin3-dependent degradation of the actin-crosslinking BTB-domain protein Kelch. PloS one 4, e7598.

Djagaeva, I., Doronkin, S., 2009b. Dual regulation of dendritic morphogenesis in Drosophila by the COP9 signalosome. PloS one 4, e7577.

Dressel, U., Thormeyer, D., Altincicek, B., Paululat, A., Eggert, M., Schneider, S., Tenbaum, S.P., Renkawitz, R., Baniahmad, A., 1999. Alien, a highly conserved protein with characteristics of a corepressor for members of the nuclear hormone receptor superfamily. Mol. Cell. Biol. 19, 3383-3394.

Duffy, J.B., 2002. GAL4 system in Drosophila: a fly geneticist's Swiss army knife. Genesis 34, 1-15.

Fabrizio, J.J., Boyle, M., DiNardo, S., 2003. A somatic role for eyes absent (eya) and sine oculis (so) in Drosophila spermatocyte development. Dev. Biol. 258, 117-128.

Filipponi, D., Hobbs, R.M., Ottolenghi, S., Rossi, P., Jannini, E.A., Pandolfi, P.P., Dolci, S., 2007. Repression of kit expression by Plzf in germ cells. Mol. Cell. Biol. 27, 6770-6781.

Flaherty, M.S., Salis, P., Evans, C.J., Ekas, L.A., Marouf, A., Zavadil, J., Banerjee, U., Bach, E.A., 2010. chinmo is a functional effector of the JAK/STAT pathway that regulates eye development, tumor formation, and stem cell self-renewal in Drosophila. Developmental cell 18, 556-568.

Freilich, S., Oron, E., Kapp, Y., Nevo-Caspi, Y., Orgad, S., Segal, D., Chamovitz, D.A., 1999. The COP9 signalosome is essential for development of Drosophila melanogaster. Curr. Biol. 9, 1187-1190.

Fuchs, E., Tumbar, T., Guasch, G., 2004. Socializing with the neighbors: stem cells and their niche. Cell 116, 769-778.

Fuller, M.T., 1993. Spermatogenesis in Drosophila. , in: Bate, M., Martinez Arias, A. (Ed.), The development of Drosophila melanogaster. Cold Spring Harbor Laboratory Press, Cold Spring Harbor, New York, USA, pp. 71-148.

Gonczy, P., DiNardo, S., 1996. The germ line regulates somatic cyst cell proliferation and fate during Drosophila spermatogenesis. Development 122, 2437-2447.

Goriely, A., McVean, G.A., van Pelt, A.M., O'Rourke, A.W., Wall, S.A., de Rooij, D.G., Wilkie, A.O., 2005. Gain-of-function amino acid substitutions drive positive

selection of FGFR2 mutations in human spermatogonia. Proc. Natl. Acad. Sci. U. S. A. 102, 6051-6056.

Goubeaud, A., Knirr, S., Renkawitz-Pohl, R., Paululat, A., 1996. The Drosophila gene alien is expressed in the muscle attachment sites during embryogenesis and encodes a protein highly conserved between plants, Drosophila and vertebrates. Mech. Dev. 57, 59-68.

Griswold, M.D., 1998. The central role of Sertoli cells in spermatogenesis. Semin. Cell Dev. Biol. 9, 411-416.

Harari-Steinberg, O., Cantera, R., Denti, S., Bianchi, E., Oron, E., Segal, D., Chamovitz, D.A., 2007. COP9 signalosome subunit 5 (CSN5/Jab1) regulates the development of the Drosophila immune system: effects on Cactus, Dorsal and hematopoiesis. Genes Cells 12, 183-195.

Hardy, R.W., Tokuyasu, K.T., Lindsley, D.L., Garavito, M., 1979. The germinal proliferation center in the testis of Drosophila melanogaster. J. Ultrastruct. Res. 69, 180-190.

Hudson, A.G., Parrott, B.B., Qian, Y., Schulz, C., 2013. A temporal signature of epidermal growth factor signaling regulates the differentiation of germline cells in testes of Drosophila melanogaster. PloS one 8, e70678.

Issigonis, M., Tulina, N., de Cuevas, M., Brawley, C., Sandler, L., Matunis, E., 2009. JAK-STAT signal inhibition regulates competition in the Drosophila testis stem cell niche. Science 326, 153-156.

Joti, P., Ghosh-Roy, A., Ray, K., 2011. Dynein light chain 1 functions in somatic cyst cells regulate spermatogonial divisions in Drosophila. Sci Rep 1, 173.

Kiger, A.A., Jones, D.L., Schulz, C., Rogers, M.B., Fuller, M.T., 2001. Stem cell self-renewal specified by JAK-STAT activation in response to a support cell cue. Science 294, 2542-2545.

Kokkinaki, M., Lee, T.L., He, Z., Jiang, J., Golestaneh, N., Hofmann, M.C., Chan, W.Y., Dym, M., 2009. The molecular signature of spermatogonial stem/progenitor cells in the 6-day-old mouse testis. Biol. Reprod. 80, 707-717.

Leatherman, J.L., Dinardo, S., 2008. Zfh-1 controls somatic stem cell self-renewal in the Drosophila testis and nonautonomously influences germline stem cell self-renewal. Cell stem cell 3, 44-54.

Leatherman, J.L., Dinardo, S., 2010. Germline self-renewal requires cyst stem cells and stat regulates niche adhesion in Drosophila testes. Nature cell biology 12, 806-811.

Li, M.A., Alls, J.D., Avancini, R.M., Koo, K., Godt, D., 2003. The large Maf factor Traffic Jam controls gonad morphogenesis in Drosophila. Nature cell biology 5, 994-1000.

Licursi, V., Salvi, C., De Cesare, V., Rinaldi, T., Mattei, B., Fabbri, C., Serino, G., Bramasole, L., Zimbler, J.Z., Pick, E., Barnes, B.M., Bard, M., Negri, R., 2014. The COP9 signalosome is involved in the regulation of lipid metabolism and of transition metals uptake in Saccharomyces cerevisiae. The FEBS journal 281, 175-190.

Lin, H., Yue, L., Spradling, A.C., 1994. The Drosophila fusome, a germline-specific organelle, contains membrane skeletal proteins and functions in cyst formation. Development 120, 947-956.

Lyapina, S., Cope, G., Shevchenko, A., Serino, G., Tsuge, T., Zhou, C., Wolf, D.A., Wei, N., Shevchenko, A., Deshaies, R.J., 2001. Promotion of NEDD-CUL1 conjugate cleavage by COP9 signalosome. Science 292, 1382-1385.

Matunis, E., Tran, J., Gonczy, P., Caldwell, K., DiNardo, S., 1997. punt and schnurri regulate a somatically derived signal that restricts proliferation of committed progenitors in the germline. Development 124, 4383-4391.

Meng, X., Lindahl, M., Hyvonen, M.E., Parvinen, M., de Rooij, D.G., Hess, M.W., Raatikainen-Ahokas, A., Sainio, K., Rauvala, H., Lakso, M., Pichel, J.G., Westphal, H., Saarma, M., Sariola, H., 2000. Regulation of cell fate decision of undifferentiated spermatogonia by GDNF. Science 287, 1489-1493.

Mundt, K.E., Porte, J., Murray, J.M., Brikos, C., Christensen, P.U., Caspari, T., Hagan, I.M., Millar, J.B., Simanis, V., Hofmann, K., Carr, A.M., 1999. The COP9/signalosome complex is conserved in fission yeast and has a role in S phase. Curr. Biol. 9, 1427-1430.

Nagano, M., Ryu, B.Y., Brinster, C.J., Avarbock, M.R., Brinster, R.L., 2003. Maintenance of mouse male germ line stem cells in vitro. Biol. Reprod. 68, 2207-2214.

Oron, E., Tuller, T., Li, L., Rozovsky, N., Yekutieli, D., Rencus-Lazar, S., Segal, D., Chor, B., Edgar, B.A., Chamovitz, D.A., 2007. Genomic analysis of COP9 signalosome function in Drosophila melanogaster reveals a role in temporal regulation of gene expression. Molecular systems biology 3, 108.

Pan, L., Wang, S., Lu, T., Weng, C., Song, X., Park, J.K., Sun, J., Yang, Z.H., Yu, J., Tang, H., McKearin, D.M., Chamovitz, D.A., Ni, J., Xie, T., 2014. Protein

competition switches the function of COP9 from self-renewal to differentiation. Nature.

Pan, Z.Q., Kentsis, A., Dias, D.C., Yamoah, K., Wu, K., 2004. Nedd8 on cullin: building an expressway to protein destruction. Oncogene 23, 1985-1997.

Phelps, C.B., Brand, A.H., 1998. Ectopic gene expression in Drosophila using GAL4 system. Methods 14, 367-379.

Qian, Y., Dominado, N., Zoller, R., Ng, C., Kudyba, K., Siddall, N.A., Hime, G.R., Schulz, C., 2014. Ecdysone signaling opposes epidermal growth factor signaling in regulating cyst differentiation in the male gonad of Drosophila melanogaster. Dev. Biol. 394, 217-227.

Richardson, K.S., Zundel, W., 2005. The emerging role of the COP9 signalosome in cancer. Molecular cancer research : MCR 3, 645-653.

Sarikas, A., Hartmann, T., Pan, Z.Q., 2011. The cullin protein family. Genome biology 12, 220.

Sarkar, A., Parikh, N., Hearn, S.A., Fuller, M.T., Tazuke, S.I., Schulz, C., 2007. Antagonistic roles of Rac and Rho in organizing the germ cell microenvironment. Curr. Biol. 17, 1253-1258.

Schlessinger, J., 2004. Common and distinct elements in cellular signaling via EGF and FGF receptors. Science 306, 1506-1507.

Schulz, C., Kiger, A.A., Tazuke, S.I., Yamashita, Y.M., Pantalena-Filho, L.C., Jones, D.L., Wood, C.G., Fuller, M.T., 2004. A misexpression screen reveals effects of bag-of-marbles and TGF beta class signaling on the Drosophila male germ-line stem cell lineage. Genetics 167, 707-723.

Schulz, C., Wood, C.G., Jones, D.L., Tazuke, S.I., Fuller, M.T., 2002. Signaling from germ cells mediated by the rhomboid homolog stet organizes encapsulation by somatic support cells. Development 129, 4523-4534.

Seeger, M., Kraft, R., Ferrell, K., Bech-Otschir, D., Dumdey, R., Schade, R., Gordon, C., Naumann, M., Dubiel, W., 1998. A novel protein complex involved in signal transduction possessing similarities to 26S proteasome subunits. FASEB J. 12, 469-478.

Sheng, X.R., Brawley, C.M., Matunis, E.L., 2009. Dedifferentiating spermatogonia outcompete somatic stem cells for niche occupancy in the Drosophila testis. Cell stem cell 5, 191-203.

Stratmann, J.W., Gusmaroli, G., 2012. Many jobs for one good cop - the COP9 signalosome guards development and defense. Plant science : an international journal of experimental plant biology 185-186, 50-64.

Suarez-Alvarez, B., Lopez-Vazquez, A., Lopez-Larrea, C., 2012. Mobilization and homing of hematopoietic stem cells. Adv. Exp. Med. Biol. 741, 152-170.

Tulina, N., Matunis, E., 2001. Control of stem cell self-renewal in Drosophila spermatogenesis by JAK-STAT signaling. Science 294, 2546-2549.

Walker, M.R., Patel, K.K., Stappenbeck, T.S., 2009. The stem cell niche. J. Pathol. 217, 169-180.

Watt, F.M., Hogan, B.L., 2000. Out of Eden: stem cells and their niches. Science 287, 1427-1430.

Wei, N., Chamovitz, D.A., Deng, X.W., 1994. Arabidopsis COP9 is a component of a novel signaling complex mediating light control of development. Cell 78, 117-124.

Wei, N., Deng, X.W., 1998. Characterization and purification of the mammalian COP9 complex, a conserved nuclear regulator initially identified as a repressor of photomorphogenesis in higher plants. Photochem. Photobiol. 68, 237-241.

Wei, N., Tsuge, T., Serino, G., Dohmae, N., Takio, K., Matsui, M., Deng, X.W., 1998. The COP9 complex is conserved between plants and mammals and is related to the 26S proteasome regulatory complex. Curr. Biol. 8, 919-922.

Yan, J., Walz, K., Nakamura, H., Carattini-Rivera, S., Zhao, Q., Vogel, H., Wei, N., Justice, M.J., Bradley, A., Lupski, J.R., 2003. COP9 signalosome subunit 3 is essential for maintenance of cell proliferation in the mouse embryonic epiblast. Mol. Cell. Biol. 23, 6798-6808.

Yoshida, S., Sukeno, M., Nabeshima, Y., 2007. A vasculature-associated niche for undifferentiated spermatogonia in the mouse testis. Science 317, 1722-1726.

Zoller, R., Schulz, C., 2012. The Drosophila cyst stem cell lineage: Partners behind the scenes? Spermatogenesis 2, 145-157.

CHAPTER 4

COMEBACK – A NOVEL GENE REGULATES GERMLINE DIFFERENTIATION VIA STRUCTURING ESCORT CELLS IN OVARIES OF *DROSOPHILA MELANOGASTER*[1]

[1] Qian Y and Schulz C. To be submitted.

Abstract

Studies of stem cells as well as their daughters have disclosed the importance of local signals from the microenvironment, or "niche", in governing tissue regeneration. In gonads of *Drosophila melanogaster*, germline and somatic cell lineage intimately associate with each other. In the female gonad, signaling from the germ cells to their somatic support cells regulates the proliferation and differentiation of the somatic cell lineage, and vice versa. We have discovered that female flies bearing a mutation, *comeback* (*coba*), are defective in oogenesis. Our detailed phenotypic analyses revealed that the germline cells in *coba* mutants were accompanied but not encapsulated by cytoplasmic extensions of somatic escort cells (ECs). Furthermore, germline stem cell (GSC) daughters failed to differentiate. Mosaic analysis showed that *coba* was not required in the germline, suggesting that *coba* may act in the soma. DNA sequencing of *coba* alleles indicated single nucleotide substitutions, leading to premature stop codons in a novel gene *CG14961* from two alleles, respectively. We propose that *CG14961* functions in ECs to form and/or maintain the germline microenvironment and govern germline differentiation in fly ovaries.

Introduction

Multicellular organism homeostasis relies on stem cells to establish and replenish tissue lineages, while setting aside a population of cells that remain undifferentiated precursor cells. For example, the epidermal layer of the skin turns over about every 60 days in humans (Hunter et al., 1995). Epidermal stem cells constantly proliferate and differentiate into different types of epithelial cells to make up for the dead cells that

slough off the body every day. The capacity of skin stem cells to self-renew and differentiate into specialized cell types requires intrinsic factors within stem cells as well as extrinsic cues from a local microenvironment, commonly referred as a “niche” (reviewed in Hsu et al., 2014).

In adult mammalian ovaries, the existence of female GSCs, also known as oogonial stem cells (OSCs), and primordial follicles in postnatal females has been heavily debated (Bukovsky, 2011; reviewed in Ghazal, 2013). Over half a century ago, it was believed that the oogenesis occurs only in fetal gonads, and oogonia neither persist nor mitotically divide during sexual maturity. But recently, scientists have confirmed the presence of populations of mitotically active OSCs from postnatal mouse and human ovaries (Woods and Tilly, 2013; Pacchiarotti et al., 2010). Also, very small pluripotent stem-like cells were discovered in the ovarian surface epithelium (OSE) from adult rabbit, sheep, monkey, and menopausal human. The OSE is a relatively less differentiated, uncommitted layer of cells that are positive for both epithelial and mesenchymal markers (Parte et al., 2011). However, the definitive location of the OSC microenvironment is still ambiguous. In light and scanning electron microscopic studies of OSCs during ovulatory cycles, the OSE, or “germinal” epithelium, was found to frequently evaginate (turn inside out) into villous-like projections, or papillae, varying largely in number, size, and distribution (reviewed in Van Blerkom and Motta, 1979). The OSC microenvironment from the OSE has not been successfully identified until in a recent study, it was demonstrated that the hilum region, the transitional area between the OSE, mesothelium and oviductal epithelium, is a previously unrecognized OSC microenvironment in the mouse ovary (Flesken-Nikitin et al., 2013). In this study, hilum

cells were shown to express stem and/or progenitor cell markers and display long-term stem cell properties *ex vivo* and *in vivo*. Yet the molecular and cellular mechanisms regulating the interactions of the OSE and OSC lineages are still not very well characterized.

While it has been difficult to study the germline and somatic cell lineage in mammals due to their anatomical complexities, *Drosophila* ovaries have long been studied to reveal cellular microenvironments regulating proliferation and differentiation of stem cells and their daughter cells (Spradling, 1993a; reviewed in Scadden, 2014). An adult female fly has a pair of ovaries and each consists of an average of 16 ovarioles, depending on genetic or environmental variation (Spradling, 1993b; Wayne et al., 1997) (Fig. 1.2A). An ovariole contains a series of stages of oogenesis in an assembly-line fashion, starting from the very anterior structure, named the germarium, to the most developed oocyte in the very distal egg chamber (Fig. 1.2B).

Drosophila oogenesis starts with an asymmetrical cell division of a GSC, during which a new stem cell and a cystoblast (CB) are produced. The new stem cell remains attached to the GSC niche, which is composed of three cell types at the anterior apex of a germarium. The most apical cells are a distinguishable stack of somatic cells, known as the terminal filament (TF). Posterior to the TF are 5-7 cap cells (CpCs) and 4-6 escort stem cells (ESCs) (Kirilly and Xie, 2007) (Fig. 1.2C). TF, CpCs, and ESCs are associated with 2-3 GSCs and control GSC self-renewal and differentiation (Xie and Spradling, 2000; Kirilly et al., 2011). A number of signaling pathways have been well characterized to reveal the interplay between GSCs and their microenvironmental cells (Xie and

Spradling, 1998; Cox et al., 2000; King et al., 2001; Chen and McKearin, 2003; Wang et al., 2008; Lopez-Onieva et al., 2008; Chen and McKearin, 2005; Ward et al., 2006).

The CB moves out of the GSC niche and initiates differentiation. It undergoes precisely four rounds of synchronous mitotic divisions with incomplete cytokinesis, producing 2-, 4-, 8-, and 16-differentiating cystocytes (CCs) located progressively more posterior along the germarium. Each unit of the interconnected dividing CCs is called a germline cyst. CBs and clusters of CCs are encased in the cytoplasmic extensions of the microenvironmental cells, known as ECs or inner germarial sheath cells (IGSCs) (Margolis and Spradling, 1995). Conventionally, the germarium is divided into four regions (1, 2A, 2B and 3) that correspond to the various stages of cyst development (Mahowald and Kambysellis, 1980) (Fig. 1.2D). When a cyst reaches region 2B, one of the 16 CCs that connects four mitotic sister cells is determined to become an oocyte, whereas the remaining 15 cells will become nurse cells (Fig. 4.1C, as indicated), providing the oocyte with nutrients, mRNAs, proteins, and organelles throughout oogenesis and early embryogenesis (Pritchett et al., 2009).

Epidermal growth factor (EGF) signaling is one of the most important signaling pathways that recur between the germline and somatic cell lineage. Signaling from the germline cells activates the EGF receptors on somatic support cells to regulate germline encapsulation by the cytoplasmic extensions of somatic support cells, and promotes germline differentiation in both males and females (Kiger et al., 2000; Tran et al., 2000; Schulz et al., 2002; Sarkar et al., 2007; Kirilly et al., 2011). In females, EGF signaling in ECs represses Dally, a glypican required for Decapentaplegic (Dpp) extracellular

movement and stability, which spatially restricts bone morphogenic protein (BMP) signaling to allow GSC maintenance and CB differentiation (Liu et al., 2010).

In addition to the important role of EGF signaling, JAK/STAT signaling is also required in germline enclosure during early gametogenesis in both genders. While it is required in the testis GSC niche, called the hub, for GSC self-renewal (Tulina and Matunis, 2001; Kiger et al., 2001), JAK/STAT signaling is indispensable in the ovarian ESC lineage to control the morphology and proliferation of ESCs as well as their progeny (Decotto and Spradling, 2005). Reduced JAK/STAT signal via a temperature-sensitive mutation leads to a significant reduction of somatic cells at the tip of the germarium and loss of cytoplasmic extensions of ECs. They therefore form a monolayer of epithelial cells surrounding the germ cells, which eventually results in precocious GSC loss and the disruption of the anterior germarium and its surrounding sheath.

A role for steroid hormone, the ecdysone signaling, is shown to control CB differentiation, possibly through control of the potency of transforming growth factor beta (TGF-β) signaling and adjustment of adhesion complexes and cytoskeletal proteins in the EC lineage (Konig et al., 2011). More recently, ecdysone signaling is shown to be essential in maintaining cytoplasmic extensions of somatic support cells specifically in the female gonad, but not in males (Morris and Spradling, 2012; Qian et al., 2014). Reduction of ecdysone signals from the ECs through RNA interference (RNAi) disrupts germline enclosure and results in a failure of the germline to differentiate (Morris and Spradling, 2012).

Here, we show that animals carrying mutations in *coba* have tiny ovaries. The germaria of *coba* females show germline enclosure defects and accumulating CBs. DNA

sequencing of *coba* alleles revealed that two alleles carry nonsense mutations in a novel gene, named *CG14961*. Clonal analysis indicated that *coba* acts outside of the germline. We propose that CG14961, as a new molecule that has not yet been characterized, may be functional in the somatic cell lineage to contribute to the structure of germline microenvironment and govern germline cell fate determination in fly ovaries.

Material and Methods

Fly stocks

Flies were raised on standard cornmeal, molasses and agar medium at room temperature unless otherwise stated. The original *comeback* allele ($coba^{1}$) was identified in a P-element insertion screen for male sterility. 6 potential *coba* alleles ($coba^{1060, 1458, 1468, 1632, 1663, 2836}$), out of a collection of 3579 EMS induced viable lines, were isolated on a *TM6B, Humeral, ebony* chromosome in a screen that failed to complement a chromosome carrying the $coba^{1}$ allele in our laboratory. The *coba* mutant phenotype was analyzed in flies transheterozygous for loss-of-function alleles $coba^{1060}$, $coba^{1458}$, $coba^{1468}$, $coba^{1632}$, $coba^{1663}$ and $coba^{2836}$ over $coba^{1}$. Unless otherwise indicated, images of *coba* mutant ovaries shown were from $coba^{1}/Df(3L)E1$ animals. All the other *Drosophila* mutants and balancer chromosomes are as described elsewhere (Lindsley and Zimm, 1992). *Df(3L)E1* was discovered by Munroe et al., 1998. *traffic jam*-Gal4 [104055] was obtained from Kyoto *Drosophila* Genetic Resource Center. Lines expressing *CG14961* RNAi constructs [v15272, v15273 and v106865] were obtained from the Vienna RNAi Stock Center. All other stocks were obtained from the Bloomington *Drosophila* Stock Center.

Immunofluorescence microscopy

Ovaries were dissected in 1x Tissue Isolation Buffer (1x TIB: 183 mM KCl, 47 mM NaCl, 10 mM Tris, pH 6.9) and fixed with 4% formaldehyde in 1x PBT (1x PBS with 0.1 % Triton X-100, pH 7.5; 1x PBS: 137 mM NaCl, 2.7 mM KCl, 10 mM Na_2HPO_4, 1.8 mM KH_2PO_4, pH 7.4) for 30 minutes at room temperature. Ovaries were then washed at least 3 x 20 minutes in PBT and incubated with primary antibodies overnight at 4°C in PBT. After incubation, ovaries were washed at least 3 x 20 minutes in PBT, incubated with fluorophore-conjugated secondary antibodies in PBT for 2 hours at room temperature, and washed again at least 3 x 20 minutes in PBT. Ovaries were then embedded in SlowFade Gold Antifade Reagent with DAPI (Life Technologies). The following hybridoma/monoclonal antibodies were obtained from the Developmental Studies Hybridoma Bank, developed under the auspices of the NICHD, and maintained by The University of Iowa, Department of Biological Sciences, Iowa City, IA 52242: mouse anti-Spec (3A9) (1:10), mouse anti-Sxl (1:100) and mouse anti-Bam (1:50). Goat anti-Vasa (1:150) and rabbit anti-Arm (1:400) were obtained from Santa Cruz Biotechnology. Mouse anti-BrdU (1:2) and rabbit anti-pHH3 (1:1000) were obtained from EMD Millipore. Mouse anti-GFP (1:200) was obtained from Invitrogen. Guinea-pig anti-Tj (1:5000) is a gift from Dr. Dorothea Godt (used in Li et al., 2003); rabbit anti-pMad (1:2500) is a gift from Dr. Ed Laufer. Alexa-488-, Cy3-, and Cy5-conjugated secondary antibodies (Invitrogen) were used at 1:500. Immunofluorescence was performed following standard procedures (Ashburner, 1989). Samples were observed using a Zeiss Axiophot microscope in fluorescent microscopy. Images were taken with a

CCD camera using an Apotome and Axiovision Rel Software. *P*-values were calculated using Fisher's and chi-squared exact test.

BrdU labeling in vitro

Ovaries were dissected in 163 mM BrdU (EMD Millipore) in 1x PBS for 15 minutes, transferred to an Eppendorf tube with fresh 163 mM BrdU in PBS, incubated for 30 minutes at room temperature, rinsed twice with PBS, fixed for 30 minutes in 4% formaldehyde in 1x PBT, washed 3 x 20 minutes in PBT and incubated with anti-BrdU overnight at 4°C in PBT. The rest of the procedure was as for other antibodies.

UAS/Gal4 expression studies

Expression in the somatic cell lineage was induced with the UAS/Gal4 expression system (Brand and Perrimon, 1993). Crosses were set up at room temperature or other temperatures outlined in the results, and the animals were shifted to 29°C to maximize the Gal4 activity.

Mitotic clonal analysis

Mitotic clones were generated using the FLP/FRT system of site-specific recombination (Theodosiou and Xu, 1998). All FLP/FRT strains were obtained from Bloomington Stock Center. The allele *coba*^{1} was recombined onto an *FRT-80* chromosome (*FRT-80-coba*). Males carrying the *FRT-80-coba* chromosome and control animals carrying the *FRT-80* chromosome were mated to females carrying the FLP recombinase gene under the control of a heat-shock promoter and an *FTR-80*

chromosome marked with a nuclear targeted GFP (*hs-FLP; FRT-80-GFP*). Progeny were heat-shocked as adults for 2 hours x 7 days in a 37°C water bath. Ovaries from adult females were dissected 7 days after the heat-shock. On average, one out of 5 germaria showed GFP-clones. Under these conditions, control animals often contained 2-3 clusters of GFP-cells, and same number of clusters of GFP-clones was observed from females carrying the *FRT-80-coba* chromosome.

EMS induced mutagenesis and non-complementation screen

A total of 1000 w^{1118} male flies were starved overnight, fed for 8 hours with 50 mM EMS (M0880, Sigma) dissolved in 1% sucrose solution, recovered for 24 hours in clean fly bottles bottomed with Kimwipes (Kimtech science) soaked in sucrose solution, then mated in bulk to $coba^{1}$/*TM6B* virgin females. After 4 days, all males were discarded and the mated females were transferred into new fly bottles provided with standard food. A total of 5000 F_1 */*TM6B* (* indicates potential mutations) male progeny were collected after eclosion, mated to $coba^{1}$/*TM6B* virgin females, one male and ten females per vial. 3579 out of 5000 lines were able to produce progeny. F_2 */$coba^{1}$ females were screened for non-complementation of *coba* according to Bökel, 2008, and their */*TM6B* siblings were collected established as stocks for further analysis. 6 lines of potential new *coba* alleles were established and the rest of flies were discarded.

Genetic mapping of coba

coba was localized to polytene chromosome interval 63D1-63D2 with the following deficiencies obtained from the Bloomington Stock Center: *Df(3L)HR232*

(63C1;63D2) [BL#3648] and *Df(3L)E1* (63C6;63E1) [BL#4515], but not with *Df (3L)BSC129* (63C1;63D1) [BL#9294] and *Df (3L)Exel6094* (63D2;63E1) [BL#7573]. The molecularly defined endpoints of deficiencies are described in Parks et al., 2004 and Cook et al., 2012. Ten potential transcription units (PIG-C, CG12016, CG42456, CG11526, PHGPx, CG14961, CG14969, Drsl1, Drsl6 and karst) and one non-protein-coding sequence (CR45380) were listed in this approximate 40kb area. *Df(3L)E1* virgin females were mated to $coba^{1, 1060, 1458, 1468, 1632, 1663, 2836}$ males respectively, genomic DNAs from $coba^{*}/Df(3L)E1$ progeny were obtained as templates for sequencing *coba* candidate genes. *karst* (*kst*) was excluded because known loss-of-function alleles (kst^{1} and $kst^{14.1}$ were gifts from Dr. Graham Thomas) complemented *coba* mutants. Others were excluded because no lesions were detected in coding regions when sequencing several *coba* alleles. Primers to amplify and sequence *coba* candidates:

PIG-C Forward 1:	5’-GCATCACTATGACAGTGTGACCA-3’
PIG-C Forward 2:	5’-CGGCTACTTATTCTCACCGATGC-3’
PIG-C Reverse:	5’-CACAACCAAGCCAAAAAACTCACC-3’
CG12016 (CG42456) Forward 1:	5’-CAAGCAGAAGTGACTCGCCTAC-3’
CG12016 (CG42456) Reverse 1:	5’-CCTATCATCACTAGTCGTCGGTG-3’
CG12016 (CG42456) Forward 2:	5’-GTTGGCAGTGTACGAGGATGAAC-3’
CG12016 (CG42456) Reverse 2:	5’-CGACTGACTATCGCTCTTCCTTG-3’
CG12016 (CG42456) Forward 3:	5’-CATCGCCGCGTTCTCCTTTTAC-3’
CG12016 (CG42456) Reverse 3:	5’-GACCTTCTTGTCCCTCAGCTG-3’
CG12016 (CG42456) Forward 4:	5’-GTCTATCAATATCCGCCACAGCAG-3’
CG12016 (CG42456) Reverse 4:	5’-CGAACCACCCTTAGAGTAGCTTAC-3’

CG12016 (CG42456) Forward 5:	5’-GGATTACTTCTCCGAATCGTGGC-3’
CG12016 (CG42456) Reverse 5:	5’-GTTCTGCGAGCCCTTGAAACG-3’
CG11526 Forward 1:	5’-CGAGCATTTGGCGAACACTC-3’
CG11526 Reverse 1:	5’-GGACTGTGTTTTCGCGTAGC-3’
CG11526 Forward 2:	5’-GCAGGATACACATACACGAGTAGC-3’
CG11526 Reverse 2:	5’-GGACAACCTTCTTCATGGGGAAC-3’
CG11526 Forward 3:	5’-GCCGACTCCTTTGTGCAAG-3’
CG11526 Reverse 3:	5’-GTTCCTAGCTATGTCCTCCTCC-3’
CG11526 Forward 4:	5’-CAGTTTCTGGACATTTCGCGG-3’
CG11526 Reverse 4:	5’-GCACCTTAAGCGTCTTCTTCAGG-3’
CG11526 Forward 5:	5’-CGTGTTCTCCTGCATAAACCTG-3’
CG11526 Reverse 5:	5’-CGCATGTGGATATTAGAGCAGCTG-3’
PHGPx Forward 1:	5’-GCTGTGTGGTCGGAAAATACC-3’
PHGPx Reverse 1:	5’-GCCATTGTTCGAGTTGATTGGAC-3’
PHGPx Forward 2:	5’-GTTTGTCGTCGGGTTGTCGA-3’
PHGPx Reverse 2:	5’-GCAGACATGTCGATCTGGAAGC-3’
PHGPx Forward 3:	5’-CACTGCAATGAACCGCGTAG-3’
PHGPx Reverse 3:	5’-GCCAGACGGTTACAAGCTAAAG-3’
CG14961 Forward 1:	5’-CGCTCCCCCAATTTTGATTCC-3’
CG14961 Reverse 1:	5’-CCTCCAATCGTCACCAGTTTCTG-3’
CG14961 Forward 2:	5’-CAGGAGTTCGAGCGGTACATC-3’
CG14961 Reverse 2:	5’-CCAGCTCGACTACCAGAGTTC-3’
CG14961 Forward 3:	5’-GGTACGAGGACTATGCCGATC-3’

CG14961 Reverse 3:	5’-GATATTCGCCGGAGAAGTAGTCG-3’
CG14961 Forward 4:	5’-CTCTCACCCAAGATGATCCAGC-3’
CG14961 Reverse 4:	5’-CAGTCCGGAGCAATAGTGGTG-3’
CG14961 Forward 5:	5’-CGATACAGTACGGAGAGCCAG-3’
CG14961 Reverse 5:	5’-CATCATGGAAAGGGCCCTTC-3’
CG14969 Forward 1:	5’-GTGTGCAGAGGGTAAGAATGTGAG-3’
CG14969 Reverse 1:	5’-CGAGTCCGGTTCATCTAAGCAAAAG-3’
CG14969 Forward 2:	5’-GAATCTGCTAGTTCGGATTTAGTTTGC-3’
CG14969 Reverse 2:	5’-GTGTTTTGTTTTTGGTTAGGCTCAAGG-3’
Drsl1 Forward:	5’-CAGATCAATGCATTGTTATATTCGGCAC-3’
Drsl1 Reverse:	5’-GCGGGGCAGTAGTAATGCTAAAATA-3’
Drsl6 Forward:	5’-GACATCGACTAGTCCAGCCCTA-3’
Drsl6 Reverse:	5’-TTTACACTCAGTACGACGACGC-3’
CR45380 Forward:	5’-GAAAGGACCTTGATCAATTAGTCTGAGT-3’
CR45380 Reverse:	5’-CATTTGAGCGATGATGCATTCAACAA-3’

Genomic-DNA and cDNA rescue constructs

All molecular techniques were performed using standard protocols (Sambrook et al., 1989). cDNA clone IP20641 was available at *Drosophila* Genomics Resource Center (DGRC). This purchased plasmid contained a 259 bp of 3’ UTR including the polyadenylation site, however, it lacked the first 666 bp of the open reading frame (ORF) at the 5’ terminus and there was a two-nucleotide (TC) deletion mutation at 1615-1616 bp of the wildtype ORF. A forward primer with an EcoRI site and a reverse primer

following the deletion mutation site were designed to amplify the missing 5' terminus by polymerase chain reaction (PCR), using wildtype fly genomic DNA as a template. The 1815 bp PCR product was digested with restriction endonucleases EcoRI and PvuI, and was directionally cloned to the original IP20641 clone to generate a construct consisting of an intact *CG14961* ORF and the 3' UTR. The 5' regulatory region of *CG14961* was predicted to be located within 1.4 kilobases upstream of the ORF, which is the distance to the 3' end of the neighbor gene. A forward primer with an EcoRV site and a reverse primer following a PciI site were designed to amplify the 5' regulatory region of *CG14961* by PCR, using wildtype fly genomic DNA as a template. The 2183 bp PCR product was digested with restriction endonucleases EcoRV and PciI, and was directionally cloned in front of the *CG14961* ORF. Primers with an XbaI site were designed to PCR the entire fragment containing the 5' regulatory region, the ORF and the 3' UTR. The 4592 bp PCR product was recovered and then digested by restriction endonuclease XbaI and fused into a pCaSpeR4 plasmid that contains sequences necessary for integration into the fly genome. The genomic-DNA rescue construct was sequenced to assure that no mutation was to disrupt normal function of *CG14961*.

To generate a cDNA rescue construct, primers were designed to amplify the *CG14961* ORF. The ~2.8 kb amplicon was directionally cloned into the Entry clone and was positively selected according to the protocol provided by the pENTR/D-TOPO Cloning Kit (Invitrogen catalog # K240020). To allow proper expression in *Drosophila* tissue, the positive Entry clone containing the *CG14961* ORF was recombined with a Destination clone, processed with a Gateway LR Clonase Enzyme Mix kit (Invitrogen catalog # 11791). Two Destination clones, an N-terminal and a C-terminal FLAG/UASt

fusion vectors (Vector name: pTFW and pTWF, Barcode: 1115 and 1116) were purchased from the *Drosophila* Gateway™ vector collection vended by DGRC, each contains a 3xFLAG tag at the N- or C-terminal end, respectively. The final cDNA rescue constructs were sequenced to assure that the 3xFLAG tag was in frame with the *CG14961* ORF.

Primers to amplify the missing 5' terminus and the deletion mutation:

Forward (EcoRI): 5'-GAAAGGGAATTCATGTTCCGAGGAGTGCTGG-3'

Reverse (14961-3): 5'-GATATTCGCCGGAGAAGTAGTCG-3'

Primers to amplify the 5' regulatory region:

Forward (EcoRV): 5'-CTGACTGATATCGCACGTACTTTGATCGGTAGTTGG-3'

Reverse (14961-1): 5'-CCTCCAATCGTCACCAGTTTCTG-3'

Primers to amplify the *CG14961* genomic region:

Forward (XbaI): 5'-ATGCTTCTAGAGCACGTACTTTGATCGGTAGTTGG-3'

Reverse (XbaI): 5'-ATGCATCTAGAGGTGACACTATAGAACTCGAGTTTTTT TTT-3'

Primers to amplify the *CG14961* ORF:

pTFW Forward: 5'-CACCATGTTCCGAGGAGTGCTGG-3'

pTFW Reverse: 5'-TTATCCGTATAGATTGCCATGGGC-3'

pTWF Forward: 5'-CACCATGTTCCGAGGAGTGCTGG-3'

pTWF Reverse: 5'-TCCGTATAGATTGCCATGGGC-3'

RNA preparation for RT-PCR and qRT-PCR

Total RNA from fly ovaries was isolated and purified using TRIzol Reagent with the PureLink RNA Mini Kit as described by the manufacturer (Life Technologies catalog

12183018A). First strand cDNA was generated using Oligo-dT primers provided in Invitrogen SuperScript III First-Strand Synthesis System for RT-PCR kit. Gene-specific PCR primers were designed manually and verified by IDT OligoAnalyzer 3.1. PCR reactions were run on 0.8% agarose gel to purify products, which were then excised and purified using the QIAquick Gel Extraction Kit and used as a template for secondary PCR to further amplify products and then sequenced by Macrogen USA. *CG14961* Forward 4 and Reverse 4 primers and *ß3 tubulin* control (Forward: 5'-ATCATTTCCGA GGAGCACGGC-3'; Reverse: 5'-GCCCAGCGAGTGCGTCAATTG-3') were used for qRT-PCR, all of which were designed close to the 3' end, ensuring that the reverse transcriptase does not fall off from primer-templates when approaching the 5' end. Additionally, when products obtained from RT-PCR were sequenced, we noted no intronic sequence present. *CG14961* Forward 2 and Reverse 2 primers were used in performing RT-PCR.

in situ hybridization

Whole-mount *in situ* hybridization was performed as described in Tautz and Pfeifle, 1989, with modifications for RNA probes described by Klingler and Gergen, 1993. Ribonucleotide probes were generated from linearized plasmid using the DIG RNA Labeling Kit (SP6/T7, Roche).

Western blotting

Ovaries of young flies were dissected in 1x TIB, lysed by homogenization in appropriate volumes of Laemmli sample buffer (Bio-Rad) containing 5% 2-

Mercaptoethanol and 1% Halt Protease Inhibitor Cocktail (Thermo Scientific). After 5 minutes of denaturation in boiling water, the protein mixture was centrifuged at 13,000 rpm for 20 minutes at 4°C. The supernatant was fractionated by 10% SDS-PAGE, transferred onto Amersham Hybond ECL Nitrocellulose Membrane (GE Healthcare) and the blots were preincubated in the blocking solution (1x TBST: 5% BSA in Tris-buffered saline and 0.1% Tween 20) overnight at 4°C with gentle agitation. Membranes were incubated with mouse anti-FLAG (F1804, 1:5000; Sigma) in the blocking solution overnight at 4°C. Peroxidase conjugated secondary antibodies were 1:10,000 diluted in the blocking solution and used for detecting the primary antibodies bound on the blots. After 1 hour of incubation at room temperature, the proteins were visualized by Amersham ECL Prime Western Blotting Detection Reagent (GE Healthcare).

Results

coba caused severe ovary defects

Disruption of *coba* causes approximately 25% (n>300) pupal lethality and $coba^{1/1}$ animals rarely survive to adulthood (<1%), suggesting that *coba* may play an essential role in the pupa-to-adult transition during development. In particular, *coba* mutant ($coba^{1}$*/Df(3L)E1*) females are sterile. However, these animals are viable and show no other gross morphological abnormalities compared to control sibling females ($coba^{1}$*/TM6B* and *Df(3L)E1/TM6B*), indicating that *coba* may have a specific function in fly ovary development.

The control females had normal ovaries, each composed of 12-16 ovarioles with egg chambers maturing from the germarium to the most developed egg along the

anterior-posterior axis (Fig. 4.1A), while *coba* mutant ovaries were overall much smaller in size and composed of ovarioles with only nascent egg chambers (Fig. 4.1B). We also noticed that the ovary defects were often exacerbated when flies were aged. So unless otherwise indicated, we would use 3-day and 10-day old flies to represent young and aged flies to examine both initial and aggravated phenotypes and how the phenotypes develop over time.

To observe substructures of fly ovaries with a higher resolution, we ruptured ovarian sheaths, and split ovaries into single ovarioles. Ovaries counterstained with a fluorescent dye, 4', 6-diamidino-2-phenylindole (DAPI) that binds to DNA, revealed germline and somatic cell nuclei in fly ovarioles. The early-stage germline cells and somatic cells in the germarium had relatively small nuclei (Fig. 4.1C, large arrowhead). During egg chamber development, the nurse cells become polyploid, and therefore appear with increasingly larger nuclei (Fig. 4.1C, as indicated). Each egg chamber was surrounded by a monolayer of follicle cells with small nuclei (Fig. 4.1C, as indicated). No significant difference was seen in the aged control ovarioles compared to the young ones (Fig. 4.1E). However, egg chambers of both young and aged *coba* mutants presented aberrant morphology in terms of shape and array of the egg chambers. Some *coba* animals had certain stages of egg chambers missing (Fig. 4.1D, as indicated), and some had irregular shaped egg chambers (4.1G, medium arrowhead) rather than the normal round or ovoid shapes. Furthermore, some of the aged *coba* ovarioles were detected with increased number of large nuclei that correspond to nurse cells (Fig. 4.1G, medium arrows) rather than 15 nurse cells per egg chamber as seen in the control animals.

Atrophic germaria were often seen in *coba* mutants (Fig. 4.1F and 4.1G), and some of the *coba* germaria appeared to be depleted of early germ cell nuclei (Fig. 4.1D).

coba disrupted germline differentiation

To investigate the earliest defects of oogenesis, we focused specifically on the germarium. We asked if the drastically reduced size of the ovary was due to defects in early germline proliferation or differentiation. Immunofluorescence microscopy using anti-Vasa antibody labels germ cells and allows for the quantification of $Vasa^{+}$ cells in the germarium (Fig. 4.2A-D). For quantifying the early-stage germline cells, we specifically focused on region 1 to 2B. Young and aged control females (Figs. 4.2A and 4.2C) had average numbers of 117 and 84 germ cells per germarium, respectively. The average numbers of early-stage germline cells in *coba* mutants of both ages (Figs. 4.2B and 4.2D) were 55 and 41, respectively. This is a significant reduction in the numbers of early-stage germline cells in *coba* mutants (Fig. 4.2E).

We postulated that the early-stage germline cells in *coba* mutants may be reduced because, (1) germline cells underwent apoptosis, (2) germline cells had a limited ability to proliferate, or (3) germline cells were not able to differentiate. To distinguish between these possibilities, we first carried out terminal deoxynucleotidyl transferase dUTP nick end labeling (TUNEL) assay to detect cell death (Table 4.1). In control animals, Vasa-and-TUNEL-double-possitive ($Vasa^{+}/TUNEL^{+}$) germline cells were sporadically detected in 5% of the young and in 8% of the aged germaria, respectively. These dying germline cells were predominantly detected in region 2A and 2B where CCs are about to become surrounded by follicle cells. 6% of the young and 3% of the aged *coba* mutant

germaria contained $Vasa^+/TUNEL^+$ germline cells in the same region. $Vasa^+/TUNEL^+$ somatic cells, including TF, ECs and follicle cells were seen in 9% of the young and in 7% of the aged control germaria, and in 9% mutant germaria of either young or aged flies. These numbers suggest that neither germline cells nor somatic cells in *coba* mutants underwent significantly increased apoptosis.

To investigate germline proliferation, we assayed incorporation of a thymidine analogue, 5-Bromo-2'-deoxyuridine (BrdU) to detect cells in the S-phase of the cell cycle. Besides, we utilized a mitosis-specific marker, anti-phospho-histone H3 (anti-pHH3), to detect cells in the M-phase of the cell cycle. BrdU-and-Vasa-double-positive ($BrdU^+/Vasa^+$) cells and pHH3-and-Vasa-double-positive ($pHH3^+/Vasa^+$) cells were quantified and divided by the numbers of $Vasa^+$ cells to reveal the percentages of germ cells in the different phases of the cell cycle (Table 4.2). Slightly higher percentages of *coba* mutant germ cells were detected in the S-phase, while percentages of mutant germ cells in the M-phase were not changed dramatically in *coba* flies, compared to control flies of both ages, respectively. Together, we conclude that *coba* mutant germ cells did not have significant defects in proliferation.

To address if *coba* mutant germline cells failed to differentiate, we stained mutant and control germaria with a variety of molecular markers for cell fate. Antibodies raised against Spectrin (Spec), an adducin-like protein (Lee et al., 1993), label germline-specific organelles, the fusomes, which have different shape and sizes dependent on the developmental stage of the cells (King, 1970; Lin et al., 1994). GSCs and CBs contain round fusomes (also known as spectrosomes) (Fig. 4.3A-E, arrowheads). During the germline cyst formation, a round fusome extends to become an elongated, highly

branched structure that interconnects the CC cluster (Fig. 4.3A-D, arrows). Quantification of fusome structures shown that control animals had an average number of 4 round fusomes close to the anterior tip of each germarium and approximately 8 branched fusomes away from the tip (Fig. 4.3A, 4.3C, and 4.3F). In *coba* mutants, especially in the aged flies, the number round fusomes increased dramatically and the numbers of branched fusomes decreased (Fig. 4.3B, 4.3D, and 4.3F). In 26% of aged *coba* mutants (n=100), the round fusomes filled the entire germarium (Fig. 4.3E, arrowheads), suggesting those germline cells failed to differentiate past the single-cell stage.

We therefore investigated whether those early germline cells containing round fusomes were GSCs or had initiated differentiation as CBs. *Sex-lethal* (*Sxl*) is a female-specific sex-determination gene and serves as a marker for GSCs and CBs (Salz et al., 1989; Chau et al., 2009). *bag-of-marbles* (*bam*) is a differentiation factor and serves as a marker for CBs and CCs (Ohlstein and McKearin, 1997; McKearin and Ohlstein, 1995). Anti-pSmad1/5/8 (pMad) antibodies specifically label GSCs (Kai and Spradling, 2003; Chang et al., 2013). Immunostaining and quantification of young and aged animals revealed an increased number of Sxl^+ cells and a decreased number of Bam^+ cells in *coba* mutants compared to control animals, (Fig. 4.4A-D' and 4.4E), confirming our above findings that the germaria were filled up with early-stage germline cells. Only a small percentage of these cells were GSCs, based on anti-pMad staining. Young and aged control females usually contained an average of 1.57 and 1.60 $pMad^+$ cells per germarium, respectively. In young and aged *coba* mutant animals, we detected slightly less GSCs, with average numbers of 1.25 and 1.18 $pMad^+$ cells per germarium, respectively (Fig. 4.4A"-E). Taken together, we conclude that the accumulated early-

stage germline cells in *coba* mutant females were not GSCs but their immediate daughter CBs, and the reduction of germline cells in *coba* mutant animals was probably due to the failure of c*oba* mutant CBs to transition into CC fate.

coba mutant females had defects in germline enclosure

A failure of the germline cells to differentiate could be caused by abnormal germline-soma interactions. The stem cell niche appeared normal in *coba* mutant flies, based on the expression of nuclear Lamin C, which highly expresses in nuclear membranes of the TF and CpCs (Xie and Spradling, 2000). Control (Fig. 4.5A-A', small arrowheads) and *coba* mutant (Fig. 4.5B-B', small arrowheads) germaria contained Lamin C^+ cells at the anterior tip. Quantification of Lamin C^+ cells showed that *coba* mutants had normal numbers of TF cells and CpCs (data not shown). This finding is consistent with the normal number of GSCs in the *coba* mutant germaria and suggests that TFs and CpCs functioned normally in the *coba* mutant.

In wildtype germaria, ECs extend cytoplasmic extensions towards and around the germline cells to form the germline microenvironment and guide germline differentiation (Schulz et al., 2002; Decotto and Spradling, 2005; Xie, 2008). The *Drosophila* segment polarity gene *armadillo* (*arm*), a homolog of the vertebrate plakoglobin and β-catenin, is required for adhesive junction and integrity of the actin cytoskeleton (Peifer et al., 1993). Anti-Arm antibodies serve as a marker for cell adhesion and were used to investigate whether germ cells were in contact with cytoplasmic extensions of ECs. In control flies, Arm staining appeared as a net-like pattern around the germline cells, filling up the entire room of germaria (Fig. 4.5C and 4.5C', small arrows). In *coba* mutant flies, this net-like

pattern was disrupted and barely detectable in regions 1 to 2B (Fig. 4.5D and 4.5D'). To verify with another marker that the cytoplasmic extensions of ECs were disrupted in *coba* mutants, we expressed cytoplasmic green fluorescent protein (GFP) under the control of a *traffic jam* (*tj*)-Gal4 transcriptional activator (*tj-Gal4>UAS-GFP*). In 7-day old control germaria (*tj-Gal4/UAS-GFP;coba/TM6* or *tj-Gal4/UAS-GFP;Df/TM6*), we detected an average of 12 GFP^+ ECs with cytoplasmic extensions encasing germline cysts in region 1 and 2A of the germarium (n=10) (Fig. 4.5E and 4.5E', large arrows). In 7-day old *coba* germaria (*tj-Gal4/UAS-GFP;coba/Df*), an average of 11 GFP^+ ECs were present in the same region (n=23). However, only 39% of the *coba* germaria contained ECs with detectable cytoplasmic extensions, while 61% only had EC's cell bodies adjoining germline cysts without cytoplasmic extension being detected (Fig. 4.5F and 4.5F', large arrowheads). Based on these findings, we hypothesize that the observed germline defects in *coba* mutants are caused by the lack of a proper germline microenvironment.

Wildtype coba gene appeared to function outside of the germline in the germarium

To address if *coba* normally functions in the germline or somatic cells, we generated $coba^{1/1}$ germline clones upon induction of flippase-mediated mitotic recombination. *Ubi*-GFP (GFP controlled by the *Ubiquitin* promoter) served as a marker for clones and Spec was a phenotypic reporter for the developmental stage of the germline cells. GFP-negative, $coba^{1/1}$ germ cell clones contained elongated and branched fusome structures as were seen in control animals, ruling out the possibility that *coba* is required in the germline lineage (Fig. 4.6A-D). This, together with our observation that ECs failed to encapsulate the germline in the *coba* mutant, led us to propose that *coba*

acts in ECs for forming or maintaining the cytoplasmic extensions, which in turn regulates germline differentiation.

coba was possibly mapped to a novel gene CG14961

To decipher the genetics basis of this mutant, deletion mapping confined *coba* to a 40 kb region in chromosomal interval between 63C6 to 63D2, where 11 genes were mapped (Fig. 4.7). We sequenced coding regions of each candidate gene (except for *karst*), and performed a non-complementation experiment assured that *karst* complemented *coba*. A premature stop codon was identified in the coding region of a predicted gene *CG14961* that translates into a predicted protein of 914 amino acids (Fig. 4.8). The gene *CG14961* is novel and no prediction of its molecular function can be made based on its amino acid sequence, and neither a conserved domain has been predicted based on the sequence.

EMS induced mutagenesis screen for non-complementation of coba discovered a second null allele of CG14961

To generate more *coba* alleles, w^{1118} male flies were treated with EMS, and the mutagenized males were mated to $coba^{1}$ virgin females to test for non-complementation according to Bökel, 2008. A total number of 3597 mutagenized single males were mated to $coba^{1}$ individually, and their progeny were screened for tiny ovaries (Fig. 4.9). Six potential *coba* alleles ($coba^{1060}$, $coba^{1458}$, $coba^{1468}$, $coba^{1632}$, $coba^{1663}$, and $coba^{2836}$) were found because of the female infertility and tiny ovaries. Among them, homozygous mutant $coba^{1468}$ had a lethality about 30% (n>300) at the pupal stage, which was much

higher than the lethality rate of the other five strains (~5%, n>300). But this *coba*^{1468} strain did not show a severer ovary defect compared to the other strains. Stocks were established for the six alleles. Their genomic DNA was sequenced for potential lesions in *CG14961* and the other nine candidate genes in the *coba* interval. We detected a premature stop codon in the coding region of *CG14961* in *coba*^{1468} (Fig. 4.8).

Previous studies showed that this EMS treatment regimen results in a good survival rate (90%) and a high mutation frequency (1 in 155.6 kb) that corresponds to 1 nonsense mutation per 1000 mutagenized flies (Winkler et al., 2005; Grigliatti, 1986). Based on these numbers, having six alleles out of 3597 strains seems much higher than the average number of EMS mutagenic hits. However, except for *coba*^{1468}, the other five strains (*coba*^{1060}, *coba*^{1458}, *coba*^{1632}, *coba*^{1663}, and *coba*^{2836}) did not have any molecular lesion in the coding region except for some single-nucleotide polymorphism (SNP) variations inherited from the parental strains. To investigate if the alleles that did not have lesions in *CG14961* could be enhancers of *coba*, they were crossed to *Df(3L)E1* and their progeny were examined for an ovary phenotype. Each allele over *Df(3L)E1* had tiny ovaries, indicating that the mutations map to the *coba* interval. In addition, trans-heterozygous progeny of interallelic crosses also had tiny ovaries, indicating that the alleles carry mutations in the same transcription unit. Together, our data suggest that all seven strains carry *coba* alleles.

One possible explanation for our failure to detect molecular lesions in the coding region of *CG14961* is that we introduced promoter mutations. However, quantitative real-time polymerase chain reaction (qRT-PCR) analysis of whole ovary mRNA samples

showed that all seven alleles, displayed *CG14961* mRNA abundances that were of no significant difference from the wildtype level (data not shown).

Validation of coba candidate gene CG14961

To restore oogenesis in *coba* mutants, we generated recombinant constructs that either contained the wildtype *CG14961* genomic region (Fig. 4.10A) or the coding region under control of yeast upstream activating sequences (UASt-*CG14961*, Fig. 4.10B and 4.10C). After transformation, we received 9 strains carrying *genomic-CG14961* (*g-14961*), 9 strains of transformants that contained UASt-*CG14961* with a N-terminal epitope tag of a FLAG protein (*UAS-FLAG-14961*), and 9 strains containing UASt-*CG14961* with a C-terminal epitope tag of a FLAG protein (*UAS-14961-FLAG*). Transgenic flies that carried either *UAS-FLAG-14961* or *UAS-14961-FLAG* were mated to transgenic flies carrying two different somatic cell-Gal4 drivers (*tj*- and *engrailed*-Gal4). Experimental flies were produced following the mating scheme shown in Fig. 4.11.

We attempted to rescue $coba^{1}$ and $coba^{1468}$, each of which contains a premature stop codon in the coding region of *CG14961*. To test if the experimental flies (*g-14961/+;coba/Df(3L)E1 and UASt-CG14961/tj-Gal4;coba/Df(3L)E1*) have a restored ovary phenotype, we dissected them a week after they were hatched. Experimental flies bearing *UAS-FLAG-14961* or *UAS-14961-FLAG* constructs were raised at 29°C all the time to maximize the Gal4 activity. To our surprise, all of the experimental animals (n>30 per strain), either carrying the genomic or coding region of *CG14961*, displayed a majority (>80%) of tiny ovaries without later stages of egg chambers, which appeared

similar as their sibling mutant controls, suggesting that none of the rescue constructs restored *coba* function in the *coba*^{1} and *coba*^{1468} female gonads.

As an alternative way to show that c*oba* corresponds to *CG14961*, we tried to knockdown *CG14961* in ovaries to see if it would phenocopy the *coba* mutant. For this, we expressed three different RNA hairpins directed against *CG14961* (UAS-*CG14961i*) in somatic cells of otherwise wildtype ovaries using two somatic cell specific drivers (*tj*- and *C784*-Gal4). To induce a higher level of expression and to observe the knockdown effect to oogenesis at different developmental stages, flies were shifted from 18°C to 29°C as embryos, 3rd instar larvae, mid-pupae and 3-day old adults. Unfortunately, we did not find a significant percentage (<20%) of tiny ovaries in any of the animals. We validated the results by quantifying *CG14961* mRNA abundances in ovaries. qRT-PCR results revealed that *CG14961* mRNA molecules from the experimental animal ovaries were not significantly decreased compared to controls (data not shown). It is thus very likely that none of the UAS-*CG14961i* constructs worked efficiently in ovaries.

Lastly, we aimed to show that *CG14961* is expressed in somatic cells of the ovary. However, *in situ* hybridization, using an antisense RNA probe that was transcribed from *CG14961* cDNA, did not reveal any signal above background in wildtype embryos, 3rd instar larval gonads, or adult ovaries. As we did detect *CG14961* by reverse transcription-polymerase chain reaction (RT-PCR), this suggests that the transcriptional level of *CG14961* in *Drosophila* may be below the detectable threshold by way of *in situ* hybridization.

Discussion

Drosophila GSCs and their daughters are regulated by somatic support cells, that form a cellular microenvironment to ensure proper and sustained gametogenesis throughout adult life. However, the research on molecular and cellular mechanisms that govern the formation or maintenance of the germline microenvironment and the feedback signaling from the germline to the somatic support cells during different stages of gametogenesis is still in its infancy. We characterized *coba* phenotypes in adult female ovaries, indicating it is likely that *coba* plays an instructive role in the ESC cell lineage to maintain the structure of the somatic microenvironment of GSC daughters and consequently, regulate the fate determination of the germline.

coba could act in a novel signaling pathway regulating germline enclosure or act in one of the known pathways. Since the *coba* mutations are specific to the female gonad and also display lethality in development similar to the ecdysone phenotypes, the most likely pathway for an interaction with *coba* is probably ecdysone signaling. Genetic interaction studies with components of EGF and Jak/STAT signaling pathways are yet to be performed to address this question.

Currently, we aim to verify that *coba* corresponds to *CG14961*. Unfortunately, introducing rescue constructs containing *CG14961* into *coba* mutants did not restore oogenesis. We anticipate several potential reasons for this. Most likely, the gene annotation of *coba* provided by FlyBase (http://flybase.org/) is incomplete. The Berkeley *Drosophila* Genome Project (BDGP, http://www.fruitfly.org/) is still ongoing and regularly incorporated new assembly data into FlyBase. It is likely that another exon of *CG14961* that has not been predicted. Our genomic-DNA rescue construct includes the

CG14961 upstream regulatory region that covers from the end of the closest neighbor gene, PHGPx (Fig. 4.7), to the start codon (about 1,400 bp), the coding region (2801 bp), and the 3' untranslated region (UTR) that begins after the stop codon to the "AATAAA" polyadenylation site (about 250 bp). Although a "TATAAA" consensus promoter sequence is present in our construct, the genomic-DNA rescue construct could be nonfunctional due to the lack of a complete upstream regulatory element or due to the lack of an alternatively spliced 5' exon. Our cDNA-rescue construct may not be functional either because we lack an exon or because the FLAG Tag interferes with Coba function. We were not able to detect FLAG expression using an anti-FLAG antibody upon expressing our *CG14961* constructs under the control of a ubiquitously expressed *actin*-Gal4 driver. Only one line showed expression at the cuticles in the larval stage, but none showed in the adult ovaries (data not shown). Western blotting using protein lysate prepared from 7-day old adult ovaries did not detect FLAG either (data not shown). Next-generation sequencing employs deep-sequencing technologies, allowing the generation of an unbiased profile of the transcriptome (Najmabadi et al., 2011; Sultan et al., 2008). Unfortunately, the available ovary transcriptome data (Daines, et al., 2011) failed to provide reliable sequence information at the 5' end of *CG14961*, probably because mRNA degradation is usually initiated from the 5' end. To undoubtedly identify the coding region of *CG14961*, we are currently establishing an extensive map of ovary transcriptome to find a potential lacking exon of *CG14961*.

Another explanation for our failure to rescue *coba* via expression of *CG14961* is that we expressed it in the incorrect somatic cell type. We excluded the possibility that *coba* functions in the germline, using mitotic clonal analysis. Yet we have not obtained

solid evidence showing that *coba* functions in the somatic support cells. To confirm this hypothesis, ideally we have to generate $coba^{1/1}$ clones in the somatic cell lineage and see if the mutant cells lack cytoplasmic extensions. However, ECs remain quiescent in the normal situation and only divide very rarely as needed (Morris and Spradling, 2011; Kirilly et al., 2011), which means it is unlikely to induce clusters of mutant ECs in the germarium. Without confirming that *coba* functions in the somatic cell lineage unequivocally, it is possible that *coba* acts in the ovarian sheath or is involved in the synthesis of certain hormones that are functional in the hemolymph, in which cases our Gal drivers would not be able to activate expression of the wildtype copy of *CG14961* in the required tissues or cell types.

Lastly, *CG14961* may not correspond to *coba*. Although we have performed experiments, including genomic/cDNA rescuing, RNAi phenocopy and *in situ* hybridization, to draw a connection between *CG14961* and *coba*, yet so far we have no direct evidence pointing that *CG14961* corresponds to *coba* or contributes to the *coba* phenotypes. However, we reason that the chances of having multiple genes mapped to the same chromosomal interval and contributing to the same phenotype is very low. Since *CG14961* did not rescue *coba*, it could be possible that a microRNA or another gene, which has not been predicted in that chromosomal interval, may contribute to *coba*.

In conclusion, we have shown that *coba* is instructive in shaping the somatic microenvironmental cells, which are important in regulating the CB-to-CC fate transition in female flies. We also disclosed the genetic mapping of *coba* to a putative novel gene *CG14961*. But since we have not yet verified *CG14961* as a *bona fide* gene

corresponding to *coba*, future experiments will address *coba*'s molecular nature and the genetic or biochemical pathways that it functions in.

Acknowledgements

We thank Dorothea Godt, Ed Laufer, and Graham Thomas for flies and reagents, and Edward Kipreos, James Lauderdale, and John Shields for critical discussions. We are grateful to members of the Schulz laboratory for comments on the manuscript. This work was supported by NSF grants #0841419 and #1355099 given to CS.

	Young (3-day old)		Aged (10-day old)	
	control (n=100)	***coba*^{1}*/Df(3L)E1*** (n=100)	**control** (n=100)	***coba*^{1}*/Df(3L)E1*** (n=65)
TUNEL^{+} germline cells per germarium	0.12	0.11	0.48	0.05
% of germaria containing TUNEL^{+} germline cells	5%	6%	8%	3%
TUNEL^{+} somatic cells per germarium	0.50	0.38	0.20	0.35
% of germaria containing TUNEL^{+} somatic cells	9%	7%	9%	9%

Table 4.1:

Negligible amounts of cell death were observed in *coba* mutants. Age, genotypes, TUNEL^{+} germline or somatic cells per germarium, percentage of germaria containing TUNEL^{+} germline or somatic cells, and number of germaria are as indicated. Neither germline cells nor somatic cells in *coba* had significantly increased apoptosis. n=number of germaria.

% of germ cells in	Young (3-day old)			Aged (10-day old)		
	control (n=200)	***coba*^{1}*/Df(3L)E1*** (n=200)	***P*-values**	**control** (n=100)	***coba*^{1}*/Df(3L)E1*** (n=100)	***P*-values**
S-phase (BrdU^{+}/Vasa^{+})	5.94%	7.26%	0.10	5.88%	9.44%	0.04
M-phase (pHH3^{+}/Vasa^{+})	0.59%	0.70%	0.51	0.34%	0.22%	0.45

Table 4.2:

coba mutant germ cells did not have significant defects in proliferation. Age, genotypes, percentage of germline cells in different phases, number of germaria, and *P*-values are as indicated. Slight increases in percentage of germline cell in the S-phase were observed in both young and aged *coba* flies, whereas the percentages of germline cells in M-phase were not changed significantly in neither age of *coba* flies. n=number of germaria.

Figure 4.1: *coba* flies had severe defects in oogenesis.

(A) and (B) Light microscopy of 7-day old fly ovaries, scale bars: 1000 μm.

(A) Three pairs of control fly ovaries. Each ovary contained more than 10 developing ovarioles with mature eggs (small arrows) at the posterior ends.

(B) Three pairs of *coba* mutant ovaries. Ovarioles were less developed with only early stages of egg chambers. No mature eggs were observed at the posterior ends of the ovarioles.

(C)-(G) DAPI stained ovarioles of young and aged flies, anterior tips of germaria to the left, scale bars: 10 μm.

(C) In a young control ovariole, the germarium (large arrowhead) was filled with only small nuclei. Egg chambers contained increasingly larger nuclei that indicated nurse cells (nc), whereas follicle cells (fc) were seen as a peripheral monolayer of smaller nuclei.

(D) A young *coba* ovariole, lacking a germarium and egg chambers of stages 7-9.

(E) An aged control ovariole appeared similar to (C) the young control.

(F) An aged *coba* ovarioles, with fractionated nuclei (large arrow) in the S8 egg chamber.

(G) An aged *coba* ovarioles, lacking early-stage germline cells in the germarium. A large nucleus indicative of a nurse cell (nc) appeared in 2B region of the germarium. The S7 egg chamber is not ovoid-shaped (medium arrowhead) and the S8 egg chamber contains more than 15 nurse cells nuclei (medium arrows).

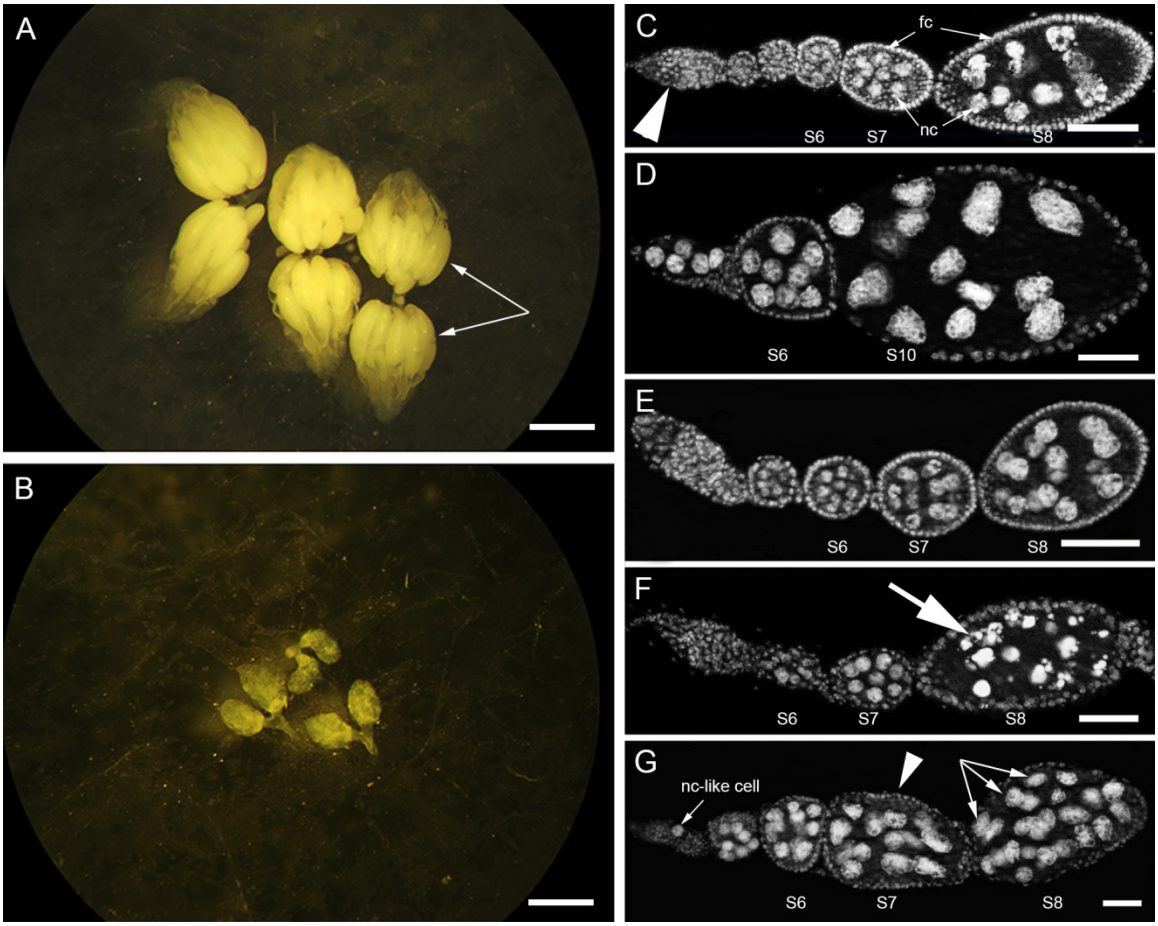
A
B
C
fc
nc
S6
S7
S8
D
S6
S10
E
S6
S7
S8
F
S6
S7
S8
G
nc-like cell
S6
S7
S8

Figure 4.2: *coba* had fewer germline cells in the germaria.

Apical tips of germaria to the left.

(A)-(D) Immuno-labeling with anti-Vasa antibody, scale bars: 10 μm.

(A) Young and (C) aged control flies had $Vasa^{+}$ cells filling up the germarium.

(B) Young and (D) aged *coba* germaria had areas depleted of $Vasa^{+}$ cells (arrows).

(E) Quantification of $Vasa^{+}$ cells per germarium (region 1 to 2B) of young and aged flies. Ages and genotypes are color-coded as indicated. *Y*-axis shows the average number of germline cells per germarium. n=number of germaria.

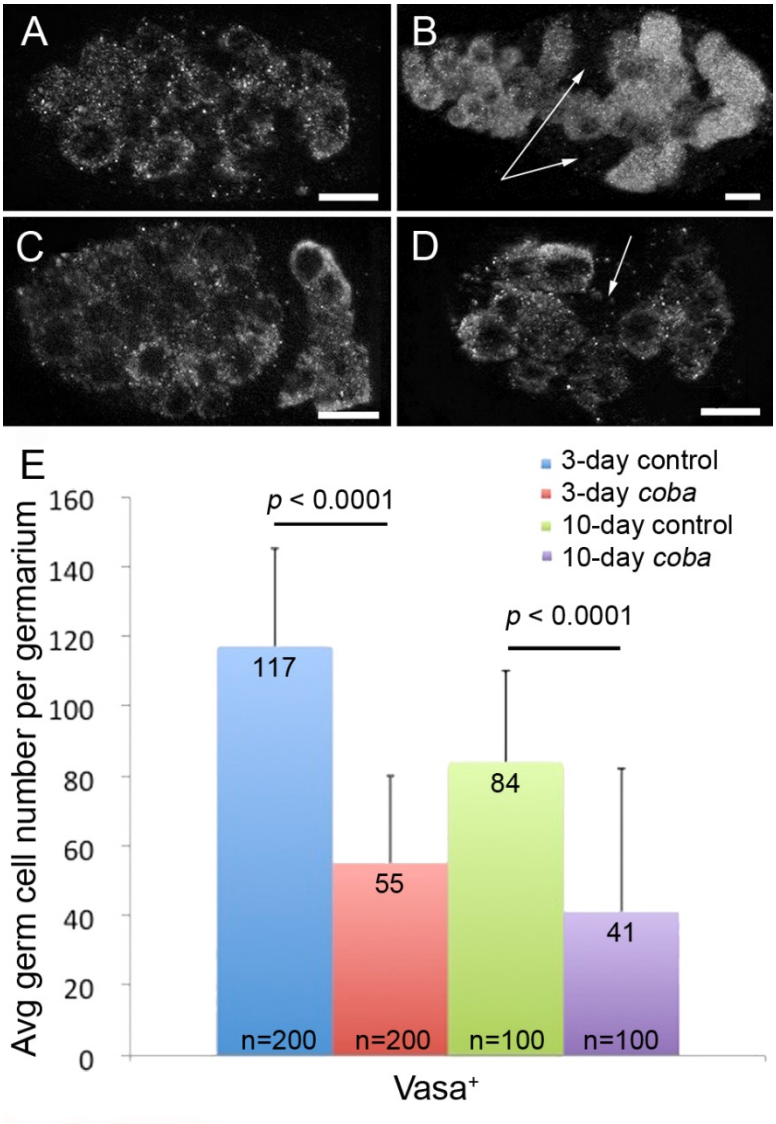
A
B
C
D
E
3-day control
3-day coba
10-day control
10-day coba
p < 0.0001
p < 0.0001
Avg germ cell number per germarium
160
140
120
100
80
60
40
20
0
117
55
84
41
n=200
n=200
n=100
n=100
Vasa+

Figure 4.3: Early-stage germline cells failed to differentiate in *coba* mutants.

Apical tips of germaria to the left.

(A)-(E) Immuno-labeling with anti-Spec antibody, scale bars: 10 μm.

(A) Young and (C) aged control flies had round fusomes appearing as single dots within region 1 of the germaria, and branched fusomes in regions 2A and 2B.

(B) Young and (D) and (E) aged *coba* mutants contained only few branched fusomes in the germaria. (E) The phenotype was seen aggravated in aged *coba* mutants, with single dots of fusomes filling the entire germaria.

(F) Quantification of round fusomes versus branched fusomes in young and aged flies, respectively. *X*-axis shows ages and genotypes, and *Y*-axis shows average number of fusomes per germarium. Fusome shapes are color-coded as indicated, n=number of germaria.

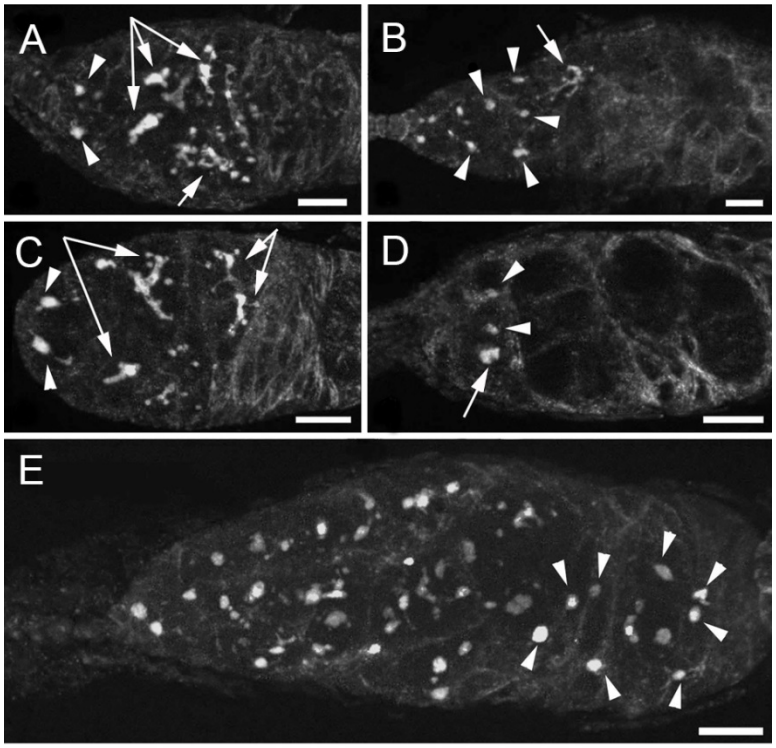
A
B
C
D
E

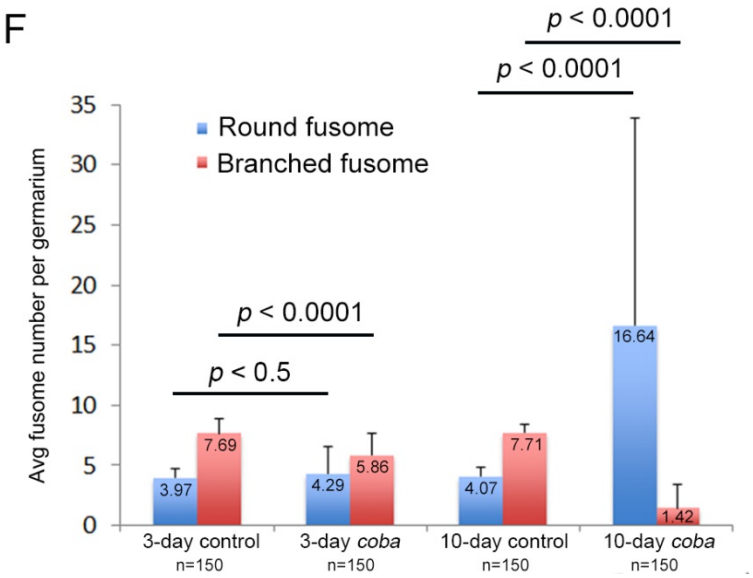
F
p < 0.0001
p < 0.0001
p < 0.0001
p < 0.5
Round fusome
Branched fusome
Avg fusome number per germarium
35
30
25
20
15
10
5
0
3.97
7.69
4.29
5.86
4.07
7.71
16.64
1.42
3-day control
n=150
3-day coba
n=150
10-day control
n=150
10-day coba
n=150

Figure 4.4: Accumulating early-stage germline cells in *coba* mutants were not GSCs but CBs.

Apical tips of germaria to the left.

(A)-(D") Immuno-labeling with molecular markers, as indicated, scale bars: 10 μm. Germaria from (A)-(A") young control, (B)-(B") young *coba*, (C)-(C") aged control, and (D)-(D") aged *coba* animals.

(A) and (C) Control germaria with a few Sxl^+ cells in region 1.

(B) A germarium from a young *coba* mutant fly with an enlarged area of Sxl^+ cells, and (D) a germarium from an aged *coba* mutant fly filled with Sxl^+ cells.

(A') and (C') Control germaria with Bam^+ cells in region 2A.

(B') A germarium from a *coba* mutant fly with fewer Bam^+ cells within region 2A, and (D') a germarium from an aged *coba* mutant fly without Bam^+ cells.

(A") and (C") Control germaria with 2 $pMad^+$ cells (outlined by yellow dashed circles) close to the anterior tip.

(B") and (D") *coba* germaria with 2 $pMad^+$ cells (outlined by yellow dashed circles).

(E) Quantification of Sxl^+, Bam^+, and $pMad^+$ cells in young and aged control and *coba* mutant germaria. Ages and genotypes are color-coded as indicated, *X*-axis shows different molecular markers, and *Y*-axis shows the average numbers of marker-positive germline cells per germarium.

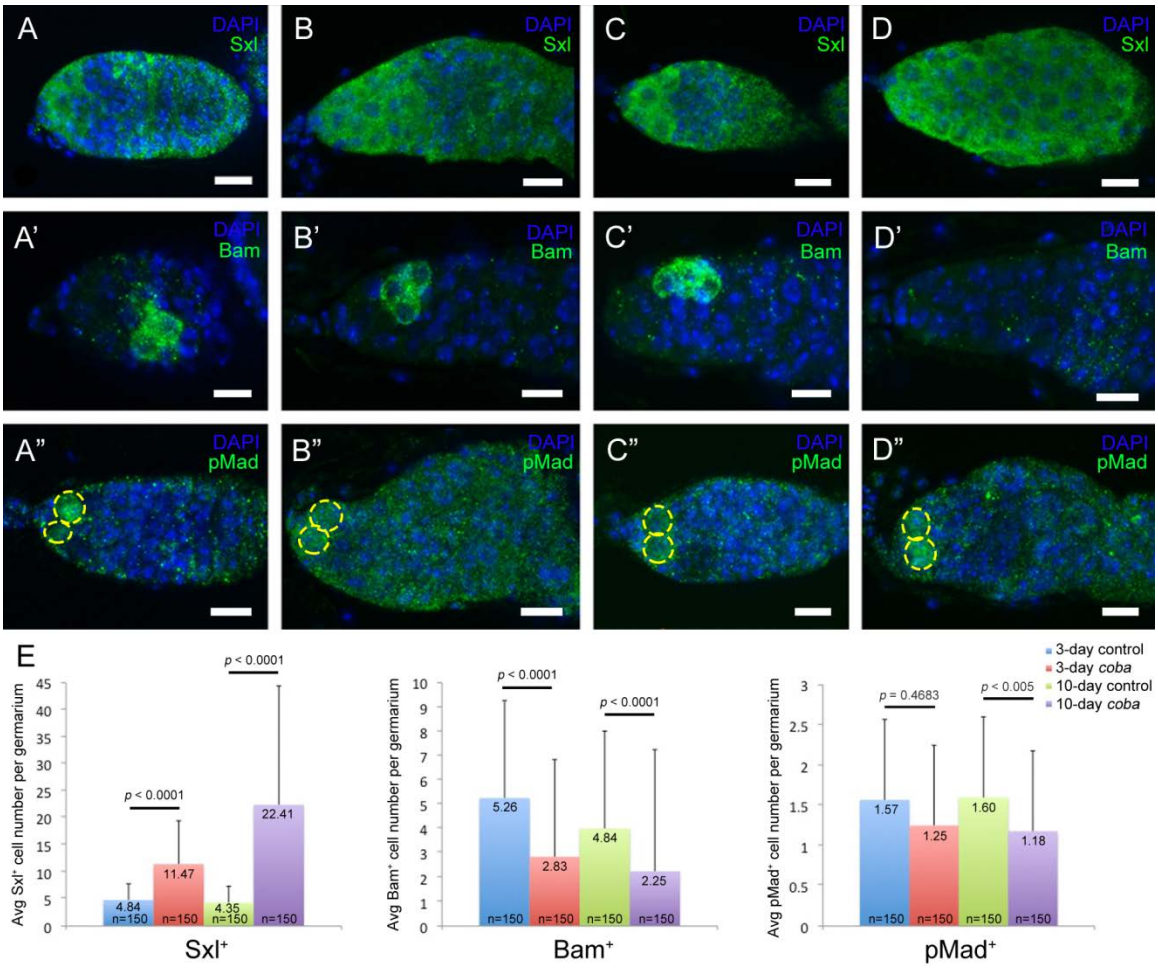
A
DAPI
Sxl
B
DAPI
Sxl
C
DAPI
Sxl
D
DAPI
Sxl
A'
DAPI
Bam
B'
DAPI
Bam
C'
DAPI
Bam
D'
DAPI
Bam
A"
DAPI
pMad
B"
DAPI
pMad
C"
DAPI
pMad
D"
DAPI
pMad
E
3-day control
3-day coba
10-day control
10-day coba
Avg Sxl+ cell number per germarium
p < 0.0001
p < 0.0001
4.84
n=150
11.47
n=150
4.35
n=150
22.41
n=150
Sxl+
Avg Bam+ cell number per germarium
p < 0.0001
p < 0.0001
5.26
n=150
2.83
n=150
4.84
n=150
2.25
n=150
Bam+
Avg pMad+ cell number per germarium
p = 0.4683
p < 0.005
1.57
n=150
1.25
n=150
1.60
n=150
1.18
n=150
pMad+

Figure 4.5: In germaria from *coba* mutant animals, ECs were present but did not contain cytoplasmic extensions around the germline.

Apical tips of germaria to the left, small arrowheads indicate the GSC niche (TF and CpCs), small arrows point to the cytoplasmic extensions labeled by Arm, large arrows point to the cytoplasmic extensions labeled by GFP, large arrowheads point to the cell bodies of ECs.

(A)-(F') Immuno-labeling with molecular markers, as indicated, scale bars: 10 μm.

(A) and (A') A control germarium with strong Lamin C staining in TF and CpCs (small arrowheads) at the tip.

(B) and (B') A germarium from a *coba* mutant animal showing the GSC niche cells (small arrowheads) at the apical tip based on strong Lamin C labeling. Note the there is no obvious difference in numbers or shapes between the control and *coba* Lamin C^+ cells.

(C) and (C') A control germarium showing an Arm^+, net-like pattern of cytoplasmic extensions (small arrows) around the germline. Note the GSC niche cells were also stained strongly with Arm.

(D) and (D') A germarium from a *coba* mutant animal without an Arm^+, net-like pattern of cytoplasmic extensions around the germline. The GSC niche was still present, based on the Arm staining (small arrow) at the tip.

(E) and (E') A control germarium with GFP-labeled ECs, showing the squamous EC cytoplasmic extensions (large arrows) encasing the germline.

(F) and (F') A germarium from a *coba* mutant animal with GFP-labeled cell bodies of ECs (large arrowheads), but lacking cytoplasmic extensions around the germline.

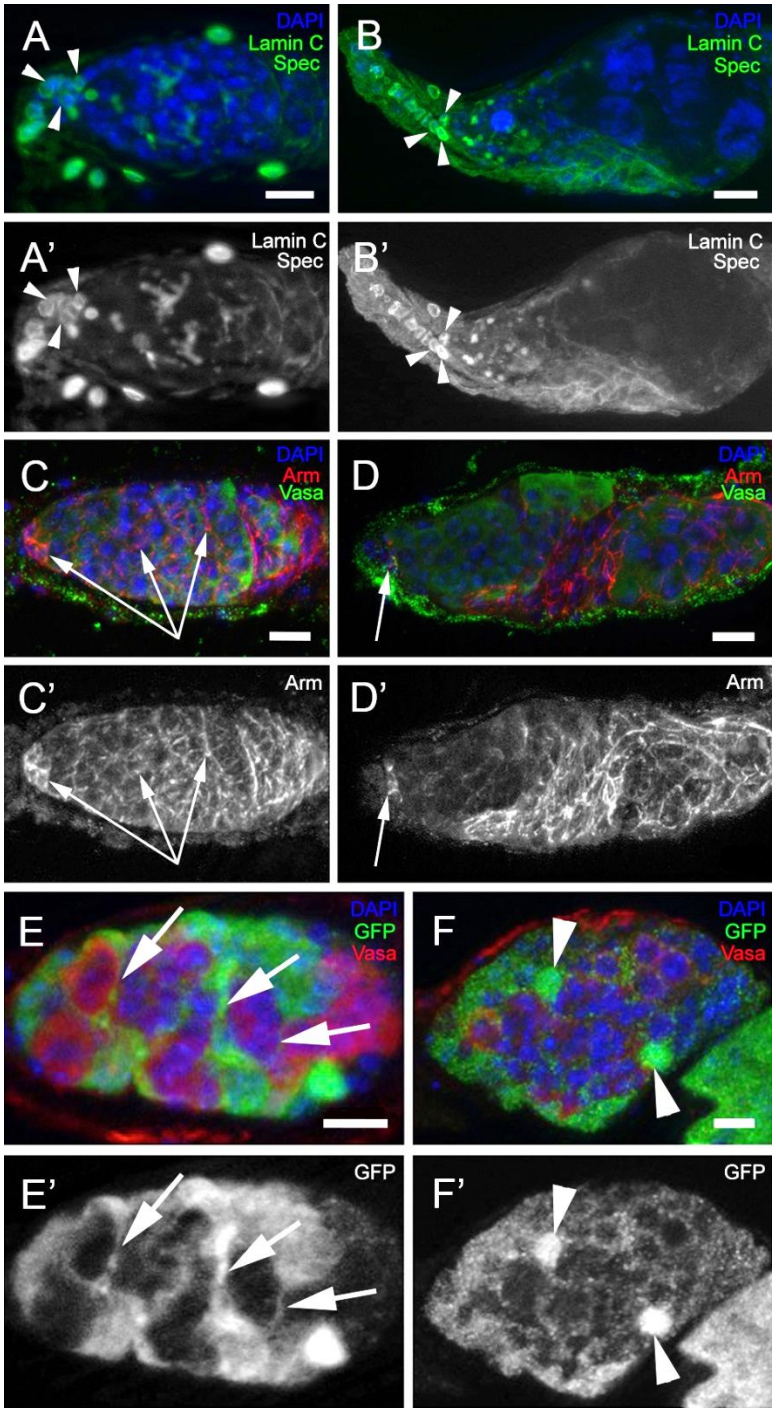
A
DAPI
Lamin C
Spec
B
DAPI
Lamin C
Spec
A'
Lamin C
Spec
B'
Lamin C
Spec
C
DAPI
Arm
Vasa
D
DAPI
Arm
Vasa
C'
Arm
D'
Arm
E
DAPI
GFP
Vasa
F
DAPI
GFP
Vasa
E'
GFP
F'
GFP

Figure 4.6: *coba* does not act in the germline.

Apical tips of germaria to the left.

(A)-(D) Immuno-labeling with molecular markers, as indicated, scale bars: 10 μm.

(A) A control germarium showing branched fusomes in control GFP^- clones (outlined by yellow dashes).

(B)-(D) Three germaria with $coba^{1/1}$ germline clones represented by GFP^- cells (outlined by yellow dashes). Note that the fusomes were branched as in the control.

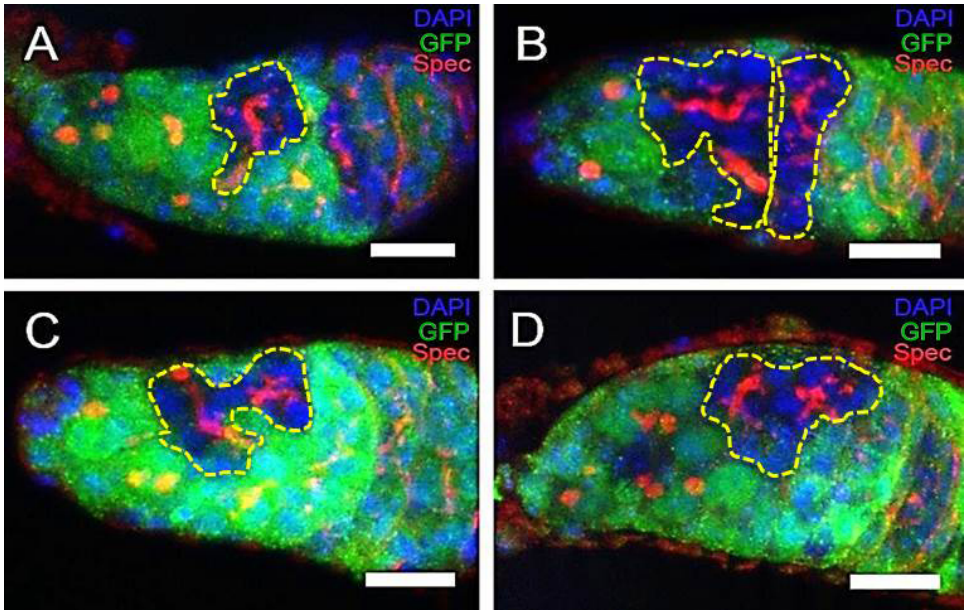
A
DAPI
GFP
Spec
B
DAPI
GFP
Spec
C
DAPI
GFP
Spec
D
DAPI
GFP
Spec

Figure 4.7: *coba* was mapped to a novel gene, *CG14961*.

coba was mapped to a 40 kb region of the chromosomal interval 63C6 to 63D2. The region contains 11 candidate genes. Deficiency lines covering *coba* are color-coded in blue, deficiencies not covering *coba* are in red. *CG14961* is framed in red.

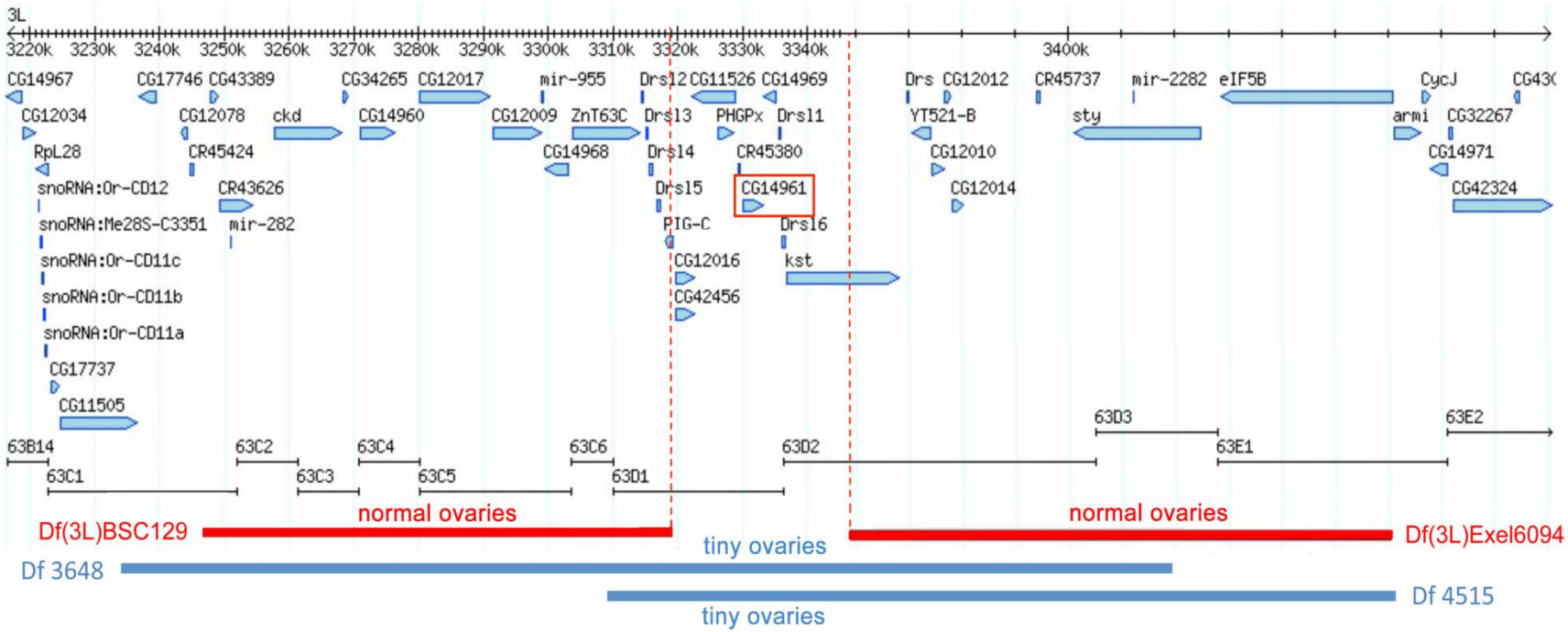
3L
3220k 3230k 3240k 3250k 3260k 3270k 3280k 3290k 3300k 3310k 3320k 3330k 3340k 3400k
CG14967 CG17746 CG43389 CG34265 CG12017 mir-955 Drs12 CG11526 CG14969 Drs CG12012 CR45737 mir-2282 eIF5B CycJ CG43(
CG12034 CG12078 ckd CG14960 CG12009 ZnT63C Drs13 PHGPx Drs11 YT521-B sty armi CG32267
RpL28 CR45424 CG14968 Drs14 CR45380 CG12010 CG14971
snoRNA:Or-CD12 CR43626 Drs15 CG14961 CG12014 CG42324
snoRNA:Me28S-C3351 mir-282 PIG-C Drs16
snoRNA:Or-CD11c CG12016 kst
snoRNA:Or-CD11b CG42456
snoRNA:Or-CD11a
CG17737
CG11505
63D3 63E2
63B14 63C2 63C4 63C6 63D2 63E1
63C1 63C3 63C5 63D1
normal ovaries
normal ovaries
Df(3L)BSC129
tiny ovaries
Df(3L)Exel6094
Df 3648
Df 4515
tiny ovaries

Figure 4.8: DNA sequence of *CG14961* gene region.

The nucleotide and amino acid sequence of *CG14961*. The intronic region in white and shaded in blue. Two nonsense mutations identified in $coba^{1}$ and $coba^{1468}$ are highlighted in red, and the red numbers in parentheses indicate the position of the mutations.


* (335) coba1468
* (783) coba1

Figure 4.9: Crossing scheme of the EMS induced mutagenesis for non-complementation of *coba*.

A total of 1000 w^{1118} male starter flies were fed with EMS, mated in bulk to virgins with the 3rd chromosome balanced, 3597 lines of male progeny were collected and mated individually to $coba^{1}$ virgins for non-complementation screen, and 6 lines ($coba^{1060}$, $coba^{1458}$, $coba^{1468}$, $coba^{1632}$, $coba^{1663}$, and $coba^{2836}$) were identified having tiny ovaries without other obvious gross morphological defects. Phenotypic traits like eye color, body color, and bristle number are indicated within brackets.

* Only mutations on the 3rd chromosome are illustrated, "m" stands for mutation, numeric subscripts stand for different mutations occurred on the same chromosome.

** Strains that were neither mated nor maintained.

♂ w^{1118} ; + ; + ⇜ *EMS*

[white eyes]

↓

G_0: ♂ w^{1118} ; + ; $m_{(1, 2, 3,..., n)}$ * x w^{1118} ; + ; $coba^1$/*TM6B, Hum* ♀♀

[white eyes] [orange eyes, more humeral bristles]

↓

F_1: w^{1118} ; + ; $m_{(1, 2, 3,..., n)}$/$coba^1$ **

[orange eyes]

♂ w^{1118} ; + ; $m_{(1, 2, 3,..., n)}$/*TM6B, Hum* x w^{1118} ; + ; $coba^1$/*TM6B, Hum* ♀♀

[white eyes, more humeral bristles] [orange eyes]

↓ 3597 single male crosses

F_2: w^{1118} ; + ; $m_{(1, 2, 3,..., n)}$/$coba^1$ (screen for non-complementation)

[orange eyes]

w^{1118} ; + ; $m_{(1, 2, 3,..., n)}$/*TM6B, Hum* (establish stocks)

[white eyes, more humeral bristles]

w^{1118} ; + ; $coba^1$/*TM6B, Hum* **

[orange eyes, more humeral bristles]

Figure 4.10: Maps of the *CG14961* genomic- and coding-DNA rescue constructs.

(A) The genomic-DNA rescue construct. The recombined construct has the long terminal repeat (LTR) flanking the *mini-white* reporter gene, Ampicillin-resistant gene (Amp^r), Origin of replication (*Ori*), *CG14961* regulatory region (5'UTR), coding region, and downstream regulatory region (3'UTR).

(B) and (C) Two coding-DNA rescue constructs. The recombined constructs both have the LTR flanking the *mini-white* reporter gene, Amp^r, *Ori*, UASt promoter region, *CG14961* coding region, and 3xFLAG sequence (highlighted in yellow boxes). The 3xFLAG sequence is tagged either (B) in front of or (C) behind the coding region.

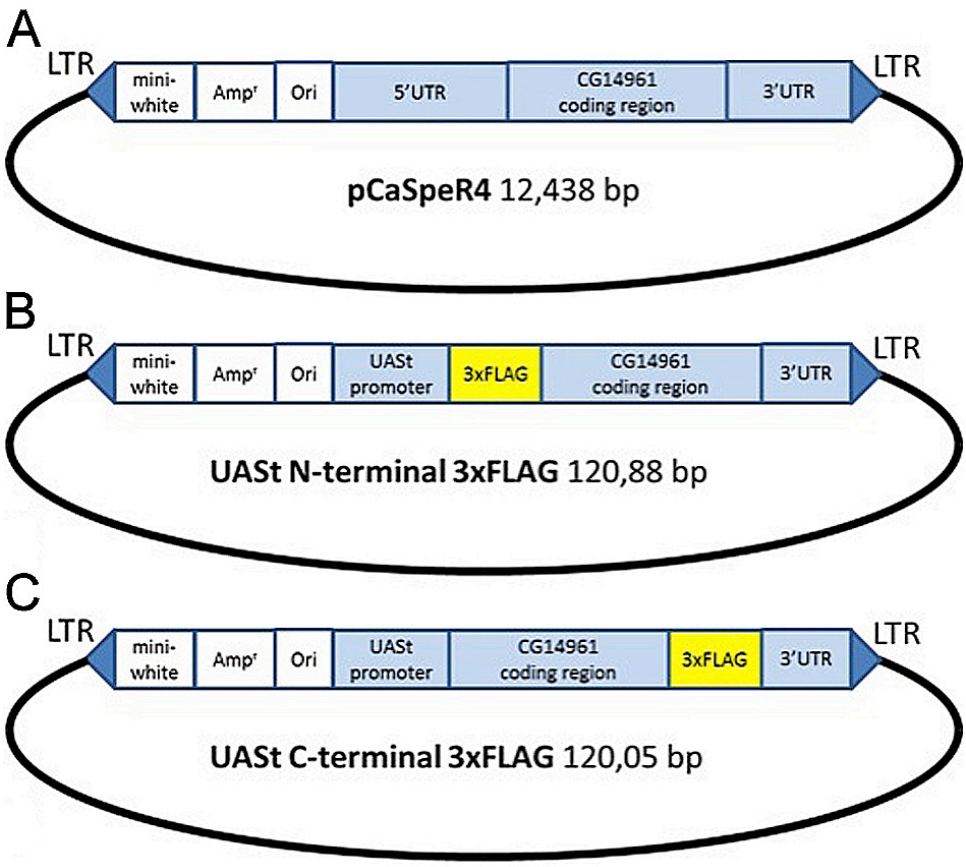
A
LTR
mini-white
Amp^r
Ori
5'UTR
CG14961 coding region
3'UTR
LTR
pCaSpeR4 12,438 bp
B
LTR
mini-white
Amp^r
Ori
UASt promoter
3xFLAG
CG14961 coding region
3'UTR
LTR
UASt N-terminal 3xFLAG 120,88 bp
C
LTR
mini-white
Amp^r
Ori
UASt promoter
CG14961 coding region
3xFLAG
3'UTR
LTR
UASt C-terminal 3xFLAG 120,05 bp

Figure 4.11: Cross schemes of rescuing *coba* with flies transformed with genomic- and coding-DNA constructs.

Flies transformed with (A) genomic-DNA or (B) coding-DNA of *CG14961* were crossed to flies contain *coba*^{1} or *Df(3L)E1* to generate experimental and control lines. Phenotypic traits like eye color, body color, bristle number, and wing trait are indicated within brackets.

* "*g-14961*"stands for genomic-DNA rescue construct containing genomic region of *CG14961*, and "*mw*" stands for *mini-white*, serving as a positive marker of transgene incorporation.

** "*N/C-14961*" stands for cDNA rescue UASt constructs containing *coding-CG14961*, either following a N-terminal epitope tag of a FLAG protein (*UAS-FLAG-14961*) or followed by a C-terminal epitope tag of a FLAG protein (*UAS-14961-FLAG*), respectively.


A
G0: w1118 ; g-14961mw/CyO ; ftz, e/TM6B, e* x w1118 ; tj-Gal4mw/CyO ; coba1 mw/TM6B, e
[light orange eyes, curly wings, ebony body color, more humeral bristles] [red eyes, curly wings, normal body color, more humeral bristles]
F1: w1118 ; g-14961mw/CyO ; coba1 mw/TM6B, e x w1118 ; tj-Gal4mw ; Df(3L)E1/TM6B, e
[orange eyes, curly wings, normal body color, more humeral bristles] [red eyes, straight wings, normal body color, more humeral bristles]
F2: w1118 ; g-14961mw/tj-Gal4mw ; coba1 mw/Df(3L)E1 (experimental)
[orange eyes, straight wings, normal body color, normal humeral bristles]
w1118 ; tj-Gal4mw/CyO ; coba1 mw/Df(3L)E1 (control)
[red eyes, curly wings, normal body color, normal humeral bristles]
B
G0: w1118 ; N/C-14961mw/CyO ; ftz, e/TM6B, e** x w1118 ; spi/CyO ; Df(3L)E1/TM6B, e
[light orange eyes, curly wings, ebony body color, more humeral bristles] [white eyes, curly wings, normal body color, more humeral bristles]
F1: w1118 ; N/C-14961mw/CyO ; Df(3L)E1/TM6B, e x w1118 ; tj-Gal4mw ; coba1 mw/TM6B, e
[light orange eyes, curly wings, normal body color, more humeral bristles] [red eyes, straight wings, normal body color, more humeral bristles]
F2: w1118 ; N/C-14961mw/tj-Gal4mw ; coba1 mw/Df(3L)E1 (experimental)
[orange eyes, straight wings, normal body color, normal humeral bristles]
w1118 ; tj-Gal4mw/CyO ; coba1 mw/Df(3L)E1 (control)
[red eyes, curly wings, normal body color, normal humeral bristles]

References

Ashburner, M., 1989. Drosophila. A Laboratory Manual. Cold Spring Harbor Laboratory Press, New York.

Bökel, C. EMS Screens: From Mutagenesis to Screening and Mapping. In: Dahmann, C. (ed.), 2008, Methods in Molecular Biology: Drosophila. pp. 119-138. Humana Press, Totowa, NJ

Brand, A.H., Perrimon, N., 1993. Targeted gene expression as a means of altering cell fates and generating dominant phenotypes. Development 118, 401-415.

Bukovsky, A., 2011. Ovarian stem cell niche and follicular renewal in mammals. Anatomical record 294, 1284-1306.

Chang, Y.J., Pi, H., Hsieh, C.C., Fuller, M.T., 2013. Smurf-mediated differential proteolysis generates dynamic BMP signaling in germline stem cells during Drosophila testis development. Developmental biology 383, 106-120.

Chau, J., Kulnane, L.S., Salz, H.K., 2009. Sex-lethal facilitates the transition from germline stem cell to committed daughter cell in the Drosophila ovary. Genetics 182, 121-132.

Chen, D., McKearin, D., 2005. Gene circuitry controlling a stem cell niche. Current biology : CB 15, 179-184.

Chen, D., McKearin, D.M., 2003. A discrete transcriptional silencer in the bam gene determines asymmetric division of the Drosophila germline stem cell. Development 130, 1159-1170.

Cook, R.K., Christensen, S.J., Deal, J.A., Coburn, R.A., Deal, M.E., Gresens, J.M., Kaufman, T.C., Cook, K.R., 2012. The generation of chromosomal deletions to

provide extensive coverage and subdivision of the Drosophila melanogaster genome. Genome biology 13, R21.

Cox, D.N., Chao, A., Lin, H., 2000. piwi encodes a nucleoplasmic factor whose activity modulates the number and division rate of germline stem cells. Development 127, 503-514.

Daines, B., Wang, H., Wang, L., Li, Y., Han, Y., Emmert, D., Gelbart, W., Wang, X., Li, W., Gibbs, R., Chen, R., 2011. The Drosophila melanogaster transcriptome by paired-end RNA sequencing. Genome research 21, 315-324.

Decotto, E., Spradling, A.C., 2005. The Drosophila ovarian and testis stem cell niches: similar somatic stem cells and signals. Developmental cell 9, 501-510.

Flesken-Nikitin, A., Hwang, C.I., Cheng, C.Y., Michurina, T.V., Enikolopov, G., Nikitin, A.Y., 2013. Ovarian surface epithelium at the junction area contains a cancer-prone stem cell niche. Nature 495, 241-245.

Ghazal, S., 2013. Oogonial stem cells: do they exist and may they have an impact on future fertility treatment? Current opinion in obstetrics & gynecology 25, 223-228.

Grigliatti, T., 1986. Mutagenesis. In Drosophila. A practical approach (ed. D.B. Roberts), pp. 39-59. IRL Press Ltd., Oxford, UK.

Hsu, Y.C., Li, L., Fuchs, E., 2014. Emerging interactions between skin stem cells and their niches. Nature medicine 20, 847-856.

Hunter, J.A.A., Savin, J., and Dahl, M.V., 1995. Clinical Dermatology (2nd edition). Blackwell Science, Oxford.

Kai, T., Spradling, A., 2003. An empty Drosophila stem cell niche reactivates the proliferation of ectopic cells. Proceedings of the National Academy of Sciences of the United States of America 100, 4633-4638.

Kiger, A.A., Jones, D.L., Schulz, C., Rogers, M.B., Fuller, M.T., 2001. Stem cell self-renewal specified by JAK-STAT activation in response to a support cell cue. Science 294, 2542-2545.

Kiger, A.A., White-Cooper, H., Fuller, M.T., 2000. Somatic support cells restrict germline stem cell self-renewal and promote differentiation. Nature 407, 750-754.

King, F.J., Szakmary, A., Cox, D.N., Lin, H., 2001. Yb modulates the divisions of both germline and somatic stem cells through piwi- and hh-mediated mechanisms in the Drosophila ovary. Molecular cell 7, 497-508.

King, R.C., 1970. In Ovarian Development in Drosophila melanogaster. New York: Academic Press.

Kirilly, D., Wang, S., Xie, T., 2011. Self-maintained escort cells form a germline stem cell differentiation niche. Development 138, 5087-5097.

Kirilly, D., Xie, T., 2007. The Drosophila ovary: an active stem cell community. Cell research 17, 15-25.

Klingler, M., Gergen, J.P., 1993. Regulation of runt transcription by Drosophila segmentation genes. Mechanisms of development 43, 3-19.

Konig, A., Yatsenko, A.S., Weiss, M., Shcherbata, H.R., 2011. Ecdysteroids affect Drosophila ovarian stem cell niche formation and early germline differentiation. The EMBO journal 30, 1549-1562.

Lee, J.K., Coyne, R.S., Dubreuil, R.R., Goldstein, L.S., Branton, D., 1993. Cell shape and interaction defects in alpha-spectrin mutants of Drosophila melanogaster. The Journal of cell biology 123, 1797-1809.

Li, M.A., Alls, J.D., Avancini, R.M., Koo, K., Godt, D., 2003. The large Maf factor Traffic Jam controls gonad morphogenesis in Drosophila. Nature cell biology 5, 994-1000.

Lin, H., Yue, L., Spradling, A.C., 1994. The Drosophila fusome, a germline-specific organelle, contains membrane skeletal proteins and functions in cyst formation. Development 120, 947-956.

Lindsley, D.L., and Zimm, G.G., 1992, The Genome of Drosophila melanogaster. Academic Press, San Diego, California.

Liu, M., Lim, T.M., Cai, Y., 2010. The Drosophila female germline stem cell lineage acts to spatially restrict DPP function within the niche. Science signaling 3, ra57.

Lopez-Onieva, L., Fernandez-Minan, A., Gonzalez-Reyes, A., 2008. Jak/Stat signalling in niche support cells regulates dpp transcription to control germline stem cell maintenance in the Drosophila ovary. Development 135, 533-540.

Mahowald, A.P. and Kambysellis, M.P., 1980. Oogenesis. In Genetics and Biology of Drosophila 2nd. (eds. M. Ashburner and T. R. F. Wright), pp. 141-223. New York: Academic Press.

Margolis, J., Spradling, A., 1995. Identification and behavior of epithelial stem cells in the Drosophila ovary. Development 121, 3797-3807.

McKearin, D., Ohlstein, B., 1995. A role for the Drosophila bag-of-marbles protein in the differentiation of cystoblasts from germline stem cells. Development 121, 2937-2947.

Morris, L.X., Spradling, A.C., 2011. Long-term live imaging provides new insight into stem cell regulation and germline-soma coordination in the Drosophila ovary. Development 138, 2207-2215.

Morris, L.X., Spradling, A.C., 2012. Steroid signaling within Drosophila ovarian epithelial cells sex-specifically modulates early germ cell development and meiotic entry. PloS one 7, e46109.

Najmabadi, H., Hu, H., Garshasbi, M., Zemojtel, T., Abedini, S.S., Chen, W., Hosseini, M., Behjati, F., Haas, S., Jamali, P., Zecha, A., Mohseni, M., Puttmann, L., Vahid, L.N., Jensen, C., Moheb, L.A., Bienek, M., Larti, F., Mueller, I., Weissmann, R., Darvish, H., Wrogemann, K., Hadavi, V., Lipkowitz, B., Esmaeeli-Nieh, S., Wieczorek, D., Kariminejad, R., Firouzabadi, S.G., Cohen, M., Fattahi, Z., Rost, I., Mojahedi, F., Hertzberg, C., Dehghan, A., Rajab, A., Banavandi, M.J., Hoffer, J., Falah, M., Musante, L., Kalscheuer, V., Ullmann, R., Kuss, A.W., Tzschach, A., Kahrizi, K., Ropers, H.H., 2011. Deep sequencing reveals 50 novel genes for recessive cognitive disorders. Nature 478, 57-63.

Ohlstein, B., McKearin, D., 1997. Ectopic expression of the Drosophila Bam protein eliminates oogenic germline stem cells. Development 124, 3651-3662.

Pacchiarotti, J., Maki, C., Ramos, T., Marh, J., Howerton, K., Wong, J., Pham, J., Anorve, S., Chow, Y.C., Izadyar, F., 2010. Differentiation potential of germ line

stem cells derived from the postnatal mouse ovary. Differentiation; research in biological diversity 79, 159-170.

Parks, A.L., Cook, K.R., Belvin, M., Dompe, N.A., Fawcett, R., Huppert, K., Tan, L.R., Winter, C.G., Bogart, K.P., Deal, J.E., Deal-Herr, M.E., Grant, D., Marcinko, M., Miyazaki, W.Y., Robertson, S., Shaw, K.J., Tabios, M., Vysotskaia, V., Zhao, L., Andrade, R.S., Edgar, K.A., Howie, E., Killpack, K., Milash, B., Norton, A., Thao, D., Whittaker, K., Winner, M.A., Friedman, L., Margolis, J., Singer, M.A., Kopczynski, C., Curtis, D., Kaufman, T.C., Plowman, G.D., Duyk, G., Francis-Lang, H.L., 2004. Systematic generation of high-resolution deletion coverage of the Drosophila melanogaster genome. Nature genetics 36, 288-292.

Parte, S., Bhartiya, D., Telang, J., Daithankar, V., Salvi, V., Zaveri, K., Hinduja, I., 2011. Detection, characterization, and spontaneous differentiation in vitro of very small embryonic-like putative stem cells in adult mammalian ovary. Stem cells and development 20, 1451-1464.

Peifer, M., Orsulic, S., Sweeton, D., Wieschaus, E., 1993. A role for the Drosophila segment polarity gene armadillo in cell adhesion and cytoskeletal integrity during oogenesis. Development 118, 1191-1207.

Pritchett, T.L., Tanner, E.A., McCall, K., 2009. Cracking open cell death in the Drosophila ovary. Apoptosis : an international journal on programmed cell death 14, 969-979.

Qian, Y., Dominado, N., Zoller, R., Ng, C., Kudyba, K., Siddall, N.A., Hime, G.R., Schulz, C., 2014. Ecdysone signaling opposes epidermal growth factor signaling

in regulating cyst differentiation in the male gonad of Drosophila melanogaster. Dev. Biol. 394, 217-227.

Salz, H.K., Maine, E.M., Keyes, L.N., Samuels, M.E., Cline, T.W., Schedl, P., 1989. The Drosophila female-specific sex-determination gene, Sex-lethal, has stage-, tissue-, and sex-specific RNAs suggesting multiple modes of regulation. Genes & development 3, 708-719.

Sambrook, J., Fritschi, E.F. and Maniatis, T., 1989. Molecular cloning: a laboratorymanual. Cold Spring Harbor Laboratory Press, New York.

Sarkar, A., Parikh, N., Hearn, S.A., Fuller, M.T., Tazuke, S.I., Schulz, C., 2007. Antagonistic roles of Rac and Rho in organizing the germ cell microenvironment. Current biology : CB 17, 1253-1258.

Scadden, D.T., 2014. Nice neighborhood: emerging concepts of the stem cell niche. Cell 157, 41-50.

Schulz, C., Wood, C.G., Jones, D.L., Tazuke, S.I., Fuller, M.T., 2002. Signaling from germ cells mediated by the rhomboid homolog stet organizes encapsulation by somatic support cells. Development 129, 4523-4534.

Spradling, A.C., 1993a. Developmental genetics of oogenesis. In The development of Drosophila melanogaster 1st. (eds. M. Bate and A. M. Arias). Cold Spring Harbor, NY: Cold Spring Harbor Laboratory Press, pp. 3-4.

Spradling, A.C., 1993b. Germline cysts: communes that work. Cell 72, 649-651.

Sultan, M., Schulz, M.H., Richard, H., Magen, A., Klingenhoff, A., Scherf, M., Seifert, M., Borodina, T., Soldatov, A., Parkhomchuk, D., Schmidt, D., O'Keeffe, S., Haas, S., Vingron, M., Lehrach, H., Yaspo, M.L., 2008. A global view of gene

activity and alternative splicing by deep sequencing of the human transcriptome. Science 321, 956-960.

Tautz, D., Pfeifle, C., 1989. A non-radioactive in situ hybridization method for the localization of specific RNAs in Drosophila embryos reveals translational control of the segmentation gene hunchback. Chromosoma 98, 81-85.

Theodosiou, N.A., Xu, T., 1998. Use of FLP/FRT system to study Drosophila development. Methods 14, 355-365.

Tran, J., Brenner, T.J., DiNardo, S., 2000. Somatic control over the germline stem cell lineage during Drosophila spermatogenesis. Nature 407, 754-757.

Tulina, N., Matunis, E., 2001. Control of stem cell self-renewal in Drosophila spermatogenesis by JAK-STAT signaling. Science 294, 2546-2549.

Van Blerkom, J. and Motta, P., 1979. Morphodynamic aspects of the ovarian superficial epithelium as revealed by transmission, scanning and high voltage electron microscopy. Ann. Biol. Anim. Biophys. 19:1559-1567.

Wang, L., Li, Z., Cai, Y., 2008. The JAK/STAT pathway positively regulates DPP signaling in the Drosophila germline stem cell niche. The Journal of cell biology 180, 721-728.

Ward, E.J., Shcherbata, H.R., Reynolds, S.H., Fischer, K.A., Hatfield, S.D., Ruohola-Baker, H., 2006. Stem cells signal to the niche through the Notch pathway in the Drosophila ovary. Current biology : CB 16, 2352-2358.

Wayne, M.L., Hackett, J.B. and Mackay, T.F.C., 1997. Quantitative Genetics of Ovariole Number in Drosophila melanogaster: I. Segregating Variation and Fitness. Evolution 51, 1156-1163.

Winkler, S., Schwabedissen, A., Backasch, D., Bokel, C., Seidel, C., Bonisch, S., Furthauer, M., Kuhrs, A., Cobreros, L., Brand, M., Gonzalez-Gaitan, M., 2005. Target-selected mutant screen by TILLING in Drosophila. Genome research 15, 718-723.

Woods, D.C., Tilly, J.L., 2013. Isolation, characterization and propagation of mitotically active germ cells from adult mouse and human ovaries. Nature protocols 8, 966-988.

Xie, T., 2008. Germline stem cell niches, StemBook, Cambridge (MA).

Xie, T., Spradling, A.C., 1998. decapentaplegic is essential for the maintenance and division of germline stem cells in the Drosophila ovary. Cell 94, 251-260.

Xie, T., Spradling, A.C., 2000. A niche maintaining germ line stem cells in the Drosophila ovary. Science 290, 328-330.

CHAPTER 5

CONCLUSION

Studies in this thesis have demonstrated regulation of progression through early stages of germ cell lineage non-autonomously by several signaling pathways in *Drosophila melanogaster*: (1) ecdysone signaling modulates the effects of EGF signaling by promoting an undifferentiated state in early-stage cyst cells; (2) CSN acts via distinct CRLs to selectively target proteins for degradation in CySCs and enable cyst cells to respond to external EGF and Upd signals; (3) Comeback fosters the CB-to-CC fate transition possibly through transducing ecdysone signaling pathway in the EC lineage in fly ovaries. The molecules and signaling pathways shown in this study potentially play crucial roles in the somatic support cells to guarantee an intimate germline-soma interaction, and therefore control the survival and developmental stages of germ cells. My thesis data show that without the proper fate determination of and the encapsulation by the somatic cell lineage, germ cells are not properly instructed with external signals from the cellular microenvironment, and therefore severe gametogenic impediment occurs in both male and female flies.

In the gonad of most metazoan animals, the germ cells are shown normally differentiate in close contact with their somatic support cells (Lei et al., 2006; Seydoux et al., 1990; Gilboa and Lehmann, 2006). In the mammalian gonad, interactions between the germ and somatic cell lineages regulate gametogenesis in both genders – the differentiating male germ cells are enclosed in a compartment encompassed by two

Sertoli cells (Yoshida et al., 2007; Akama et al., 2002), while the individual female primordial germ cells are enclosed by somatic granulosa cells to form primordial follicles (Byskov, 1986; Guigon and Magre, 2006; Hirshfield, 1991; Gilchrist et al., 2004; reviewed in Pepling, 2006). In the hermaphrodite gonad of *Caenorhabditis elegans*, the somatic distal tip cell (DTC) extends several thin cytoplasmic arms to associate with the germline, maintaining distal germ cell nuclei in mitosis and promoting proximal nuclei to enter meiosis (Crittenden et al., 2006; reviewed in Kimble and Crittenden, 2005), while somatic cells of the sheath and spermathecal lineage are required for multiple biological events, including germline proliferation, exit from meiotic pachytene stage, gamete differentiation, and the ovulation of the oocyte (McCarter et al., 1997). In *Drosophila melanogaster*, germ cells are enclosed by somatic support cells that to co-regulate each lineage in both sexes (Hardy et al., 1979; Morris and Spradling, 2012; Sarkar et al., 2007; Schulz et al., 2002; reviewed in Zoller and Schulz, 2012). The nature of such germline-soma communication is overwhelmingly complex and highly context-dependent. The genetic tractability of *Drosophila* and the relative anatomical simplicity of fly gonads present a valuable experimental opportunity to probe fundamental questions regarding what signals reciprocally conveyed between the germ and somatic cell lineages, how they interact to each other, and specifically, how the cellular microenvironment is formed and/or maintained to direct germline proliferation and differentiation during different developmental stages.

In this thesis, we tried to approach these questions by utilizing both male and female gonads as tools. The somatic microenvironments for GSCs and their daughters at the tip of *Drosophila* testes and ovaries have been shown to share conspicuous

similarities, and are broadly regulated by some common mechanisms (Decotto and Spradling, 2005; reviewed in Li and Xie, 2005). ESCs in fly ovaries are morphologically and functionally reminiscent of CySCs in fly testes, and they both divide asymmetrically to produce new stem cells to maintain the stem cell niche, and differentiate into ECs and cyst cells, respectively, that encapsulate developing germ cells for proper signal activation and transduction. Both microenvironments relay common signaling, including TGF-β, JAK/STAT, Notch, EGF, and ecdysone (McKearin and Spradling, 1990; Decotto and Spradling, 2005; Kitadate and Kobayashi, 2010; Morris and Spradling, 2012; Qian et al., 2014).

In so far the main evidence for the function of somatic support cells, including CySC and ESC lineages, came from the analysis of individual signal transduction pathways that establish a crosstalk between the soma and the germline. Now we know that the encapsulation of germ cells by the cytoplasmic extensions of somatic support cells are imperative for setting up a functional germline microenvironment and the integrity of both lineages. To this end, it is important to further characterize the local germline-soma association with focus on: (1) what signaling promotes the directional scaffolds within the somatic cell lineage; (2) how the signals are relayed to the germline to effect this intercellular contact; (3) how the somatic support cells act as safeguard of germline function. Resolving the basics of germline-soma coordination and somatic microenvironment will benefit the study of more complex questions in the future such as molecular and cellular mechanisms used for coordinated growth, regeneration and homeostasis. Furthermore, the use of a combination of genetics, biochemistry, transcriptomics, and super-resolution light microscopy to address these questions will

enable us to adapt tools that have already established and maneuvered in other model systems to *Drosophila* research.

References

Akama, T.O., Nakagawa, H., Sugihara, K., Narisawa, S., Ohyama, C., Nishimura, S., O'Brien, D.A., Moremen, K.W., Millan, J.L., Fukuda, M.N., 2002. Germ cell survival through carbohydrate-mediated interaction with Sertoli cells. Science 295, 124-127.

Byskov, A.G., 1986. Differentiation of mammalian embryonic gonad. Physiological reviews 66, 71-117.

Crittenden, S.L., Leonhard, K.A., Byrd, D.T., Kimble, J., 2006. Cellular analyses of the mitotic region in the Caenorhabditis elegans adult germ line. Molecular biology of the cell 17, 3051-3061.

Decotto, E., Spradling, A.C., 2005. The Drosophila ovarian and testis stem cell niches: similar somatic stem cells and signals. Developmental cell 9, 501-510.

Gilboa, L., Lehmann, R., 2006. Soma-germline interactions coordinate homeostasis and growth in the Drosophila gonad. Nature 443, 97-100.

Gilchrist, R.B., Ritter, L.J., Armstrong, D.T., 2004. Oocyte-somatic cell interactions during follicle development in mammals. Animal reproduction science 82-83, 431-446.

Guigon, C.J., Magre, S., 2006. Contribution of germ cells to the differentiation and maturation of the ovary: insights from models of germ cell depletion. Biology of reproduction 74, 450-458.

Hardy, R.W., Tokuyasu, K.T., Lindsley, D.L., Garavito, M., 1979. The germinal proliferation center in the testis of Drosophila melanogaster. Journal of ultrastructure research 69, 180-190.

Hirshfield, A.N., 1991. Development of follicles in the mammalian ovary. International review of cytology 124, 43-101.

Kimble, J., Crittenden, S.L., 2005. Germline proliferation and its control. WormBook: the online review of C. elegans biology, 1-14.

Kitadate, Y., Kobayashi, S., 2010. Notch and Egfr signaling act antagonistically to regulate germ-line stem cell niche formation in Drosophila male embryonic gonads. Proceedings of the National Academy of Sciences of the United States of America 107, 14241-14246.

Lei, L., Zhang, H., Jin, S., Wang, F., Fu, M., Wang, H., Xia, G., 2006. Stage-specific germ-somatic cell interaction directs the primordial folliculogenesis in mouse fetal ovaries. Journal of cellular physiology 208, 640-647.

Li, L., Xie, T., 2005. Stem cell niche: structure and function. Annual review of cell and developmental biology 21, 605-631.

McCarter, J., Bartlett, B., Dang, T., Schedl, T., 1997. Soma-germ cell interactions in Caenorhabditis elegans: multiple events of hermaphrodite germline development require the somatic sheath and spermathecal lineages. Developmental biology 181, 121-143.

McKearin, D.M., Spradling, A.C., 1990. bag-of-marbles: a Drosophila gene required to initiate both male and female gametogenesis. Genes & development 4, 2242-2251.

Morris, L.X., Spradling, A.C., 2012. Steroid signaling within Drosophila ovarian epithelial cells sex-specifically modulates early germ cell development and meiotic entry. PloS one 7, e46109.

Pepling, M.E., 2006. From primordial germ cell to primordial follicle: mammalian female germ cell development. Genesis 44, 622-632.

Qian, Y., Dominado, N., Zoller, R., Ng, C., Kudyba, K., Siddall, N.A., Hime, G.R., Schulz, C., 2014. Ecdysone signaling opposes epidermal growth factor signaling in regulating cyst differentiation in the male gonad of Drosophila melanogaster. Dev. Biol. 394, 217-227.

Sarkar, A., Parikh, N., Hearn, S.A., Fuller, M.T., Tazuke, S.I., Schulz, C., 2007. Antagonistic roles of Rac and Rho in organizing the germ cell microenvironment. Current biology : CB 17, 1253-1258.

Schulz, C., Wood, C.G., Jones, D.L., Tazuke, S.I., Fuller, M.T., 2002. Signaling from germ cells mediated by the rhomboid homolog stet organizes encapsulation by somatic support cells. Development 129, 4523-4534.

Seydoux, G., Schedl, T., Greenwald, I., 1990. Cell-cell interactions prevent a potential inductive interaction between soma and germline in C. elegans. Cell 61, 939-951.

Yoshida, S., Sukeno, M., Nabeshima, Y., 2007. A vasculature-associated niche for undifferentiated spermatogonia in the mouse testis. Science 317, 1722-1726.

Zoller, R., Schulz, C., 2012. The Drosophila cyst stem cell lineage: Partners behind the scenes? Spermatogenesis 2, 145-157.

APPENDIX

RIGHTSLINK PRINTABLE LICENSE

ELSEVIER LICENSE
TERMS AND CONDITIONS

Sep 12, 2014

This is a License Agreement between Yue Qian ("You") and Elsevier ("Elsevier") provided by Copyright Clearance Center ("CCC"). The license consists of your order details, the terms and conditions provided by Elsevier, and the payment terms and conditions.

All payments must be made in full to CCC. For payment instructions, please see information listed at the bottom of this form.

Supplier	Elsevier Limited The Boulevard,Langford Lane Kidlington,Oxford,OX5 1GB,UK
Registered Company Number	1982084
Customer name	Yue Qian
Customer address	Room 604, Dept of Cellular Biology ATHENS, GA 30602
License number	3466540196878
License date	Sep 12, 2014
Licensed content publisher	Elsevier
Licensed content publication	Developmental Biology
Licensed content title	Ecdysone signaling opposes epidermal growth factor signaling in regulating cyst differentiation in the male gonad of Drosophila melanogaster
Licensed content author	Yue Qian,Nicole Dominado,Richard Zoller,Chun Ng,Karl Kudyba,Nicole A. Siddall,Gary R. Hime,Cordula Schulz
Licensed content date	Available online 26 August 2014
Licensed content volume number	n/a
Licensed content issue number	n/a
Number of pages	1
Start Page	None
End Page	None
Type of Use	reuse in a thesis/dissertation
Portion	full article
Format	both print and electronic
Are you the author of this Elsevier article?	Yes
Will you be translating?	No

Title of your thesis/dissertation	SIGNALING PATHWAYS REGULATING ENCAPSULATION OF GERMLINE CELLS BY SOMATIC SUPPORT CELLS IN DROSOPHILA MELANOGASTER
Expected completion date	Dec 2014
Estimated size (number of pages)	
Elsevier VAT number	GB 494 6272 12
Permissions price	0.00 USD
VAT/Local Sales Tax	0.00 USD / 0.00 GBP
Total	0.00 USD
Terms and Conditions	

INTRODUCTION

1. The publisher for this copyrighted material is Elsevier. By clicking "accept" in connection with completing this licensing transaction, you agree that the following terms and conditions apply to this transaction (along with the Billing and Payment terms and conditions established by Copyright Clearance Center, Inc. ("CCC"), at the time that you opened your Rightslink account and that are available at any time at http://myaccount.copyright.com).

GENERAL TERMS

2. Elsevier hereby grants you permission to reproduce the aforementioned material subject to the terms and conditions indicated.

3. Acknowledgement: If any part of the material to be used (for example, figures) has appeared in our publication with credit or acknowledgement to another source, permission must also be sought from that source. If such permission is not obtained then that material may not be included in your publication/copies. Suitable acknowledgement to the source must be made, either as a footnote or in a reference list at the end of your publication, as follows:

"Reprinted from Publication title, Vol /edition number, Author(s), Title of article / title of chapter, Pages No., Copyright (Year), with permission from Elsevier [OR APPLICABLE SOCIETY COPYRIGHT OWNER]." Also Lancet special credit - "Reprinted from The Lancet, Vol. number, Author(s), Title of article, Pages No., Copyright (Year), with permission from Elsevier."

4. Reproduction of this material is confined to the purpose and/or media for which permission is hereby given.

5. Altering/Modifying Material: Not Permitted. However figures and illustrations may be altered/adapted minimally to serve your work. Any other abbreviations, additions, deletions and/or any other alterations shall be made only with prior written authorization of Elsevier Ltd. (Please contact Elsevier at permissions@elsevier.com)

6. If the permission fee for the requested use of our material is waived in this instance, please be advised that your future requests for Elsevier materials may attract a fee.

7. Reservation of Rights: Publisher reserves all rights not specifically granted in the combination of (i) the license details provided by you and accepted in the course of this licensing transaction, (ii) these terms and conditions and (iii) CCC's Billing and Payment terms and conditions.

8. License Contingent Upon Payment: While you may exercise the rights licensed immediately upon issuance of the license at the end of the licensing process for the transaction, provided that you have disclosed complete and accurate details of your proposed use, no license is finally effective unless and until full payment is received from you (either by publisher or by CCC) as provided in CCC's Billing and Payment terms and conditions. If full payment is not received on a timely basis, then any license preliminarily granted shall be deemed automatically revoked and shall be void as if never granted. Further, in the event that you breach any of these terms and conditions or any of CCC's Billing and Payment terms and conditions, the license is automatically revoked and shall be void as if never granted. Use of materials as described in a revoked license, as well as any use of the materials beyond the scope of an unrevoked license, may constitute copyright infringement and publisher reserves the right to take any and all action to protect its copyright in the materials.

9. Warranties: Publisher makes no representations or warranties with respect to the licensed material.

10. Indemnity: You hereby indemnify and agree to hold harmless publisher and CCC, and their respective officers, directors, employees and agents, from and against any and all claims arising out of your use of the licensed material other than as specifically authorized pursuant to this license.

11. No Transfer of License: This license is personal to you and may not be sublicensed, assigned, or transferred by you to any other person without publisher's written permission.

12. No Amendment Except in Writing: This license may not be amended except in a writing signed by both parties (or, in the case of publisher, by CCC on publisher's behalf).

13. Objection to Contrary Terms: Publisher hereby objects to any terms contained in any purchase order, acknowledgment, check endorsement or other writing prepared by you, which terms are inconsistent with these terms and conditions or CCC's Billing and Payment terms and conditions. These terms and conditions, together with CCC's Billing and Payment terms and conditions (which are incorporated herein), comprise the entire agreement between you and publisher (and CCC) concerning this licensing transaction. In the event of any conflict between your obligations established by these terms and conditions and those established by CCC's Billing and Payment terms and conditions, these terms and conditions shall control.

14. Revocation: Elsevier or Copyright Clearance Center may deny the permissions described in this License at their sole discretion, for any reason or no reason, with a full refund payable to you. Notice of such denial will be made using the contact information provided by you. Failure to receive such notice will not alter or invalidate the denial. In no event will Elsevier or Copyright Clearance Center be responsible or liable for any costs, expenses or damage incurred by you as a result of a denial of your permission request, other than a refund of the amount(s) paid by you to Elsevier and/or Copyright Clearance Center for denied permissions.

LIMITED LICENSE

The following terms and conditions apply only to specific license types:

15. **Translation**: This permission is granted for non-exclusive world **English** rights only unless your license was granted for translation rights. If you licensed translation rights you may only translate this content into the languages you requested. A professional translator must perform all translations and reproduce the content word for word preserving the integrity of the article. If this license is to re-use 1 or 2 figures then permission is granted for non-exclusive world rights in all languages.

16. **Posting licensed content on any Website**: The following terms and conditions apply as follows: Licensing material from an Elsevier journal: All content posted to the web site must maintain the copyright information line on the bottom of each image; A hyper-text must be included to the Homepage of the journal from which you are licensing at http://www.sciencedirect.com/science/journal/xxxxx or the Elsevier homepage for books at http://www.elsevier.com; Central Storage: This license does not include permission for a scanned version of the material to be stored in a central repository such as that provided by Heron/XanEdu.

Licensing material from an Elsevier book: A hyper-text link must be included to the Elsevier homepage at http://www.elsevier.com . All content posted to the web site must maintain the copyright information line on the bottom of each image.

Posting licensed content on Electronic reserve: In addition to the above the following clauses are applicable: The web site must be password-protected and made available only to bona fide students registered on a relevant course. This permission is granted for 1 year only. You may obtain a new license for future website posting.

For journal authors: the following clauses are applicable in addition to the above: Permission granted is limited to the author accepted manuscript version* of your paper.

***Accepted Author Manuscript (AAM) Definition:** An accepted author manuscript (AAM) is the author's version of the manuscript of an article that has been accepted for publication and which may include any author-incorporated changes suggested through the processes of submission processing, peer review, and editor-author communications. AAMs do not include other publisher value-added contributions such as copy-editing, formatting, technical enhancements and (if relevant) pagination.

You are not allowed to download and post the published journal article (whether PDF or HTML, proof or final version), nor may you scan the printed edition to create an electronic version. A hyper-text must be included to the Homepage of the journal from which you are licensing at http://www.sciencedirect.com/science/journal/xxxxx. As part of our normal production process, you will receive an e-mail notice when your article appears on Elsevier's online service ScienceDirect (www.sciencedirect.com). That e-mail will include the article's Digital Object Identifier (DOI). This number provides the electronic link to the published article and should be included in the posting of your personal version. We ask that you wait until you receive this e-mail and have the DOI to do any posting.

Posting to a repository: Authors may post their AAM immediately to their employer's institutional repository for internal use only and may make their manuscript publically

available after the journal-specific embargo period has ended.

Please also refer to Elsevier's Article Posting Policy for further information.

18. **For book authors** the following clauses are applicable in addition to the above: Authors are permitted to place a brief summary of their work online only.. You are not allowed to download and post the published electronic version of your chapter, nor may you scan the printed edition to create an electronic version. **Posting to a repository:** Authors are permitted to post a summary of their chapter only in their institution's repository.

20. **Thesis/Dissertation**: If your license is for use in a thesis/dissertation your thesis may be submitted to your institution in either print or electronic form. Should your thesis be published commercially, please reapply for permission. These requirements include permission for the Library and Archives of Canada to supply single copies, on demand, of the complete thesis and include permission for UMI to supply single copies, on demand, of the complete thesis. Should your thesis be published commercially, please reapply for permission.

Elsevier Open Access Terms and Conditions

Elsevier publishes Open Access articles in both its Open Access journals and via its Open Access articles option in subscription journals.

Authors publishing in an Open Access journal or who choose to make their article Open Access in an Elsevier subscription journal select one of the following Creative Commons user licenses, which define how a reader may reuse their work: Creative Commons Attribution License (CC BY), Creative Commons Attribution – Non Commercial - ShareAlike (CC BY NC SA) and Creative Commons Attribution – Non Commercial – No Derivatives (CC BY NC ND)

Terms & Conditions applicable to all Elsevier Open Access articles:

Any reuse of the article must not represent the author as endorsing the adaptation of the article nor should the article be modified in such a way as to damage the author's honour or reputation.

The author(s) must be appropriately credited.

If any part of the material to be used (for example, figures) has appeared in our publication with credit or acknowledgement to another source it is the responsibility of the user to ensure their reuse complies with the terms and conditions determined by the rights holder.

Additional Terms & Conditions applicable to each Creative Commons user license:

CC BY: You may distribute and copy the article, create extracts, abstracts, and other revised versions, adaptations or derivative works of or from an article (such as a translation), to include in a collective work (such as an anthology), to text or data mine the article, including for commercial purposes without permission from Elsevier

CC BY NC SA: For non-commercial purposes you may distribute and copy the article,

create extracts, abstracts and other revised versions, adaptations or derivative works of or from an article (such as a translation), to include in a collective work (such as an anthology), to text and data mine the article and license new adaptations or creations under identical terms without permission from Elsevier

CC BY NC ND: For non-commercial purposes you may distribute and copy the article and include it in a collective work (such as an anthology), provided you do not alter or modify the article, without permission from Elsevier

Any commercial reuse of Open Access articles published with a CC BY NC SA or CC BY NC ND license requires permission from Elsevier and will be subject to a fee.

Commercial reuse includes:

- Promotional purposes (advertising or marketing)
- Commercial exploitation (e.g. a product for sale or loan)
- Systematic distribution (for a fee or free of charge)

Please refer to Elsevier's Open Access Policy for further information.

21. **Other Conditions**:

v1.6

You will be invoiced within 48 hours of this transaction date. You may pay your invoice by credit card upon receipt of the invoice for this transaction. Please follow instructions provided at that time.
To pay for this transaction now; please remit a copy of this document along with your payment. Payment should be in the form of a check or money order referencing your account number and this invoice number RLNK501401467.
Make payments to "COPYRIGHT CLEARANCE CENTER" and send to:

Copyright Clearance Center
Dept 001
P.O. Box 843006
Boston, MA 02284-3006
Please disregard electronic and mailed copies if you remit payment in advance.
Questions? customercare@copyright.com or +1-855-239-3415 (toll free in the US) or +1-978-646-2777.

Gratis licenses (referencing $0 in the Total field) are free. Please retain this printable license for your reference. No payment is required.